In Praise & Critique of EEG for BCI Applications

Moutz Hussien WAHDOW

Scientific advisor: Dr. István ULBERT, DSc

Pázmány Péter Catholic University

Faculty of Information Technology and Bionics

Roska Tamás Doctoral School of Sciences and Technology

A thesis submitted in partial fulfilment of the requirements for the degree of Doctor of Philosophy

2023

"بسم الله الرحمن الرحيم"

Dedicated:

‘To my Family’

Acknowledgments

I want to thank my advisor Professor Ulbert Istvan for his continued cooperation and patience. It was an excellent chance for me to collaborate with him and benefit from participating in his outstanding research team as he provided wise guidance and support through the highs and lows of this exquisite and exceptional journey.

I am grateful to Pázmány Péter Catholic University, staff, administrators, lecturers, and students. The Faculty of Information Technology and Bionics has truly an inspiring appeal to seek excellence, as I have been privileged and blessed to receive the advice and support of Dr Vida Katinka, Dr Ivan Kristof, Prof. Géza Kolumban, Prof. Árpád Csurgay, Prof. Gábor Szederkenyi and Prof. Péter Szolgay, in addition to the senior colleagues in the BCI team, Dr Marton Gergely, Dr Bálint File, Dr Domokos Meszéna, Nánási Tibor, Domonkos Horváth, Ward Fadel, András Adolf, Csaba Köllőd and Dr Mahmoud Alnaanah. To all whom I mentioned, I express my heartfelt thanks and admiration.

To our patients, those suffering from neuromuscular disorders & neurodegenerative diseases. They have been and remain the primary impetus and motive to drive BCI development and research. Their courage in facing complex challenges of their lives is a tremendous inspiration to all of us. We truly thank them and encourage their involvement and partnership in all BCI studies worldwide.

To Prof. Karmos György (May he rest in peace), To my beloved father Hussien (Peace be upon him by God's will). To my dear love, My mother, Maryam and my siblings Mohammed, Hanady and Mohannad, for their unconditional love, trust, support, and company.

To 'electroencephalographers'.

Abstract

Current EEG research has enriched our literature and societies with many prospects for fruitful applications. This sophisticated yet simple device allows monitoring of the human brain in various states for clinical applications and cognitive science studies. It can accurately identify the distinct sleep stages or the depth of anaesthesia and identifies seizures and other neurological disorders to diagnose neurodegenerative diseases and track their progression. Other methods reveal robust EEG correlations with cognitive processes associated with working memory, mental calculations, and selective attention. EEG is essential in measuring coma depth or determining cerebral death. It is also used in neurofeedback rehabilitation and psychopharmacology studies, perception, awareness, language production and comprehension, structure vs function in the brain, spatial navigation, alertness monitoring, depression, and mental state studies.

Since its first inception by Hans Berger almost a century ago, EEG has carried a massive burden in its core ideology, an irony to question telepathy, the dichotomy of whether it is actual or not, or to study higher brain abilities, mind genesis, cognition, and consciousness. Or as in the concept of (BCI), an acronym for Brain Computer Interface, that has fascinated researchers all around the world, to have the ability to read, interpret and control thoughts or control machines through thoughts instinctively and intuitively, restoring abilities, skills and control for people with disabilities who lost motor functions, providing alternative new means and tools for those with severe neuromuscular disorders, paraplegia, amyotrophic lateral sclerosis (ALS), locked-in syndrome (LIS), cerebral palsy, amputation, or trauma. More benefits would also be harnessed for non-medical applications in gaming, polygraphy, and personal identification.

BCI research is one of the most interdisciplinary and multidisciplinary subjects in contemporary neuroscience and engineering. It falls at the intersection of many fields as it combines mathematics, biology, physics, physiology and psychology, medicine, information technology, computer science, biomaterials, and the mainstream engineering disciplines of electrical, mechanical, and electronic engineering, in addition to biochemistry, signal processing, machine learning, statistics, control theory and more.

EEG is the most prominent candidate to realize BCI Sensorimotor Imagery (MI) Systems due to the non-invasive nature of data acquisition, low cost of fabrication, and a high degree of mobility and portability, which makes it the preferred module among researchers rather than the bulky and expensive functional Magnetic Resonance Imaging (fMRI) and Magnetoencephalography (MEG). Aiming to replace, restore, enhance, or improve the natural Central Nervous System (CNS) output to foster healthcare service and improve life quality. Different signal analysis methods, feature extraction, dimension reduction, and classification have been proposed. Our goal of having a plug-and-play system driven and enabled by oscillatory brain waves and rhythms is still in its early stages of research and exploration.

Table of Contents

List of Figures

Abbreviations

EEG - Electroencephalography

ECG - Electrocardiography

EMG - Electromyography

CNS - Central Nervous System

PNS - Peripheral Nervous System

ANS - Autonomic Nervous System

PSPs - Postsynaptic Potentials

EPSPs - Excitatory Postsynaptic Potentials

IPSPs - Inhibitory Postsynaptic Potentials

MEA - Multi Electrode Array

BCI - Brain Computer Interface

MRI - Magnetic Resonance Imaging

NIRS - Near-Infrared Spectroscopy

PET - Positron Emission Tomography

EP - Evoked Potential

ERP - Event-related Potential

ERS - Event related synchronization

ERD - Event related Desynchronization

SCP - Slow Cortical Potentials

VEP - Visually evoked potential

SSVEP - Steady-State Visually Evoked Potential

MI - Motor Imagery

AFE - Analog Front End

ADC - Analog to digital converter

DSP - Digital Signal Processing

DL - Deep Learning

ML - Machine Learning

FFT - Fast Fourier Transform

STFT - Short-Time Fourier transform

DFFT - Discrete Fast Fourier Transform

SNR - Signal to Noise Ratio

CMRR - Common Mode Rejection Ratio

NN - Neural Network

NNE - Neural Network Ensemble

CNN - Convolutional Neural Network

RNN - Recurrent Neural Network

LSTM - Long-Short Term Memory

CWT - Complex Morlet Wavelet Transform

DC - Direct Current

DC - Direct Coupling

AP - Action Potential

FIR - Finite Impulse Response

CSP - Common Spatial Patterns

FBCSP - Filter Bank Common Spatial Patterns

GUI - Graphical User Interface

HCI - Human Computer Interaction

ICA - Independent Component Analysis

ICN - Intrinsic channel noise

kNN - K-Nearest Neighbors

LDA - linear discriminant analysis

PCA - Principal component analysis

PGA - Programmable gain amplifier

ReLU - Rectified linear unit.

REM - rapid eye movement

NREM - Non-Rapid Eye Movement

RMS - Root Mean Square (or random map selection)

SEM - signal energy map

SVM - support vector machine

TDP - time domain parameters

TFD - time-frequency distribution

LMS - Least Mean Square

GA - Genetic Algorithm

PSD - Power Spectral Density

PSO - Particle Swarm Optimization

SCI - Spinal Cord Injury

SVD - Singular Value Decomposition

WT - Wavelet Transform

WPD - Wavelet Packet Decomposition

WPT - Wavelet Packet Transform

Chapter 1: Introduction

1.1 A glimpse into EEG History

The story must begin with the name Hans Berger (1873-1941), A clinician and a Professor of Neuropsychiatry at the University of Jena in Germany. In 1924, he discovered that electrical signals emanated by the human brain could be recorded from the scalp. After five years of further study, Berger published the first of 14 articles; all of them titled "Uber das Elektrenkephalogramm des Menschen", translating to ["On the Electroencephalogram of man"] establishing electroencephalography (EEG) as an essential tool for brain research and clinical diagnosis [1].

Berger's efforts followed the work of Richard Caton (1842-1926), a pediatrician from Liverpool, who worked to explore the electrical phenomena of the exposed cerebral hemispheres of rabbits, cats, and monkeys. Caton presented his findings in 1875 with a concise report in the British Medical Journal. Caton found distinct variations in brain currents increasing during sleep and vanishing after death. He also noted that the external surface of the grey matter was positive in relation to the cerebrum's deep structures, and the cerebrum's fluctuating currents seem to relate to the underlying function. Caton deserves credit for his pioneer work on evoked potentials and the discovery of the oscillating potentials that constitute the EEG. Though, he never pursued his line of inquiry any further and dropped out of EEG research [2].

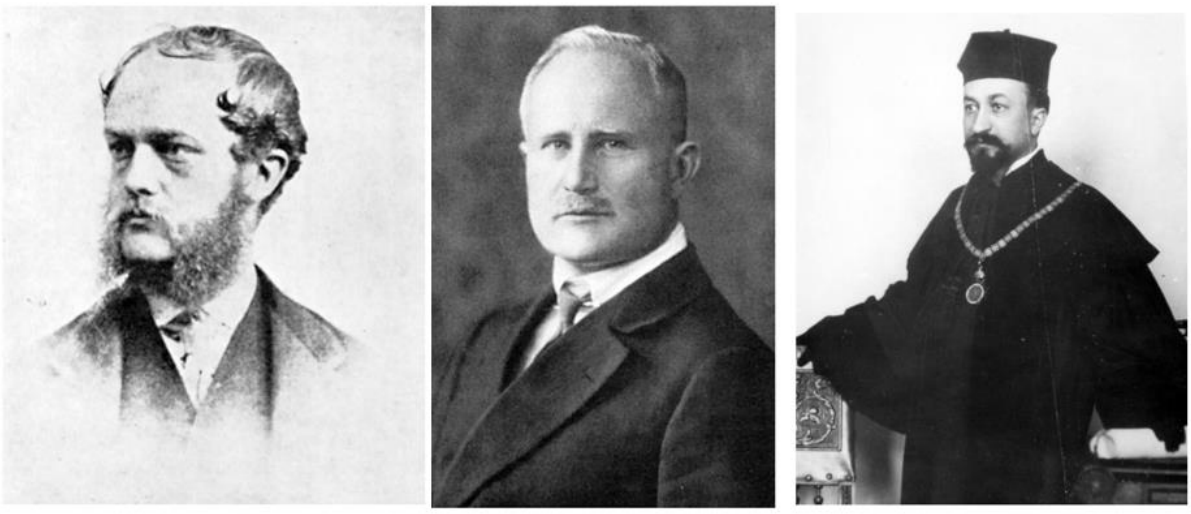

Figure 1: Scientists reported on brain electrical activity. From left to right: Richard Caton (1842-1926) from Liverpool, Hans Berger (1873-1941) from Jena and Adolf Beck (1863-1942) from Kraków.

Concurrent with Caton's work in the 1870s, a more significant impact on the neuroscientific world than Caton's demonstration of the electrical activity of the brain was the capability of the human cerebral cortex to be electrically stimulated, which was rediscovered by Gustav Fritsch (1838-1927) and Julius Eduard Hitzig (1838–1907) in a joint study in 1870 which had been reported by Giovanni Aldini earlier the 19th century [2].

Vasili Yakovlevich Danilevsky (1852-1939) defended his thesis titled "Investigations into the Physiology of the Brain" in 1877, written at the University of Kharkiv. This endeavor was based on spontaneous electrical activity and electrical stimulation in the brains of animals. Thus, Danilevsky gave full credit to Caton's priority in 1891. Danilevsky was disappointed as he expected a better correlation between the brain's spontaneous electrical activity with psychic and emotional processes. He remained profoundly involved in brain physiology and published an extensive textbook on human physiology in 1915 [2].

Caton's report passed unnoticed and remained unknown for many years, as the subject of brain waves lay dormant until the 1890s. Adolf Beck (1863-1939) was a Polish physiologist who investigated the spontaneous electrical activity of the brain in rabbits and dogs. He observed the disappearance of rhythmical oscillations when the eyes were stimulated with light and thus became a forerunner of Berger's discovery of alpha-blocking. Beck published his work in Centralblatt in 1890. Napoleon Cybulski (1854-1919), Beck's teacher in Krakow and an eminent leader in general physiology, presented experimental EEG studies in graphical form using a galvanometer with a photographic attachment. He provided EEG evidence of an epileptic seizure in a dog caused by electrical stimulation [3].

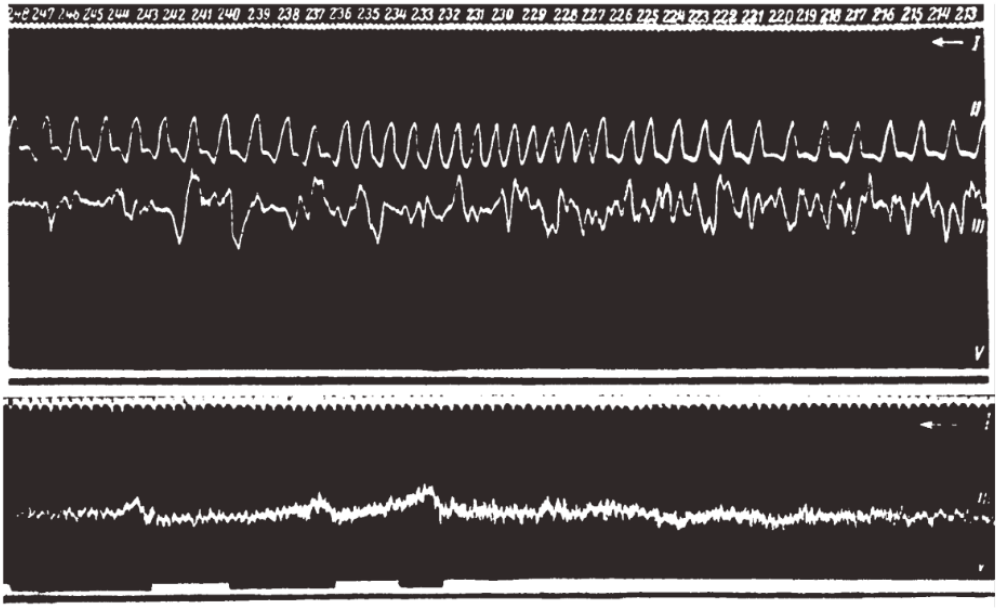

Figure 2: Neminsky's electrocerebrogram. In the upper record, the first photographs to be published of electroencephalograms as Neminsky shows the brain potentials of a curarized dog [2].

EEG research was flourishing in Eastern European countries compared to the West of Europe, and the achievements of neuroscientists and physiologists of Eastern Europe concerning the brain and its electrical activity demonstrate their independent observations and discoveries. The cortical response to electrical stimulation probably was a special incentive for studying its spontaneous electrical phenomena. Two Russian physiologists conducted further studies: Pavel Yurevich Kaufman (1877-1951) and Vladimir Vladimirovich Pravdich-Neminsky (1879-1952). Kaufman studied the effects of cortical electrical stimulation and viewed epileptic attacks as associated with abnormal electrical discharges. Neminsky recorded electrical brain activity from the dura and the intact skull of dogs with the string galvanometer. He published

the first pictorial demonstration of EEG in 1912, shown in Figure (2) above, two years earlier than Cybulski's tracings. Furthermore, he coined the term electro-Cerebro-gram, which Berger rejected purely for linguistic reasons [2].

Einthoven's introduction of the string galvanometer in 1903, a sensitive instrument that required photographic recording, became the standard instrument for Electrocardiography (ECG) at the turn of the century. Berger's first records were taken using a string galvanometer with non-polarizable pad electrodes on the skin over the skull defect. Later, needle electrodes, silver foil, or extracutaneous lead were used. In 1926, Berger substituted the Edelmann string galvanometer with the more sensitive Siemens double-coil galvanometer and, later on, with an oscillograph and an amplifier constructed for Berger by Siemens. All records were taken on photographic paper, upon which a moving mirror projected a light beam; these movements reflected the fluctuations of the cerebral potentials [2] [4].

Berger recorded the human EEG tracings using a bipolar configuration technique with frontal-occipital leads for his one-channel EEG tracings, simultaneous ECG recording, and a time marker, as shown in Figure (3). Berger always supported this photographic recording method, even when the ink writing apparatus had been developed. Between 1926 and 1929, Berger obtained good records for the alpha waves. Still, the data was often uncertain. Nevertheless, after innumerable checks and counterchecks on all possible artifact sources, he was convinced that the potential fluctuations were of genuinely cerebral origin and could be recorded from the area of the skull defects and healthy people with intact skulls. Berger finally published his first report on the human electroencephalogram in 1929 [8] [9].

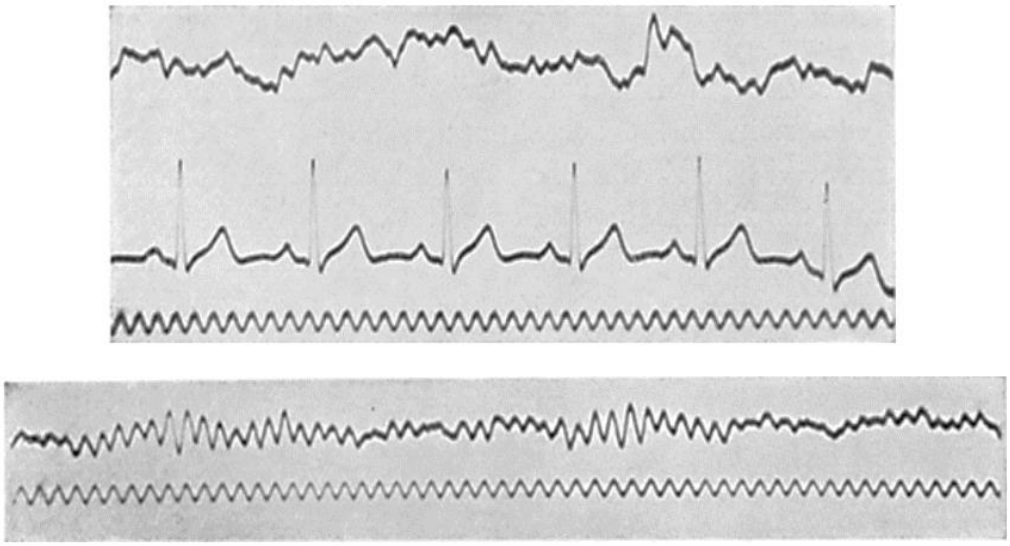

Figure 3:The first human EEG recording obtained by Hans Berger in 1925 from his son Klaus in the upper tracing. From Berger's Publication 1929. Berger has investigated the rhythm in a very large number of subjects in different conditions, e.g., sleep, anesthesia, drug intoxication, etc., and has reported certain instances of a slow rate associated with pathological states of the brain [4].

In meticulous and carefully designed experiments, Berger obsessively and painstakingly identified and eliminated all causes of artifacts that may contaminate an EEG recording. He successfully proved the cerebral origin of the waves he recorded with exquisite thoroughness.

Berger described the Alpha rhythm and Beta rhythm terms, which he introduced and proved that they could not be attributed to any cardiac, vascular, respiratory, circulatory, muscular or cutaneous currents nor any vibratory movements of the head. Therefore, these waveforms can only originate from the brain and constitute, in the true sense of the word, the electroencephalogram of man [1] [2].

On the other hand, Berger was intensely absorbed by the changes in the EEG accompanying alterations in the psychological state, both normal and abnormal; hence, his second major contribution was the EEG study of the phenomena of attention and its effect on the EEG, as well as his investigations on the EEG changes in general anesthesia, epilepsy, asphyxia, insulin coma, postictal coma and stupor and various forms of dementia and psychosis [1] [6].

Strangely enough, Berger's bold report of 1929 produced no waves in the scientific community; the idea that these signals do indeed originate in the brain was not immediately accepted. Berger was ridiculed, and his discovery was treated with disdain and disbelief until his findings were replicated and confirmed by Lord Edgar Douglas Adrian (1889-1977), Baron of Cambridge and his fellow researcher Sir Bryan Harold Cabot Matthews (1906-1986) in their 1934 publication titled "The Berger Rhythm: Potential Changes from The Occipital Lobes in Man" [5]. Moreover, only after that did the scientific community become interested in EEG technology. Since then, medical and scientific applications of EEG have proven to be of considerable importance. Lord Adrian was already a neurophysiologist of great prestige when he confirmed Berger's data, as he won the Nobel prize in 1932. Sir Matthews was Adrian's brilliant electronic engineer. The latter invented two essential pieces of technology: The Matthews oscillograph for capturing nerve activity and the differential amplifier for high gain low noise recording of electrical activity in biological systems [2] [7].

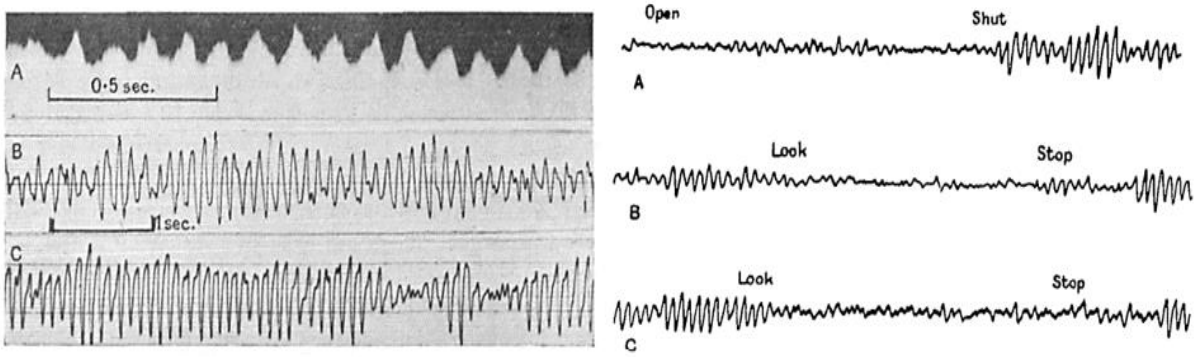

Figure 4: Records of the Berger rhythm made with pad electrodes on the head. The development of the rhythm in the absence of visual activity [5].

Eventually, recognition came at last as Berger was invited to an international congress of psychologists in Paris in 1937; this was the high point of his career. He was somewhat overwhelmed and perplexed by his recognition outside Germany. Berger's relationship with the government could have been better; at the earliest convenience, in 1938, he was abruptly made a professor emeritus and forced into retirement. Consequently, Berger developed severe depression, which remained undiagnosed. He ended his life on the 1st of June 1941, at 68 [6].

Berger's reports on the human EEG contained studies of fluctuation of consciousness, the first recording of sleep spindles, the effect of hypoxia on the human brain, and variety of diffuse

and localized brain disorders, and even some predictions on epileptic discharges. EEG interested him as the expression of the integrated activity of the whole brain. It is fascinating that as early as a century ago, Berger already speculated about the possibility of permanent structural changes induced by ongoing cortical activity, a natural outcome of diffuse cortical inhibition in attention states. Berger thought of the cortical alpha rhythm as a diffuse and homogeneous cortical process driven by a subcortical pacemaker in the thalamus or nearby upper brainstem [7].

Lastly, trying to end this section gracefully, Berger was a very complex person and investigator, an extremely meticulous and conscientious person, shy, vulnerable and sensitive yet a strict authoritarian hard-working professor. However, Berger also pursued an unscientific perspective on the nature of the EEG and telepathy. The driving force behind his research was the quest for the nature of mental energy ("psychical energy"), thought to be a partial product of metabolic energies, electricity and temperature being the other two. His contemporaries regarded him as an amateur because he may not have excelled as a clinician or psychiatrist. Nevertheless, it was the psychoneurophysiologist Berger who voyaged to search for mental energy and found the EEG. Even though the EEG is not precisely what Berger assumed, his contribution was the greatest in the history of EEG [1] [9].

Among other EEG pioneers were Herbert Jasper (1906-1999) and Wilder Penfield (1891-1976), famous for their studies of patient response to electrical stimulation of cortical tissue. Penfield and Jasper carried out numerous EEG studies of epilepsy surgery patients. Frederic Bremer (1892-1982) also quickly recognized the usefulness of EEG methods in the experimental investigation of the brain with his publication "Cerebral and Cerebellar Potentials" in 1958, and also Grey Walter (1910-1977) who was the first to assign the term "delta waves" to particular types of slow waves recorded in the EEG of humans [2] [8] [11].

1.2 Aims and motive

This thesis aims to emphasize the role of EEG in clinical diagnosis, neurorehabilitation, cognitive sciences, psychopharmacology and sleep research, perception, awareness, attention and memory, language production, spatial navigation, alertness monitoring, and BCIs. EEG is typically used to diagnose or monitor conditions such as epilepsy, sleep disorders, and brain damage. The patterns and frequencies of the brain waves recorded by the EEG can provide insight into the functioning of the brain and its responses to various stimuli.

EEG-based BCI refers to a technology that interfaces with the human brain to translate electrical activity generated by neurons into commands that control a computer or a variety of other devices and assistive technologies, exoskeletons and robotic devices. The central goal of BCI research and development is for people severely disabled by neuromuscular disorders such as (ALS), stroke, spinal cord injury (SPI), cerebral palsy, multiple sclerosis, and muscular dystrophy. BCI systems would allow individuals with physical disabilities or locked-in syndrome to interact with the world using their brain activity, bypassing their physical limitations and improving their quality of life, subsequently enabling them to live enjoyable and productive lives if provided with effective assistive technology.

Several challenges come with using and designing EEG-based BCI systems, including low signal-to-noise ratio (SNR), variability in brain signals, and the need for calibration and parameterization, in addition to the complexity of processing and interpreting neural signals. However, with improvements in signal processing and machine learning algorithms, EEG-based BCI systems are becoming more reliable and accurate. However, the rapid increase in BCI research has exposed an underappreciated problem: BCI Illiteracy. This problem remains unresolved across all major BCI approaches (P300, SSVEP, and ERD/ERS).

This work explores Convolutional Neural Networks (CNNs), which have been proven decisive for EEG signal classification and used intensively by many researchers for multi-class EEG Motor Imagery (MI) signal classification. This dissertation also comments on using EEG as a medium to construct BCIs and addresses current challenges. Three datasets are included in the evaluation process: Physionet, BCI Competition IV-2a and MTA-TTK, a private dataset belonging to Pázmány Péter Catholic University. Our results propose that CNN designs and Deep Learning (DL) algorithms are fit for implementing feature extraction and classification; using fewer channels and feature vectors would also reduce the computational complexity and increase the classifier models' speed and accuracy.

1.3 Thesis Structure

Chapter 2 overviews brain structure anatomy and physiology; Chapter 3 provides neurophysiology terminology. Chapter 4 presents EEG and its signal characteristics and their application in clinical and cognitive research as the other Data Acquisition Systems (DAQs) modalities used to implement BCIs. Datasets description, Methods, Materials and Results are presented in Chapter 5, with a brief discussion that concludes the dissertation.

Chapter 2: Overview of Human Brain Anatomy

For a long time, the Brain has fascinated scientists, philosophers, engineers, and psychologists. The delicate and enormous tasks that a relatively small organ can execute are amazingly sophisticated; judgements and reasoning, mood swings, Consciousness, subconsciousness, sleep, dreams, hallucinations, emotions, learning, awareness of self, and the unique and individualized experience of being oneself and reaching high to the soul; All Have been related to brain functionality. In our path of understanding the ways of the Brain, different approaches and tools have been exploited, such as anatomical dissections, physiologic and biological studies, chemical neurotransmitter studies, trial and error with disorders, surgeries and medications, and recently capital equipment like Computed tomography (CT), functional Magnetic Resonance Imaging (fMRI), Magnetoencephalography (MEG) in addition to EEG studies are used to explore the structure versus functionality of the Brain. These tools have immensely developed and accelerated the fields of neuroscience, psychophysiology, and cognitive neurophysiology.

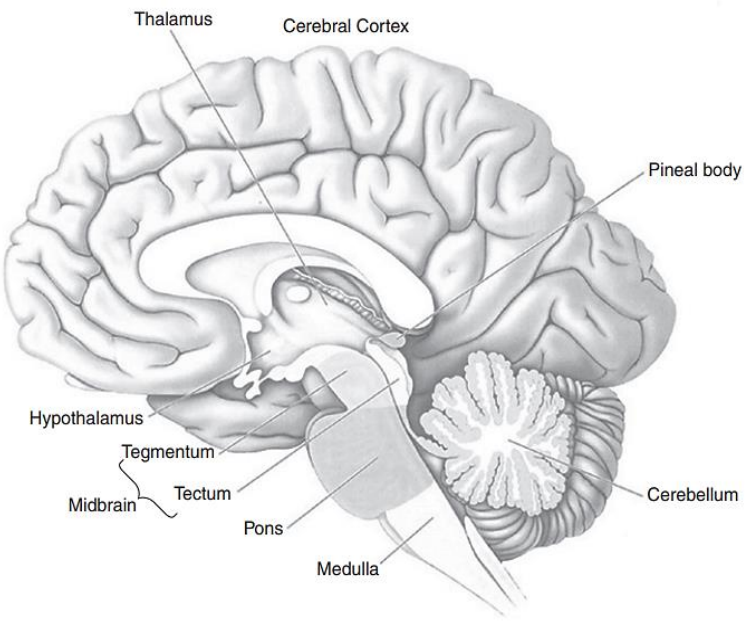

Figure 5: Major brain regions. The diagram depicts some of the major regions of the human brain. The medulla, pons, and midbrain comprise the brain stem and convey most of the information from the brain to the body. The thalamus and the hypothalamus comprise the diencephalon; the former relays sensory information to the brain, while the latter regulates basic needs. At the base of the brain is the cerebellum, which plays an active role in the coordination of movements. [15]

2.1 Nervous System and Brain Structure

The Central Nervous System (CNS) is composed of the brain and the spinal cord. It is differentiated from the peripheral nervous system (PNS), composed of the peripheral nerves, ganglia, sensory receptors, and the autonomic nervous system (ANS). The ANS is subdivided into sympathetic and parasympathetic components. It consists of neurons that innervate secretory glands and cardiac and smooth muscle and primarily control the internal

environment. The PNS mainly brings sensory inputs to the CNS and carries motor outputs to the rest of the body [15] [16] [17].

CNS activity comprises the electrophysiological, neurochemical, and metabolic phenomena such as neuronal action potentials, synaptic potentials, neurotransmitter releases, and oxygen consumption that occurs continually in the CNS. These phenomena can be monitored by measuring electric or magnetic fields, hemoglobin oxygenation, and other parameters employing sensors on the scalp, the brain's surface, or within the brain. The brain comprises three primary divisions: the Cerebrum, the Cerebellum, and the Brainstem, all included in the neurocranium (the Skull). The cerebrum consists of two cerebral hemispheres, right and left, separated by the longitudinal fissure and interconnected mainly by the corpus callosum [13][14].

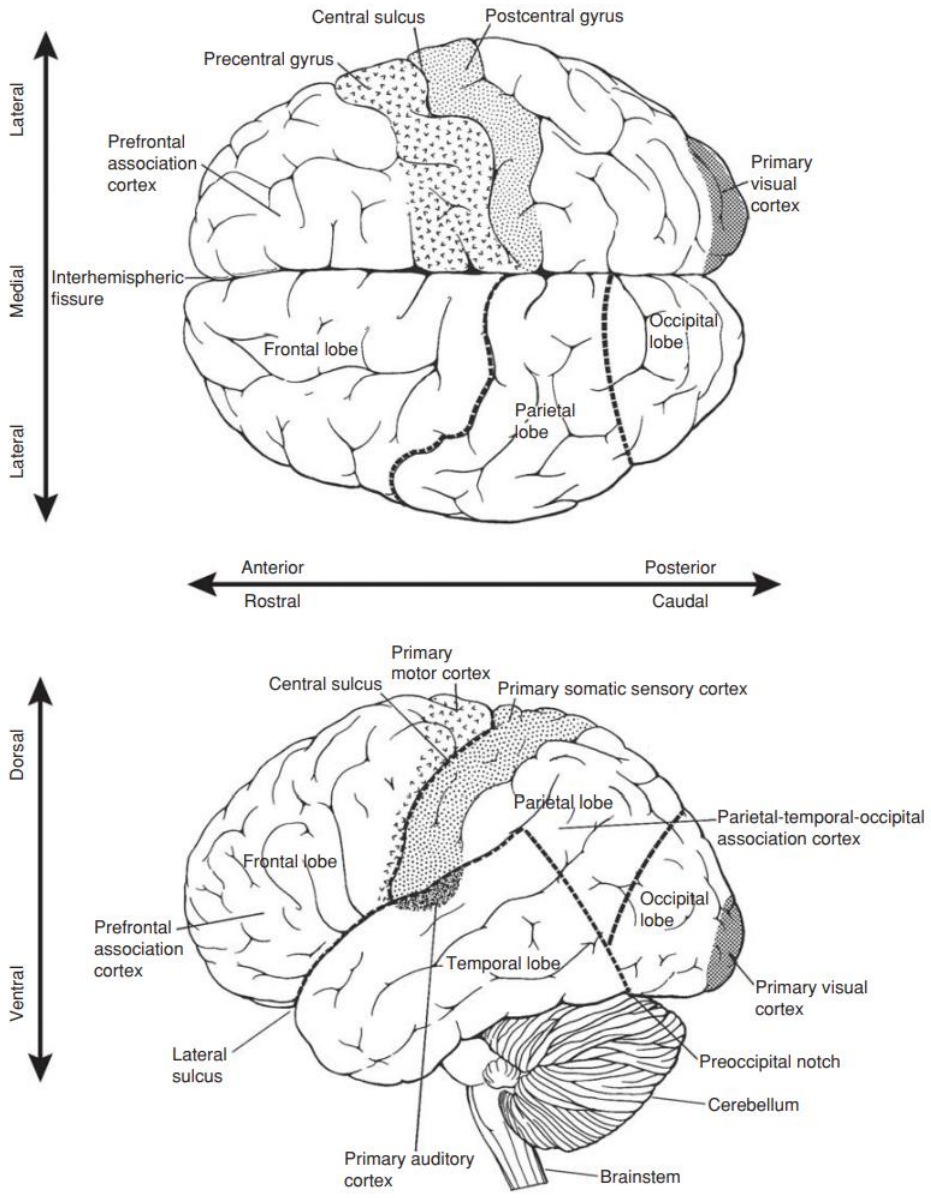

Figure 6: Major divisions of the human cerebral cortex in dorsal (from above) and lateral views. The four major lobes are (frontal, parietal, occipital, and temporal) [17].

Each hemisphere has three surfaces (lateral, medial, and basal). Meninges cover the brain (Pia mater, Arachnoid mater, and Dura mater consecutively from inward out). In mammals, the cerebrum comprises the outer grey matter, the cerebral cortex (or neocortex). The cortex is a thin, folded structure of wrinkled grey matter, varying in thickness from about 2 to 5 mm, having a total surface area of roughly 1600 to 4000 cm^2 and containing about 10^{11} neurons (nerve cells) where cortical neurons are strongly interconnected. It is thought to be responsible for the nervous system's higher functions. The gyrus is the ridge of one of those wrinkles, and a sulcus is a groove between two gyri [12].

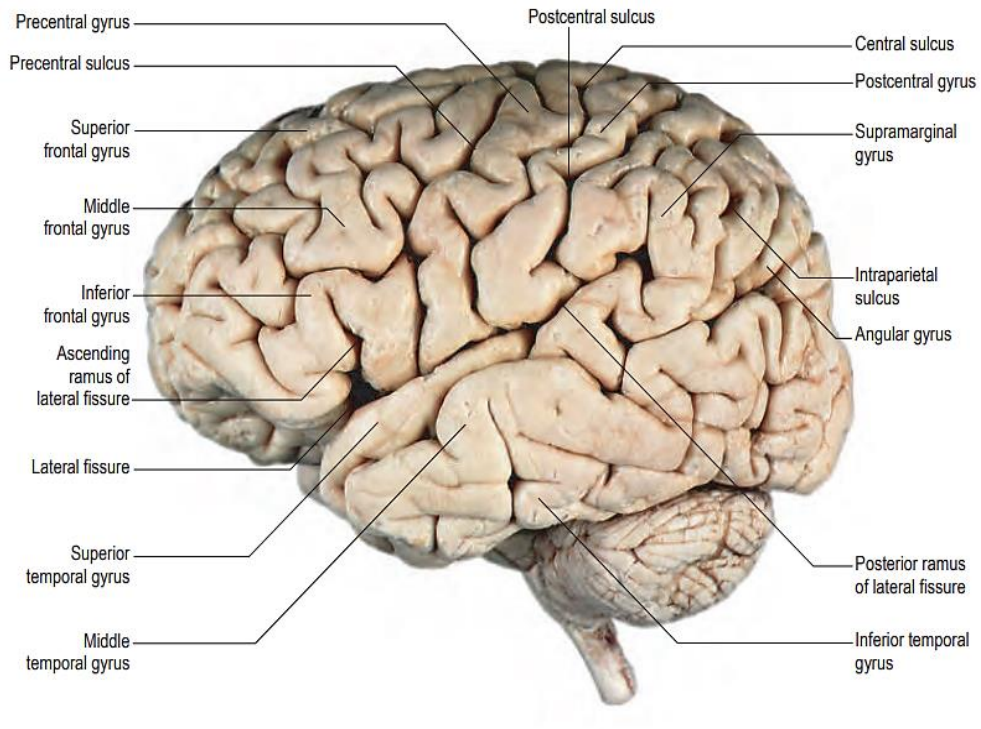

Figure 7: The lateral aspect of the left cerebral, indicating the major gyri and sulci [16]

Several other deeper grey-matter structures exist beneath the cortex, the subcortical areas, including the brainstem, basal ganglia, cerebellum, and thalamus. The cerebellum, which sits on top and to the back of the brainstem, has long been associated with the fine control of muscle movements. More recently, the cerebellum has been shown to play additional roles in cognition [13] [16].

The brain's white matter consists of the many nerve fibers that interconnect the various cortical areas and connect the cortex to subcortical areas and vice versa. The brainstem is the structure through which nerve fibers relay signals in both directions between the spinal cord and higher brain centers. The thalamus is a relay station and a crucial integrating center for all sensory input to the cortex except smell (olfaction) [17].

Grey matter is distinguished from white matter because it contains numerous cell bodies and few myelinated axons. In contrast, the white matter has relatively few cell bodies and is composed chiefly of long myelinated axons. Grey matter is distributed in the cortex, cerebellum, brainstem, and basal ganglia. White matter is formed by the fibers connecting the

cortex with sub-cortical structures and the spine. It is possible to recognize the different tracts of white matter between the distinct grey matter structures. The Grey matter – White matter duality extends to the spinal cord [6] [12] [17]. There are three different kinds of fibers that form white matter:

I. Association fibers interconnect different cortex regions within the same hemisphere.

II. Commissural fibers interconnect corresponding areas of the two hemispheres across the midline. The primary white fiber "motorway" interconnecting the hemispheres is the corpus callosum, formed by more than 200 million fibers.

III. Projection fibers are supero-inferiorly orientated, connecting the cortex with the subcortical structures and spinal cord. An exemplary projection system is a corticospinal tract, constituting the pyramidal system.

The brain has cavities within its substance named Ventricles. There are two lateral ventricles and single third and fourth ventricles. These cavities are filled with Cerebrospinal Fluid (CSF), The volume of which is around 150-200 cc [13] [14], depicted in Figure (8) below. The CSF has many purposes [18], which includes:

I. **Buoyancy**: The actual mass of the brain is about 1400-1500 g. However, when suspended in CSF, its mass is equivalent to 25-50 g. (Archimedes law: Any body entirely or partially submerged in a fluid is acted upon by an upward, upthrust or buoyant force, the magnitude of which is equivalent to the weight of the fluid displaced by the body).

II. Protection: It acts as a shock absorber.

III. Prevention of Brain ischemia.

IV. Clearing waste metabolism.

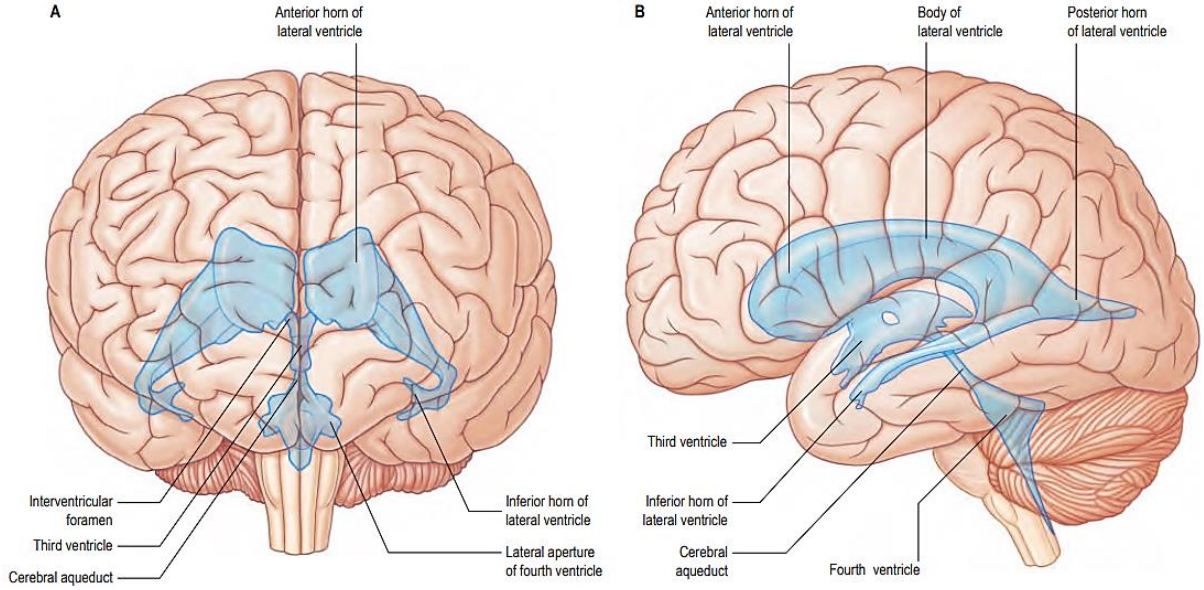

Figure 8: The ventricular system. A, Anterior view. B, Left lateral view [13].

2.1.1 Frontal lobe

The frontal lobe is the biggest lobe of the human brain, about one-third of the hemispheres. The central sulcus forms its posterior border, whilst its inferior border is the lateral sulcus. On the surface of the convexity of the frontal lobe, it is possible to recognize a vertical sulcus, the precentral sulcus; between the central sulcus and the precentral sulcus lies the precentral gyrus [13] [15] [17].

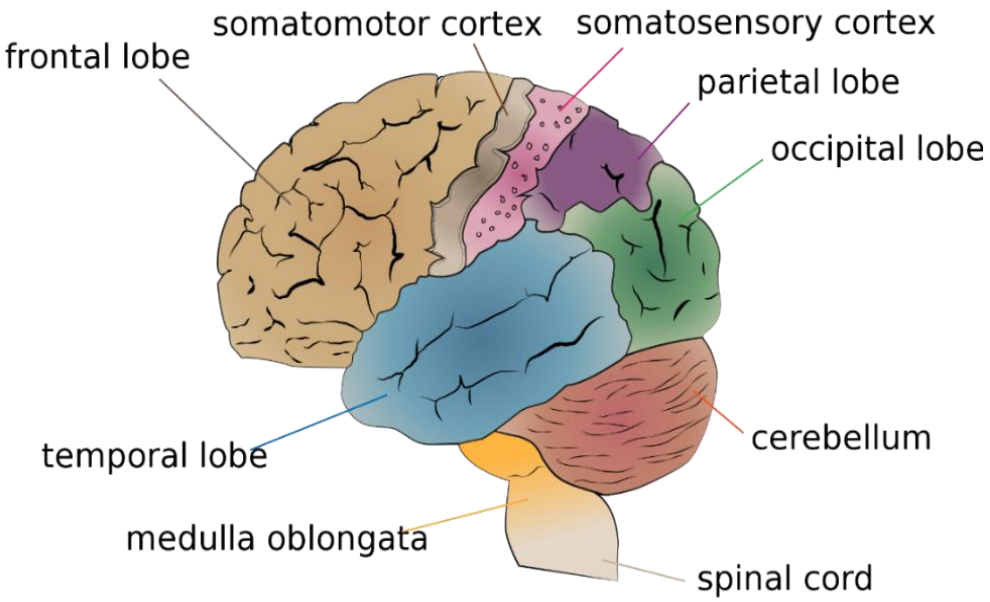

Figure 9: Frontal, Parietal, Temporal and Occipital lobes of brain, Separated by Central, Lateral and Parito-Occipital sulci [Creative Commons Attribution 4.0].

In the frontal lobe of the dominant hemisphere lies Broca's area (areas 44 and 45 of Broadmann) reference Figure (10), which is the motor speech area. The precentral gyrus, the so-called "primary motor cortex", is involved in the motor function of the contralateral side of the body. The motor cortex contains a defined body map and an area involved in sphincter control (voluntary control of bladder function).

The Premotor cortex is involved in the planning of movement, supplementary motor areas influence the generation and control of movement, and the eye-field cortex is involved in controlling the movements of the eyes. Moreover, the frontal lobe is involved in higher cognitive functions (orientation, attention, planning, personality, emotionality, sexual behaviour, mental processes, and working memory) [13].

The basal nuclei have a crucial function associated with planning movements. On the lateral surface of the cerebrum, we can identify two essential Sulci, the Central sulcus of Rolando and the lateral sulcus [19]. The parieto-occipital sulcus is the third vital sulcus to be identified. Identifying the prominent sulci on the surface of the cerebrum allows for discernment of the cerebral lobes: frontal, parietal, temporal and occipital lobes, as well as the insular lobe, hidden in the depth of the Sylvian fissure [20].

2.1.2 Parietal lobe

Korbinian Brodmann (1868 -1918), a German neurologist, extensively studied the microscopic anatomy and the cytoarchitecture of the cerebral cortex and divided the cortex into 52 separate regions based on the histology of the cortex. His work resulted in a classification system known as Brodmann's areas, shown in Figure (10) below, which is still used today to describe the anatomical distinctions within the cortex. To our interest, areas 1,2,3,4 & 6 are the areas of motor and premotor activity and motor imagery. They lie on the lateral surface of the frontal lobe, anterior to the central gyrus. Due to their superficial location relative to brain structures, they are the most amenable to EEG signal recording [13].

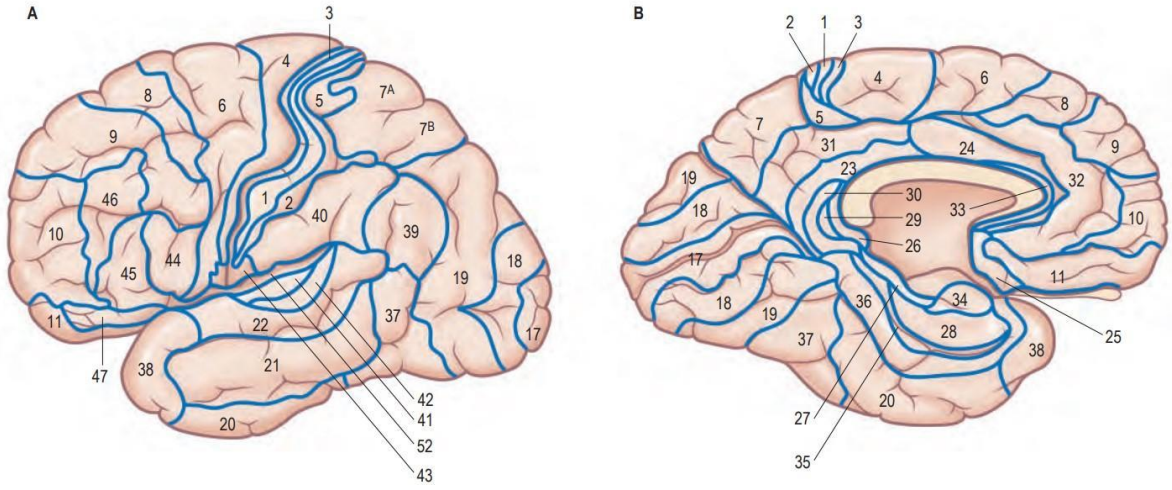

Figure 10: The lateral (A) and medial (B) surfaces of the left cerebral hemisphere depicting Brodmann's areas [13].

The **Parietal lobe** is located between the central sulcus, the parietooccipital line, and the posterior ramus of the lateral sulcus. The postcentral gyrus, the somatosensory cortex, is the cortical strip between the central sulcus and the postcentral sulcus. The somatosensory area of the cortex contains a defined body map (somatosensory homunculus). Lesions of primary somatic areas (areas 1, 2, and 3 of Broadmann) may give rise to contralateral impairment of touch, pressure, and proprioception [13] [14] [17].

Karl Wernicke (1848-1905), a German physician and neurologist, is credited with showing that damage to the back part of the temporal lobe of the left hemisphere could produce difficulties in understanding speech; similarly, problems in reading and writing were identified in some patients and were shown to result from damage to the left hemisphere, not from damage to the right hemisphere. "*Wernicke's speech region*" is also contained within the parietal lobe. Lesions involving the Wernicke's region result in receptive (or fluent) aphasia, in which the patient fluently articulates meaningless words. The parietal lobe also has some vestibular areas and many associative regions, such as those involved in planning, executing, and monitoring movements [15] [17] [21].

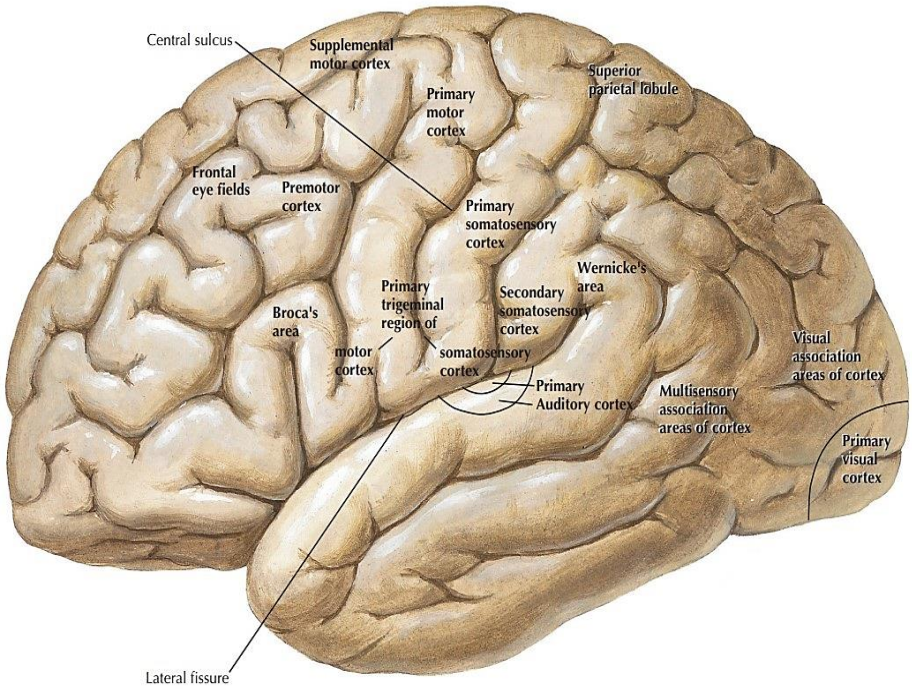

Figure 11: Lobar boundaries and nomenclature. A Lateral surface left side. The central sulcus separates the frontal from the parietal lobes. The Sylvian fissure separates the frontal from the temporal lobes [13].

A specific syndrome related to the dysfunction of the parietal lobe (angular and supramarginal gyri of the dominant hemisphere) is the Gerstmann syndrome [22], with Anomia (inability to name objects), Alexia (inability to understand written or printed language), Acalculia (inability to perform arithmetic operations), Agraphia (inability to write), finger agnosia, and inability to coordinate left and right hand sides. In the dominant hemisphere, the opercular and triangular parts of the inferior gyrus correspond to Broca's area, which is responsible for the production of spoken language [23] [24].

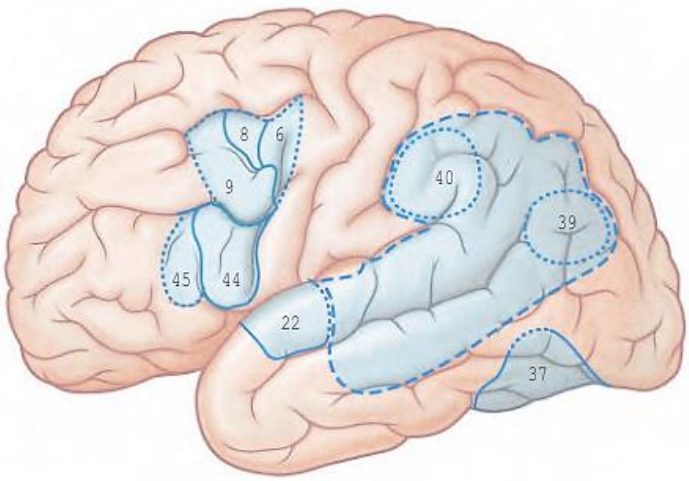

Figure 12: The lateral surface of the left cerebral hemisphere shows the frontal eye field (parts of areas 6, 8, 9), the motor speech (Broca's) area (areas 44, 45) and Wernicke's area. The perimeter of these areas is delineated by an interrupted line to indicate uncertainty as to their precise extent. [13]

2.1.3 Temporal lobe

The temporal lobe is mainly involved in auditory functions and the integration of complex information. The temporopolar cortex of the temporal lobe is a paralimbic structure. Lesions of the auditory cortex (areas 41 and 42 of Broadmann) may affect hearing or cause auditory aphasia, where the patient can hear but does not understand [13] [17].

2.1.4 Occipital lobe

The most significant sulcus of the occipital lobe is visible on its medial surface, the calcarine sulcus, where the granular cortex of the visual areas is located. The occipital lobe functions are essentially visual, with all the vision-related specific functions: shape processing, colour perception, three-dimensional reconstructions of objects, etc. Among other particular signs related to lesions of the occipital lobe, central blindness, central colour blindness (*Achromatopsia*), selective difficulty in identifying faces (*Prosopagnosia*), and dysfunction in perceiving movements (*Cortical Akinetopsia*) [13] [17].

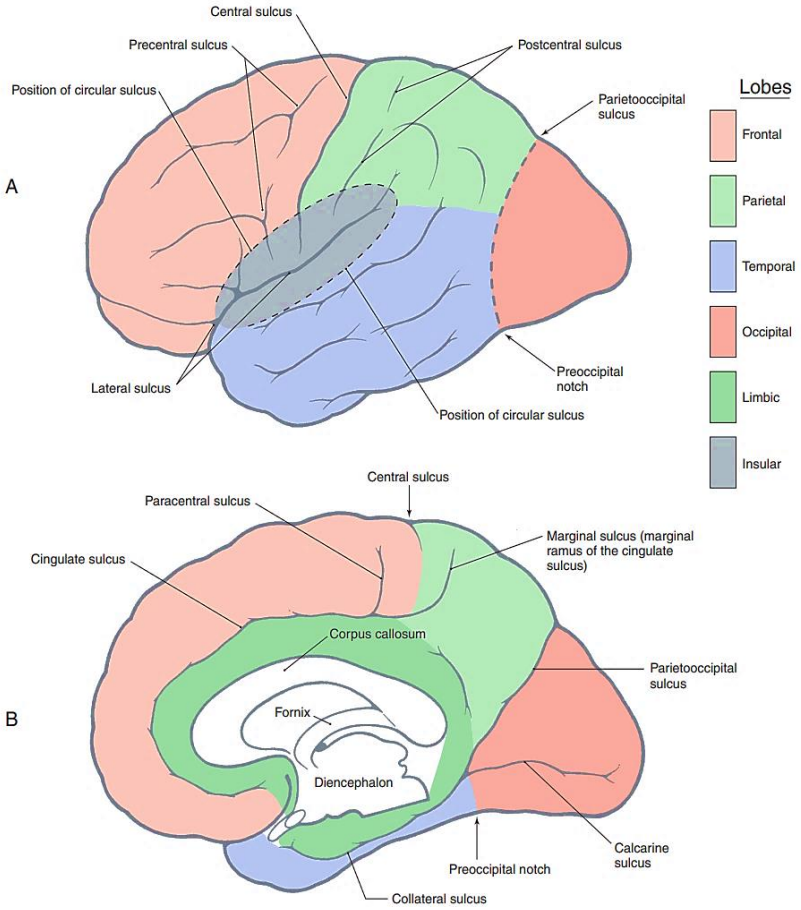

Figure 13: Lobes of the brain on the lateral surface 16]

2.1.5 Limbic lobe

The elements of the limbic system are mainly concerned with memory and the emotional aspects of behaviour and provide an affective overtone to conscious experience and an interface with subcortical areas, such as the hypothalamus, through which widespread physiological activities are integrated. Other cortical areas, primarily within the frontal region,

are concerned with the highest aspects of cognitive function and contribute to personality, judgment, foresight and planning [13] [15].

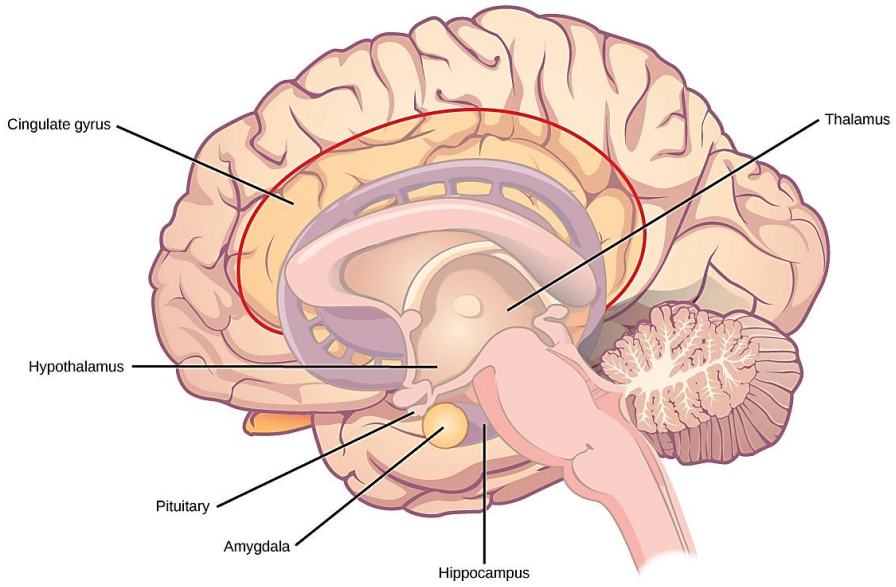

Figure 14: The Limbic System [Creative Commons Attribution 4.0]

The limbic lobe contains the cortical structures on the most medial edge of the hemisphere, with its surrounding paralimbic system, beneath the corpus callosum. The hippocampal formation, amygdala, septum pellucidum, hypothalamus, and central olfactory system form the limbic system. The Insula, cingulate gyrus and part of the orbitofrontal cortex form the paralimbic belt. Limbus means edge or border; the descriptive term limbic was first used in the sixteenth century but is more usually associated with Broca, who described the cingulate and parahippocampal gyri as the greater limbic lobe and considered the different sulci that limited these two gyri as parts of a single sulcus that he called the limbic sulcus [15] [17].

2.1.6 Insular lobe

The insular lobe sometimes called the Insula, insular cortex or “The Island of Reil”, is situated deep within the folds of the cortex. It is a paralimbic structure formed by the mesocortex, a transitional cortex between the neocortex and the archicortex of the limbic system, which includes the floor of the lateral sulcus. This brain region remains a mystery. Its location deep within the brain makes it difficult to explore, and until recent decades, doctors had little understanding of its purpose. That is changing, thanks partly to better brain imaging technologies, but much remains to be understood about this vital brain structure. The Insula is highly connected with all the brain and basal ganglia regions and is involved in many different functions [13], including:

I. Visceromotor control (e.g., gastrointestinal motility, respiration, heart control),
II. Viscerosensory functions (abdominal sensations, nausea),
III. Taste, olfaction, vestibular, somatosensory, and higher psychological functions [14].

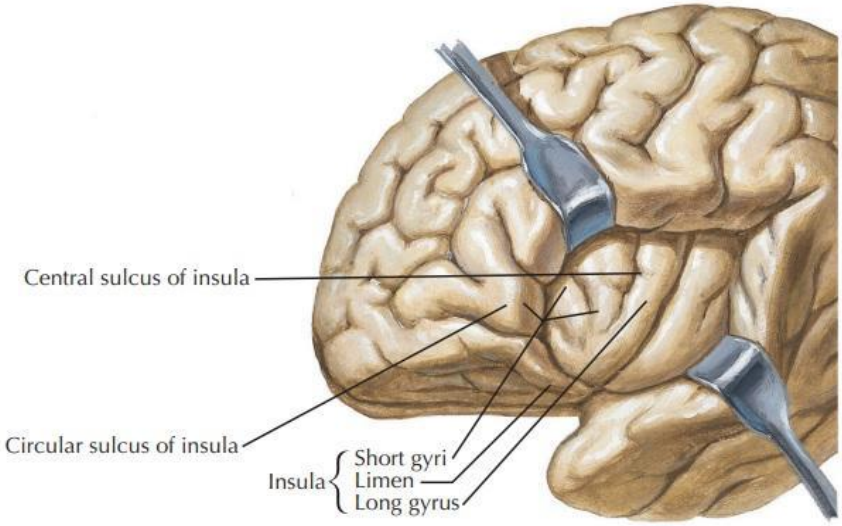

Figure 15: The Insula is embedded in the brain, and the separation of parietal and frontal cortices will reveal it. Functions of the Insula are involuntary and related to visceral functions [1314].

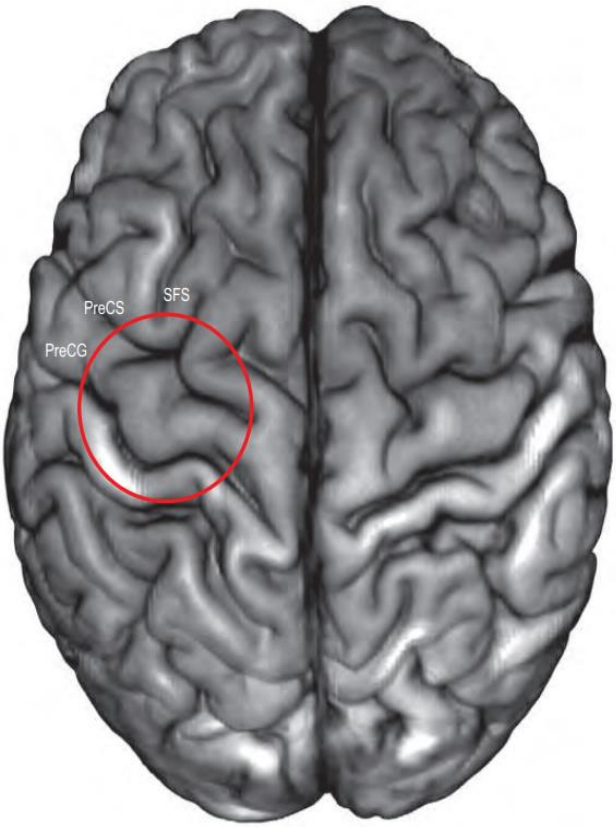

Figure 16: The hand motor activation site, corresponds to a knob-like cortical area of the contralateral precentral gyrus, which in MRI axial planes usually resembles an inverted omega shape (the area within the red circle) and may be identified by its relationship to the posterior end of the superior frontal sulcus. Abbreviations: PreCG, precentral gyrus; PreCS, precentral sulcus; SFS, superior frontal sulcus [13].

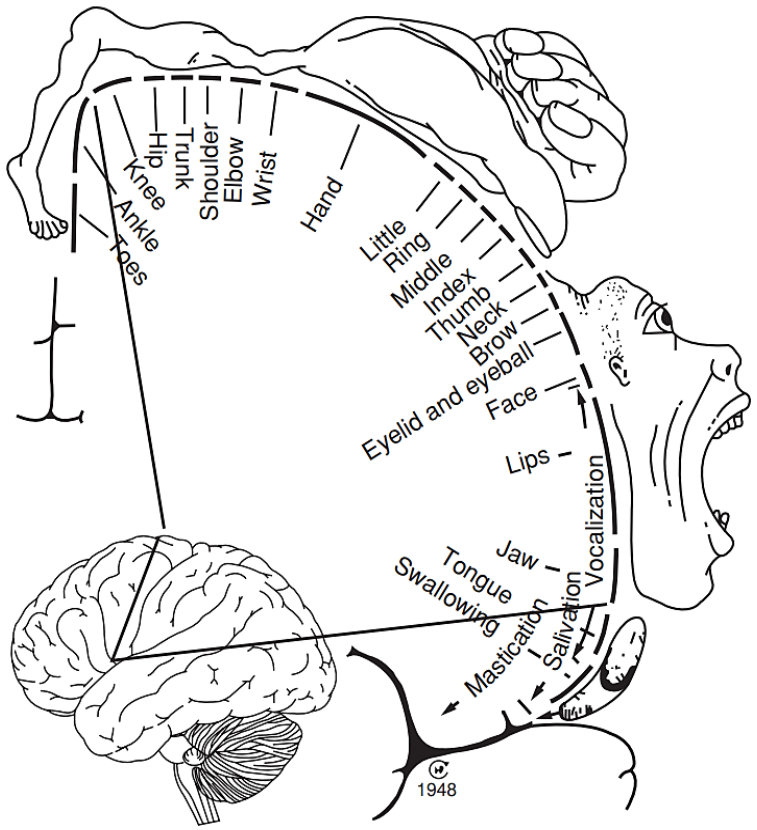

Figure 17: The motor homunculus showing proportional somatotopic representation in the primary motor area, derived by Wilder Penfield, illustrating the effects of electrical stimulation of the cortex of human neurosurgical patients [17].

2.2 Hippocampus

The hippocampus (hippocampus proper, Ammon's horn) is a convex elevation, approximately 5 cm long, within the parahippocampal gyrus inside the lateral ventricle's inferior (temporal) horn. Macroscopically, it can be divided into a head, a body, and a tail. Anteriorly, the head is expanded and bears two or three shallow grooves (pes hippocampi). The main outflow bundle of the hippocampus, the fornix, wraps around the thalamus. The hippocampus is believed to be involved in regulating emotions and storing long-term memories, making those memories resistant to forgetting, though this is a matter of debate. It is also thought to play an essential role in spatial processing and navigation, as the entorhinal cortex has reciprocal connections with the hippocampus and neocortical regions [25].

The medial temporal lobe cortex includes major subdivisions of the limbic system, such as the hippocampus and entorhinal cortex. Areas of the neocortex adjacent to these limbic regions are grouped as medial temporal association cortex. Nuclei of the amygdala project to and receive fibres from neocortical areas, predominantly of the temporal lobe and possibly the inferior parietal cortex. The density of these pathways increases towards the temporal lobe [20] [24] [26].

2.3 Amygdala

The amygdala (amygdaloid nuclear complex) is an almond-shaped structure formed by a group of lateral, central and basal nuclei lying in the dorsomedial temporal pole, anterior to the hippocampus. Laterally, the amygdala lies close to the optic tract. The amygdala primarily processes emotions and memories associated with fear and pleasure. Other recognizable structures on the Medial surface are the Uncus, Mammilary bodies, the Fornix, and the Cingulum [27] [28]. These are beyond the scope of this dissertation. The amygdaloid complex has pervasive and rich connections with many areas of the neocortex in unimodal and polymodal regions of the frontal, cingulate, insular and temporal neocortices. The amygdala receives a rich monoaminergic innervation and numerous projections from the brainstem [29].

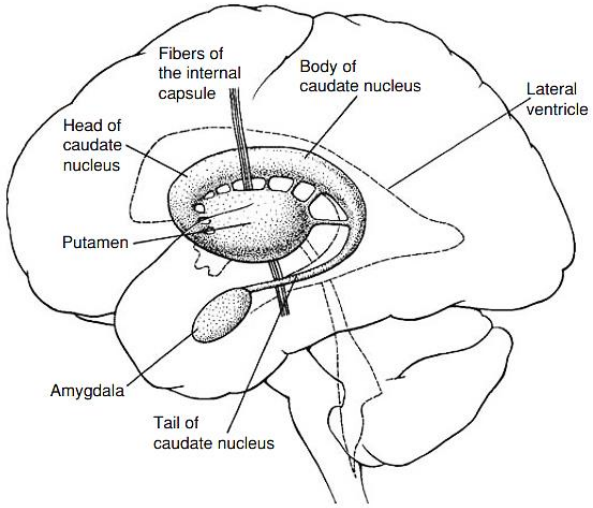

Figure 18: Location of the basal ganglia deep within the cerebral cortex. [17]

2.4 Basal Ganglia, Diencephalon & the Thalamus

The major subcortical areas of the brain that interact with the cortex and are intimately involved in motor and sensory function include the: thalamus, brainstem, basal ganglia and cerebellum [6] [13] [17]. In the center of the basal surface, one can visualize the optic system (optic nerves, optic chiasm, and optic tracts), mammillary bodies, tuber cinereum, uncus, and ventral surface of the brainstem. The basal ganglia are a group of cell masses, “grey matter in the central core of the hemispheres”, mainly the Caudate nucleus, Putamen, Globus pallidus, Claustrum and some small nuclei. The basal forebrain nuclei serve as the primary location for acetylcholine production, which modulates the overall activity of the cortex, possibly leading to greater attention to sensory stimuli [17]. The putamen and the caudate nucleus, called the striatum, are mainly involved in motor control and the mechanism of learning, cognition, and memory. The caudate nucleus is a C-shaped structure wrapped around the thalamus, involved in reward, pleasure, addiction, fear, and the placebo effect. Globus pallidus is involved with the “extrapyramidal system” for motor control. The progressive elucidation of the anatomy of basal ganglia and the pathophysiology of motor disorders has revealed a close functional interrelationship between the two systems [13] [17].

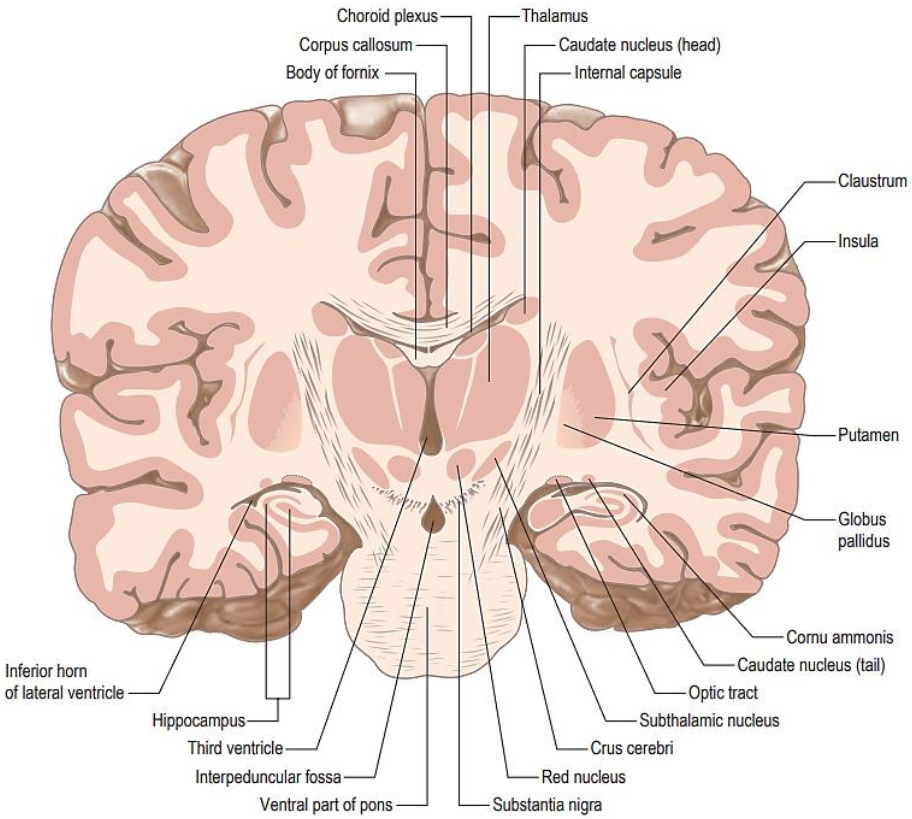

Figure 19: The principal parts of the diencephalon and Corpus callosum basal ganglia, coronal section [13].

The Diencephalon lies deep beneath the cerebrum and constitutes the walls of the third ventricle. The Pineal gland of the Epithalamus, Thalamus and Hypothalamus is collectively known as Diencephalon. All neural tracts out or into the cerebrum pass through the Diencephalon except for the olfactory pathway, which connects directly with the cerebrum. The Diencephalon is formed by four distinct longitudinal zones (to aid in remembering all the structures with the name "thalamus"), which are the epithalamus, dorsal thalamus, ventral thalamus, and Hypothalamus. The pineal gland is involved in the production of melatonin, which occurs during the night [13].

The thalamus is a large, ovoid nuclear complex in the Diencephalon. It is located below the cortex and deep within the cerebrum. It serves as a processing and distribution center, relaying and regulating information from and between the cerebral cortex, brainstem, spinal cord, and other subcortical structures, including the basal ganglia and cerebellum. The thalamus plays a crucial role in many brain functions and activities. It is involved in consciousness, circadian rhythm, memory, and sensory and motor functions. The projection to the thalamus from the cortex is precisely reciprocal; each cortical area is topographically organized to all sites in the thalamus from which it receives an input [13] [17].

The Hypothalamus is an essential organ for life, involved in a series of autonomic, endocrine, and behavioural functions maintaining wake/sleep cycles, thermoregulation, hydro electrolytic balance, reproduction, food ingestion, agonistic and sexual behaviour. Also involved in memory and emotions as part of the limbic system. Our increasing understanding of the role of the thalamus provides insights into pathological disorders of the brain. It is opening the

possibility of targeting its constituent nuclei to treat various disorders, including epilepsy, Parkinson's disease, Huntington's disease, pain, and psychiatric disorders [17].

2.5 Pyramidal / Extrapyramidal

The motor tracts can be functionally divided into two major groups; Pyramidal tracts; originate in the cerebral cortex, carrying motor fibers to the spinal cord and brainstem. They are responsible for the voluntary control of the musculature of the body and face. Extrapyramidal; originates in the brainstem, carrying motor fibers to the spinal cord. They are responsible for the involuntary and autonomic control of all musculatures, such as muscle tone, balance, posture, and locomotion. The claustrum is a thin sheet of grey matter hidden under the neocortex. ("claustrum" means in Latin "hidden away"), interconnected with all the brain areas except the auditory regions. The exact function of the claustrum is unknown [6] [12] [14] [17].

2.6 Brainstem

In vertebrate anatomy, the brainstem is the most inferior portion of the brain, situated in the posterior cranial fossa, adjoining and structurally continuous with the brain, cerebellum, and spinal cord. It gives rise to cranial nerves 3 through 12, which provide the primary motor and sensory innervation to the face and neck. Though small, it is a vital part of the brain, as damage to the brainstem is often devastating and life-threatening. The main parts of the brain that communicate with the peripheral nervous system pass through the brainstem. This includes the corticospinal tract (motor), the posterior column-medial lemniscus pathway (vibration, delicate touch, sensation, and proprioception) and the spinothalamic tract (pain, temperature, itch, and simple touch) [30] [37].

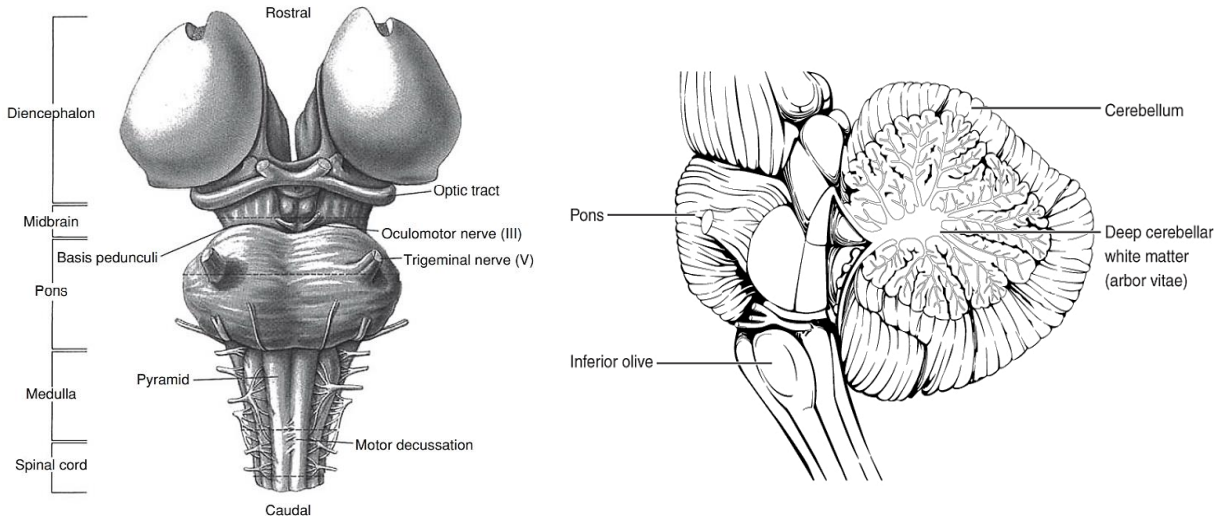

Figure 20: view of the midbrain, pons, medulla, and spinal cord; the cerebellum lies behind the pons and medulla [17] [Creative Commons Attribution 4.0]

The brainstem plays a role in regulating cardiac and respiratory functions. It regulates the CNS and is pivotal in maintaining consciousness and regulating the sleep cycle. The three components of the brainstem are the medulla oblongata, midbrain, and pons [17]. The medulla oblongata is the lower half of the brainstem, continuous with the spinal cord. The medulla

contains the cardiac, respiratory, vomiting, and vasomotor centers regulating heart rate, breathing, and blood pressure. From the medulla oblongata arise four cranial nerves:

I. Cranial nerve IX (glossopharyngeal nerve) controls swallowing, taste, and saliva production.

II. Cranial nerve X (vagus nerve) plays a role in breathing, heart function, digestion, and hormones.

III. Cranial nerve XI (accessory nerve) controls the upper back and neck muscles.

IV. Cranial nerve XII (hypoglossal nerve) controls tongue movement, speech, and swallowing [13] [20].

The midbrain is associated with vision, hearing, motor control, sleep and wake cycles, alertness, and temperature regulation. **Oculomotor & Trochlear** cranial nerves (III & IV) originate from the midbrain. Both are related to eyeball movement and Pupil sphincter control (III), which are responsible for accommodation to light.

The pons lies between the medulla oblongata and the midbrain. The pons is a structure located on the brainstem, named after the Latin word for "bridge." It contains nuclei that relay signals from the forebrain to the cerebellum, along with nuclei that deal primarily with sleep, respiration, swallowing, bladder control, hearing, equilibrium, taste, eye movement, facial expressions, facial sensation, and posture. Within the pons is the pneumotaxic center, a nucleus that regulates the change from inspiration to expiration. The pons also contains the sleep paralysis center of the brain and plays a role in generating dreams. Several cranial nerve nuclei are present in the pons [13] [17].

2.7 Cerebellum

"little brain" lies in the posterior cranial fossa, formed of two hemispheres and a midline structure called the cerebellar vermis. It has convolutions and sulci like the cerebrum. The Purkinje cells, the cerebellar output neurons, are among the giant neurons in the CNS. The cerebellum has been viewed as a motor structure involved in producing smooth, coordinated movements and in motor learning and adaptation. Responsible for comparing information from the cerebrum with sensory feedback from the periphery through the spinal cord. It is essential to fine-tune the movement details and coordinate the limbs and limb segments so that complex movements occur smoothly and automatically [12].

The cerebrum also sends information to the Thalamus, which usually communicates motor commands; this involves interactions with the cerebellum and other nuclei in the brainstem. Also, the primary output of the basal nuclei is to the Thalamus, which relays that output to the cerebral cortex [13]. Three pairs of peduncles connect the cerebellum: The inferior cerebellar peduncle, which connects mainly the cerebellum to the spinal cord. The middle cerebellar peduncle connects to the pons, and the superior cerebellar peduncle connects to the Thalamus. People with cerebellum disorders can still move, but their movements lack normal coordination; these characteristic deficits are collectively known as ataxia. [17].

Chapter 3: Background on Neurophysiology

3.1 The Neuron

Neurons are considered the basic functional computational units within the human nervous system. A single neuron consists of a dendrite, a body, an axon and axonal terminals. A neuron can be considered a leaky bag of charged liquid as a crude approximation. The neuron membrane comprises an impermeable lipid bilayer except for openings called ionic channels that selectively allow the passage of ions [37].

Neurons are structurally complex cells with long fibrous extensions specialized to receive and transmit information, conducting it over considerable distances. The neuron's cell body is only a tiny part of the neuron where the nucleus resides, termed as Soma. It gives rise to a texture of branches called dendrites, which spread out within the spinal cord to receive the bioelectric signals passed along from other neuron cells and pass them into the Soma. The axon is a thin fiber that rises from the Soma and is specialized in transmitting signals over long distances within the body, acting as a transmission path. The propagation of information within the nervous system depends on rapid electrical signals [13] [30].

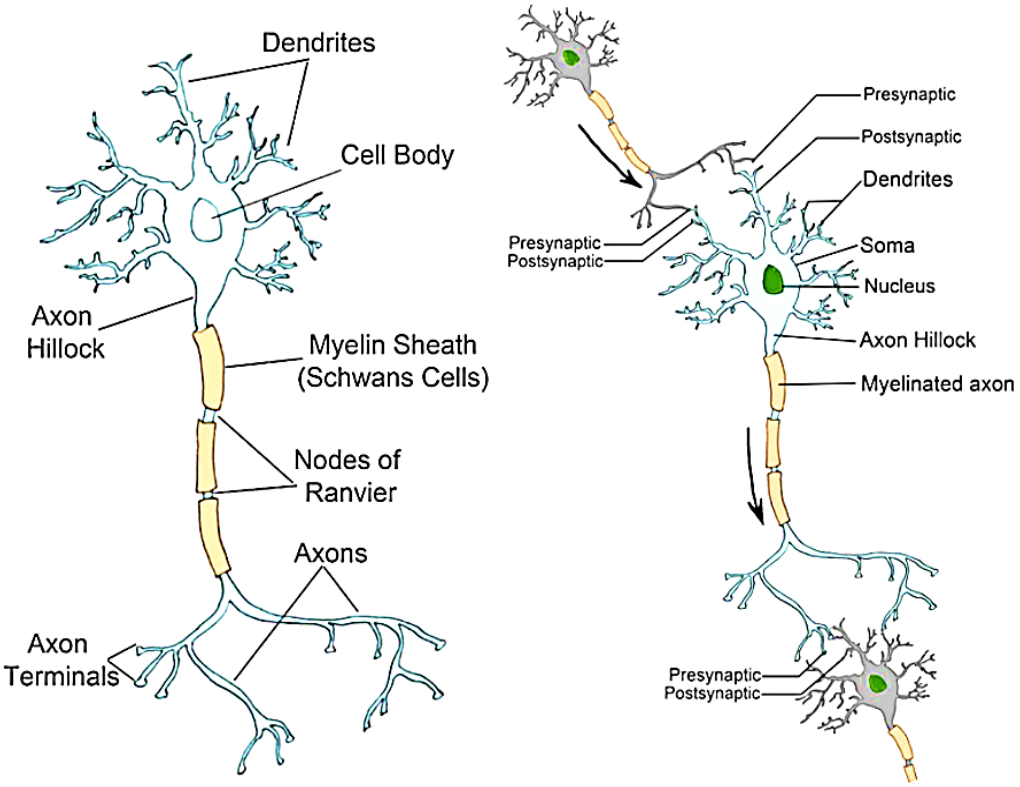

Figure 21: Although nerve cells throughout the CNS take hundreds of unique forms and shapes, most cells have standard cellular components. Shown here are the major structural features of an idealized neuron: dendrites (receiving synapses from other cells), the cell body, the axon hillock, myelination, an axon, and the axon terminals (forming synapses onto other cells) [30][37]

The action potential is a self-propagating depolarization signal that carries messages over long distances along axons in the nervous system. It is a brief (about 1 msec) explosive reversal of the neuronal membrane potential. The Resting membrane potential of a neuronal cell ranges

between -40 & -90 mV with respect to the Extracellular fluid potential, which is assigned a voltage of zero by convention. Excitation of a cell starts with an action potential that is elucidated with the influx of Na ions through gating channels into the neuronal body. Once the transmembrane potential exceeds the Threshold point (probably around -20 mV), the action potential ensues, and the cell is depolarized [30] [31].

Cations (+) and anions (−) are distributed unevenly across the neuronal cell membrane because the membrane is differentially permeable to these ions. The uneven distribution depends on the forces of charge separation and diffusion. The membrane's permeability to ions changes with depolarization (toward 0) or hyperpolarization (away from 0). The extracellular concentrations of Na+ and Cl− of 145 and 105 mEq/L, respectively, are high compared to the intracellular concentrations of 15 and 8 mEq/L. The extracellular concentration of K+ of 3.5 mEq/L is low compared to the intracellular concentration of 130 mEq/L. The resting potential of neurons is close to the equilibrium potential for K+. Na+ is actively pumped out of the cell in exchange for the inward pumping of K+ by the Na+ - K+ -ATPase membrane pump. Equivalent diagrams for Na+, K+, and Cl−are illustrated in the figure below [32].

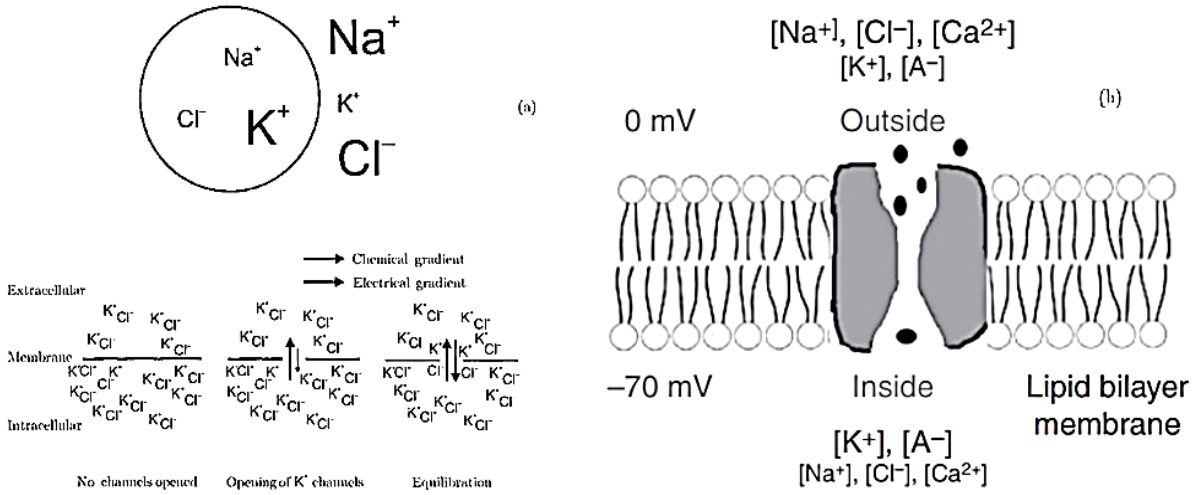

Figure 22: Intracellular and extracellular fluids Ionic concentration [30] [31].

When a cell is subjected to a stimulus, some amount of Na+ crosses the membrane; if the transmembrane potential does not reach the threshold point, the action potential is aborted; if it reaches this point, the action potential will "start". Then Na+ influx will facilitate the opening of additional Na+ channels, leading to an avalanche of Na+ influx. This fast, strongly nonlinear event will depolarize the membrane so that the inside becomes positive by about 20 millivolts as if the battery was reversed temporally.

This fast-depolarizing event is portrayed by the rising phase of the action potential (figure 23 below). At this voltage level, the process stops due to the inactivation of Na+ channels. After the depolarization has ended and propagated in the same sequence of Na+ influx across the axon, the cell will reverse to its resting state. To regain the resting voltage across the membrane more rapidly, neurons opt for another strategy: they regain charge and "reorient the ions" Voltage-dependent K+ channels are activated and quickly repolarize the cell. This fast repolarization is the falling phase of the action potential (Figure 23 below). Thus, the positive

charge created by the influx of Na+ is compensated for by the rapid efflux of equal charges carried by K+. This push-pull process, active during the action potential, takes about a millisecond (absolute refractoriness) and limits the maximum firing rate of the neuron [33] [34] [37].

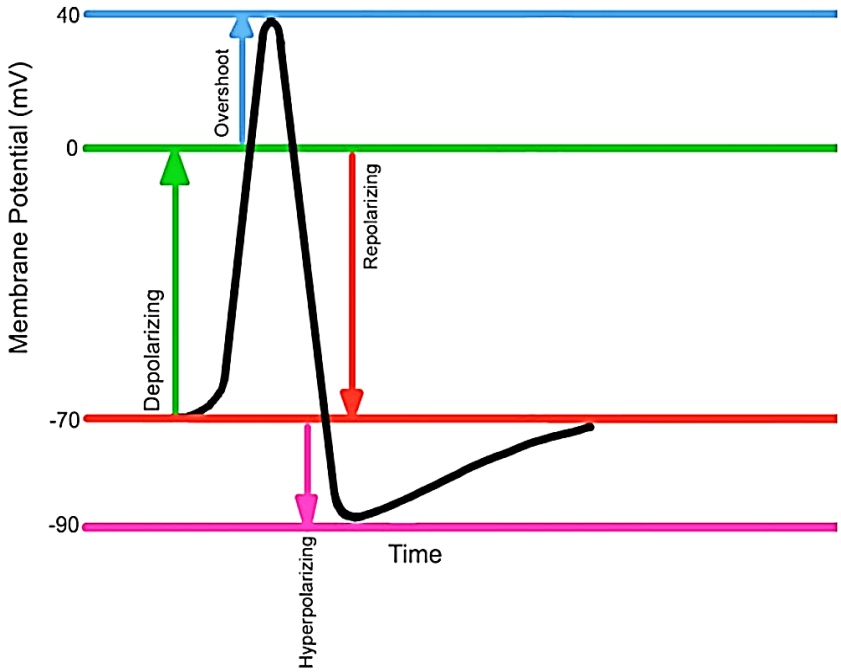

Figure 23: A general action potential waveform. Depolarization, repolarization, hyperpolarization, and overshoot changes in membrane potential are shown in relation to the resting membrane potential (horizontal red line) [30][37]

After repolarization, hyperpolarization and restoration of the resting potential, the cell is called to be in the refractory period, when further stimulation will not elucidate a new action potential. Because the action potential appeared as a short, large-amplitude event on the early chart recorders, investigators called the action potential a "spike." So, when we refer to a spiking or firing neuron, we mean that the neuron gives rise to action potentials. In contrast to the megahertz speed of computers, the speed of spike transmission by neurons is limited to a maximum of a few hundred events per second [32].

The characteristics of the action potential are:

- Action potentials are triggered by depolarization, which is a reduction in membrane potential.
- A threshold level of depolarization must be reached to trigger an action potential.
- Action potentials are (all - or - none) events.
- The amplitude of an action potential is independent of the strength of the stimulus.
- An action potential propagates without decrement throughout a neuron.
- The membrane potential reverses charge at the peak of an action potential to become positive inside.

- The absolute refractory period is brief after a neuron fires an action potential, during which it is impossible for the neuron to fire another. Typically, the membrane must be depolarized by about 10 – 20 mV in order to trigger an action potential [15] [31].

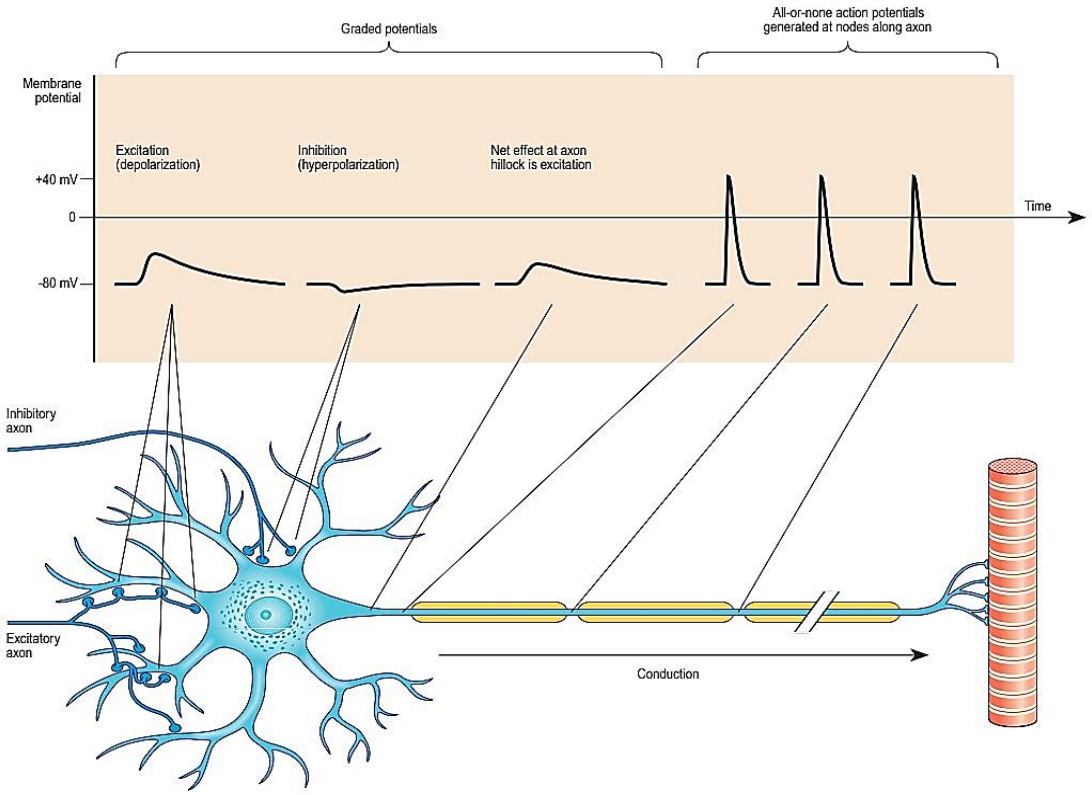

Figure 24: The types of change in electrical potential that can be recorded across the cell membrane of a motor neuron at the points indicated. Excitatory and inhibitory synapses on the surfaces of the dendrites and soma cause local graded changes of potential that summate at the axon hillock and may initiate a series of all-or-none action potentials, which in turn are conducted along the axon to the effector terminals [13].

Neurons can be divided according to the type of information they relay into:

- Afferent (sensory); these convey information from tissue and organs to CNS.
- Efferent (motor or secretory); these convey orders from CNS to peripheral tissue.
- Interneurons (processors); connect various cells within CNS to form networks.

The number ratio of these distinct types is around 1:10:200.000, respectively. Most of the neurons in the CNS are either clustered into nuclei, columns or layers or dispersed within grey matter. Neurons in the PNS are confined to the ganglia. Irrespective of location, neurons share many general features. Neurons exhibit significant variability in their size and shape. Cell bodies range from 5 to 100 µm diameter. Their surface areas are extensive because most neurons display numerous branched cell processes. Dendrites conduct electrical signals towards a soma, whereas axons conduct impulses away from it. It is worth mentioning that action potentials propagate in only a one-way direction across the neuronal cell [6] [12] [13] [14] [15].

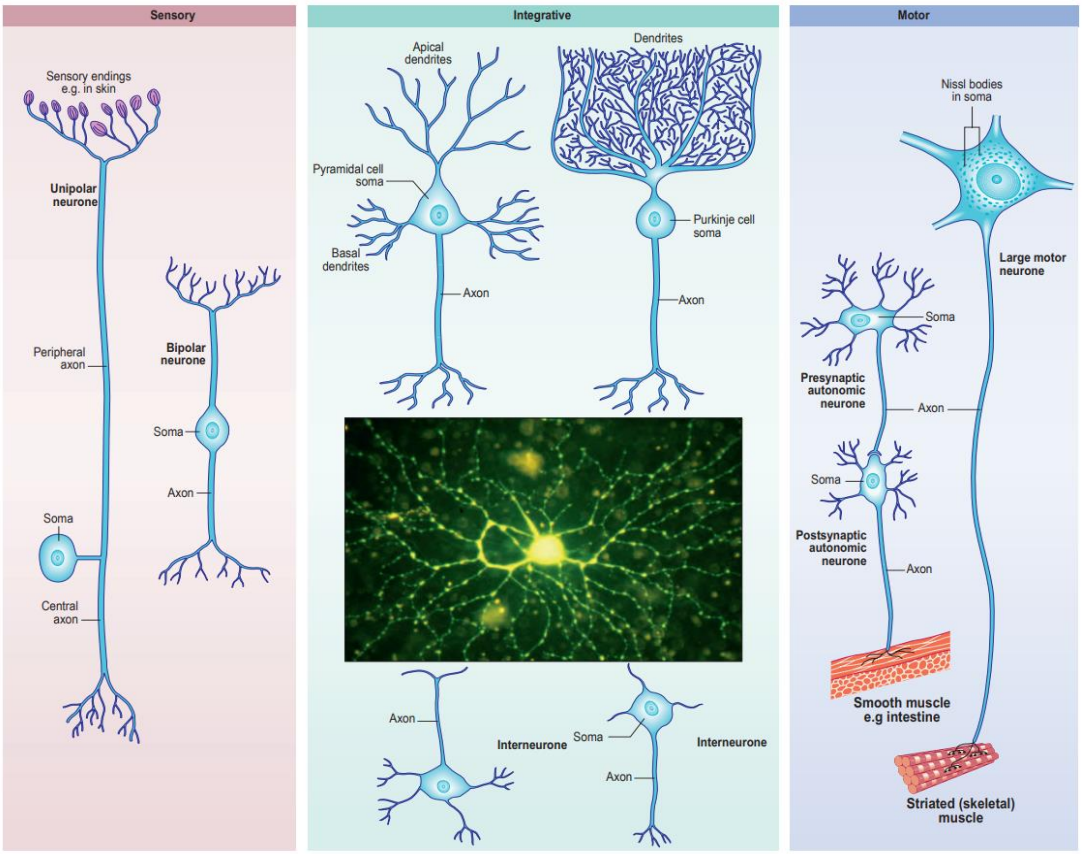

Figure 25: The variety of shapes of neurons and their processes. The inset shows a human multipolar retinal ganglion cell, filled with fluorescent dye by microinjection [13].

Besides neurons, the CNS comprises large populations of non-neuronal cells, known as neuroglia or glia cells, that are critical for maintaining cerebral tissue hemostasis, forming myelin, which plays an integral role in facilitating rapid signal transmission, providing physical and nutritional support to neurons, cleaning up brain debris, and structural scaffolding to hold neurons in place. Furthermore, though neuroglia do not generate action potentials, they convey information encoded as transient changes in the intracellular environment [13] [17].

Glia interact with neurons differently; their two-way communication is essential for regular brain activity. The glial population in the CNS consists of microglia and macroglia; the latter is subdivided into oligodendrocytes and astrocytes. The principal glial cell in the PNS is the Schwann cell. The ratio of these cells is different among different regions, but approximately it is around three glial cells per neuron in the cerebral cortex [13] [17].

3.2 Synaptic Potentials

Neurons form connections between themselves (e.g., via synapses, chemical or electrical outputs), which is the primary mechanism for information transfer within the CNS. Chemical transmission of information is widespread along CNS, e.g., dopamine in basal ganglia, serotonin in the limbic system and acetylcholine, adrenaline and noradrenaline in the autonomic system. We are focusing on electrical transmission as it is the measurable variable in EEG recordings related to our study [6] [13] [15].

In the neuron-to-neuron synapse, the presynaptic terminal is specialized to release a chemical substance, appropriately called a neurotransmitter, which then binds to specialized receptors on the postsynaptic side. All cortical pyramidal cells release glutamate, which depolarizes and discharges the target neurons; therefore, glutamate is referred to as an excitatory neurotransmitter. In contrast, GABA typically hyperpolarizes the postsynaptic resting membrane, which is why GABA's effect is called inhibitory. Neurotransmitters exert their effect by binding to receptors that reside in the membrane of the postsynaptic neuron [13] [16] [17].

3.3 Extracellular Currents

The synaptic inputs to a neuron are of two types: those that produce excitatory postsynaptic potentials (EPSPs) across the membrane of the target neuron, thereby making it easier for the target neuron to fire an action potential, and the inhibitory postsynaptic potentials (IPSPs), which act oppositely on the output neuron. EPSPs produce local membrane current sinks with corresponding distributed passive sources to preserve current conservation. IPSPs produce local membrane current sources with more distant distributed passive sinks. In addition, several other interaction mechanisms not involving action potentials have been discovered by neurophysiologists. Much of our conscious experience must involve the interaction of cortical neurons in some largely unknown manner. The cortex is also believed to be the structure that generates most of the electric potential measured on the scalp [6] [12].

Excitatory currents flow inward and outward into and away from the neuronal cell. The passive outward current far away from the synapse is a return current. Inhibitory loop currents flow in the opposite direction. The current flowing across the external resistance of the extra-neuronal space sums with the loop currents of neighboring neurons to constitute the local mean field or local field potential [6] [35] [36].

The low resistance or "shunting" effect of the extracellular fluid, the membranes of neurons, glia, and blood vessels, and the slow movement of ions attenuate current propagation in the extra-neuronal space. Passive neuron acts as a capacitive low-pass filter; this attenuation is quite discriminative: it affects fast-rising events, such as the extracellular spikes, much more than slowly undulating voltages. As a result, the effects of postsynaptic potentials can propagate much farther in the extracellular space than spikes do. Furthermore, because of their longer duration, EPSPs and IPSPs have a much higher chance of occurring in a temporally overlapping manner than the very brief action potentials. Finally, EPSPs and IPSPs are displayed by many more neurons than spikes because only a minority of neurons reach the spike threshold at any instant in time. For these reasons, the contribution of action potentials to the local field, especially to the scalp EEG, is negligible. In short, extracellular fields arise because the slow EPSPs and IPSPs allow for the temporal summation of currents of relatively synchronously activated neurons [6] [12].

The current flow between two sites can be calculated from the voltage difference and resistance using Ohm's law. The *current density* is the difference between these currents, which is a vector, reflecting the rate of current flow in a given direction through the unit surface or volume

(measured in amperes per square meter for a surface and amperes per cubic meter for a volume) [6] [12].

Current density is the current entering a volume of extracellular space divided by the volume. Current density on the scalp (a measure of the volume conduction of current generated by the neurons through the skull) is sensitive mainly to superficial sources and insensitive to deep current sources in the brain. Scalp current density is the spatial derivative of current flowing into and through the scalp. Current density depends on both the electric field strength and the conductivity (σ) of the brain. Conductance is a factor of both conductivity and the shape of the volume. Conductivity is inversely proportional to resistivity. The average resistivity of white matter is ~ 700 Ω. cm, and grey matter's is ~ 300 Ω.cm. The proportion of fibers, therefore, significantly affects tissue resistivity [12].

The source localization problem or the "inverse problem" is the task of recovering the elements and location of the neural field generators based on the spatially averaged activity detected by the scalp electrodes does not have a unique solution. The difficulty of source localization has to do with the low resistivity of neuronal tissue to electrical current flow, the capacitive currents produced by the lipid cell membranes, and the distorting and attenuating effects of glia, blood vessels, pia, dura, skull, scalp muscles, and skin. As a result, the EEG, recorded by a single electrode, is a spatially smoothed version of the local field potentials under a scalp surface and, under most conditions, has little discernible relationship with the specific patterns of activity of the neurons that generate it [6] [12].

The spatiotemporal integration problem of neuronal activity is similar to the statistical mechanics of physics in that the typical average behaviour replaces the specific details of the neuronal interactions. The EEG recorded from the scalp samples mostly the synaptic activity that occurs in the superficial layers of the cortex. The contribution of deeper layers is scaled down substantially, whereas the contribution of neuronal activity from below the cortex, in most cases, is virtually negligible. This "fish-eye lens" scaling feature of the scalp EEG is the major theoretical limitation for improving its spatial resolution [6] [12].

3.4 Divergence & Convergence.

Transported information “diverges” to multiple brain regions to have a global impact or “converge” on a single cell or group of similar cells (e.g., nuclei or ganglion) to activate or inhibit a given neural function. Divergence of neural information can occur via axon collaterals, which make such information accessible simultaneously to various parts of the CNS. For example, arousal from sleep results from a significant divergence of neuronal excitation arising from the Reticular activating system (RAS) to the rest of the brain. While in convergence, thousands of axon collaterals can converge onto the cell body of a single neuron. Convergence allows a neuron to process or integrate incoming excitatory and inhibitory signals occurring at its membrane within a short period of time (msec) [13] [17].

Chapter 4: EEG and Brain-Computer Interfaces (BCIs)

4.1 The electroencephalogram (EEG)

The ionic currents traverse the cell membrane of neurons and give rise to biopotentials. These electrical signals can be recorded with specialized instrumentation to assess physiological function, conducting neuroscience research, and even provide a novel communication medium through brain-computer interfaces (BCIs) [6] [12] [17].

Electrical recordings from the head's outer surface demonstrate continuous electrical activities within various underlying cortex regions. Both the intensities and patterns of these electrical activities are significantly determined by the overall levels of regional excitations, in other words, changes in the brain's electrical fields [2] [6] [38].

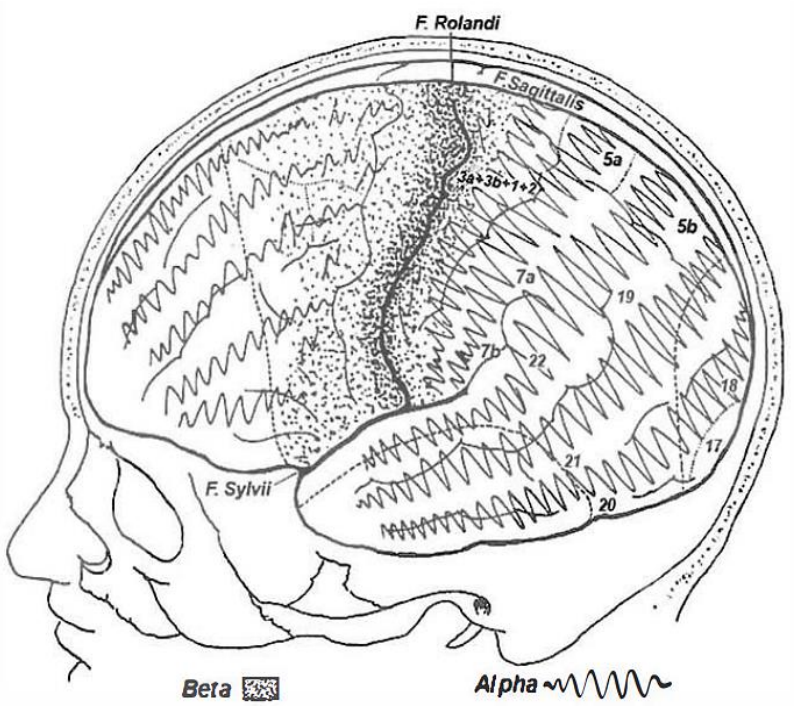

Figure 26: Cortical surface regions where alpha rhythms were recorded in a large population of epilepsy surgery patients arc indicated by wavy lines. Dotted region near the central motor strip indicates beta activity. From Nunez adapted from Jasper and Penfield (1949) [12].

The EEG is a dynamic non-invasive, relatively inexpensive technique used to monitor the state of the brain. Despite the tremendous progress in structural and functional brain imaging over the last decades, scalp EEG has remained an indispensable diagnostic tool for studying physiologic and pathologic cerebral activity. An EEG is simply a record of the brain's electrical activities, recorded as a set of surface potentials by placing electrodes on the scalp [36] [39].

Neuroscientists have always longed for a method with a sufficient spatial and temporal resolution to monitor the ever-changing patterns of brain activity. The definition of "sufficient" in this context is a complex issue, and to acquire precisely a brain activity without seriously interfering with it while compromising between spatial and temporal resolution, is indeed a dilemma [6] [12]. The desired temporal resolution is the concordance of the wave with the

speed of neurons, that is, on the millisecond scale. The desired spatial resolution, which means better localization of the source of any specific signal, depends on the goal of the investigation and expands from the global scale of the brain down to the spines of individual neurons. No current method can continuously zoom from the decimeter to the micrometer scale, which is why several approaches are being used, often in combination [6] [12].

EEG activity is a non-stationary, non-linear, non-deterministic, non-Gaussian, stochastic, and chaotic process. EEG signals have a high temporal resolution, poor spatial resolution, and discriminative spectral features. Data acquisition is affected by the skin-electrode interface, electrode material, configuration, and reference, in addition to motion artifacts like EMG, EOG, ECG, swallowing, breathing, power line interference, cross talk, volume conduction, posture, state, mood of the subject and else more of intrinsic and extrinsic sources of artifacts. [32] [35] [37] [39].

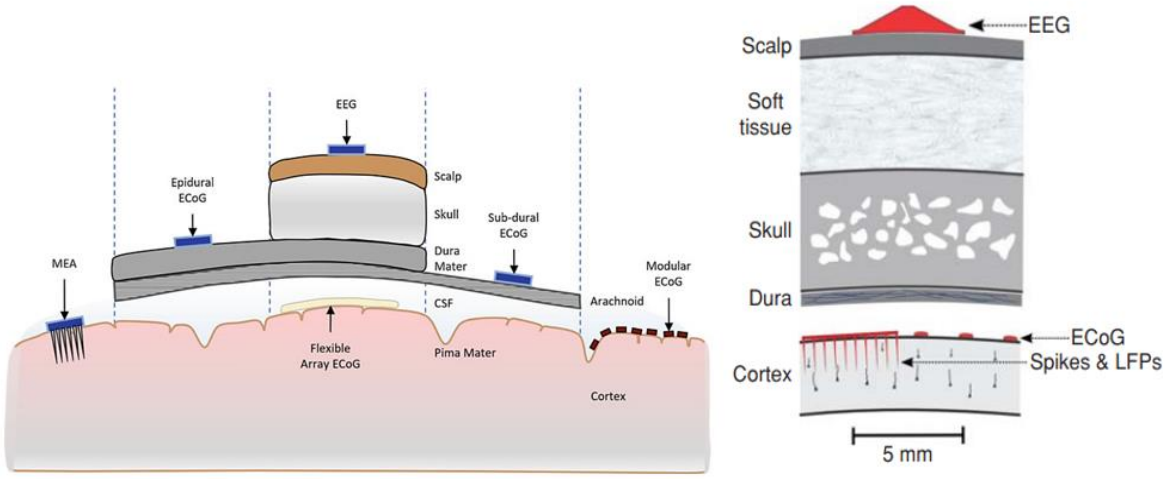

Figure 27: Scalp measurements vs ECoG and MEA recordings (The degree of invasiveness vs spatial resolution and localized measurements) [17].

These characteristics of scalp EEG depend not only on the nature and location of the current sources but also on the electrical and geometrical properties of the brain, skull, and scalp. The connection between surface and depth events is thus intimately dependent on the physics of electric field behaviour in biological tissue. Physical principles directly apply to neural tissue; we only need to interpret variables and consider tissue properties to provide a good picture of head volume conduction and how it relates to broader issues concerning EEG, brain dynamics, cell assemblies, cognition, motor and behaviour [6] [12].

As mentioned, an EEG can be recorded as a set of surface potentials by placing electrodes on the scalp. In a recording application, the electrode couples galvanically to capture the local field potential. The dimensions, geometry, and composition are paramount to design requirements. Signal degradation due to inferior electrode design or placement is unlikely to be ameliorated by design improvements in blocks further down the signal chain, thus avoiding garbage-in garbage-out (GIGO) scenarios that give inaccurate data or unreliable results. Both conductive-gel and sponge-saline electrode systems (wet electrodes) are used. The sponge-saline electrodes are easier to apply but have limited recording time (about an hour) because

impedances rise as the sponges dry. Dry electrode technology is also now available. The electrodes themselves are usually metallic and made from tin (Sn), silver/silver chloride (Ag/AgCl), gold (Au), or platinum (Pt) [35] [36].

Any voltage measurement requires both a recording electrode and a reference electrode. EEG practitioners have long been perplexed about finding a proper reference electrode for EEG recordings. Reference recordings involve choosing some fixed location, typically an ear, mastoid, or neck site, and recording all potentials with respect to this static site. The number of electrodes applied varies between 8 to 256. Increasing the number of recording sites is valid only up to a limit because scalp electrodes placed too close together will sense the same electrical fields without further enhancing spatial resolution [6] [37].

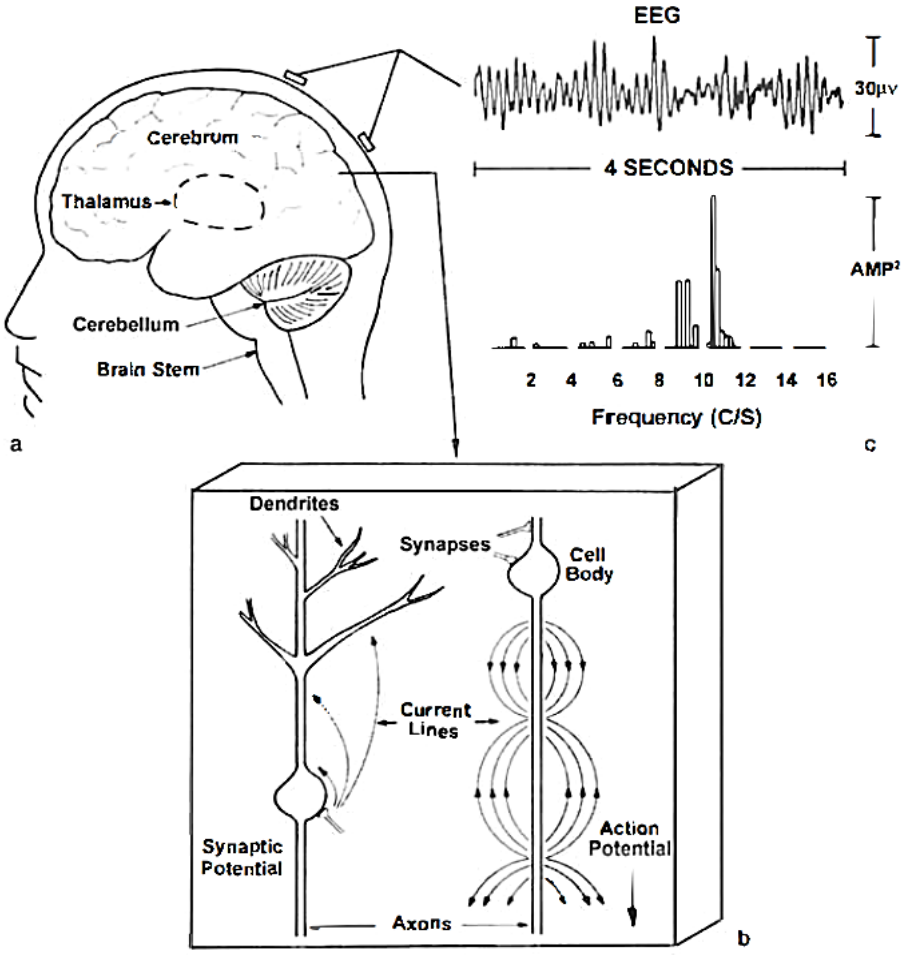

Figure 28: The human brain. (b) Section of cerebral cortex showing microcurrent sources due to synaptic and action potentials. (c) Each scalp EEG electrode records space averages over many square centimeters of cortical sources. A four-second epoch of alpha rhythm and its corresponding power amplitude [12].

The monitored signals range between 0 and 300 μV, and their frequencies range from 0.5 to approximately 50 Hz. The characteristics of the recorded waves, and the EEG patterns, are (after subtraction of artifacts) highly dependent on the degree of activities within the cerebral cortex. The features of these waves change markedly between states of wakefulness, sleep, and coma [35]. Even in a healthy individual, EEG patterns are often irregular, but distinct patterns do appear under certain conditions [15] [35].

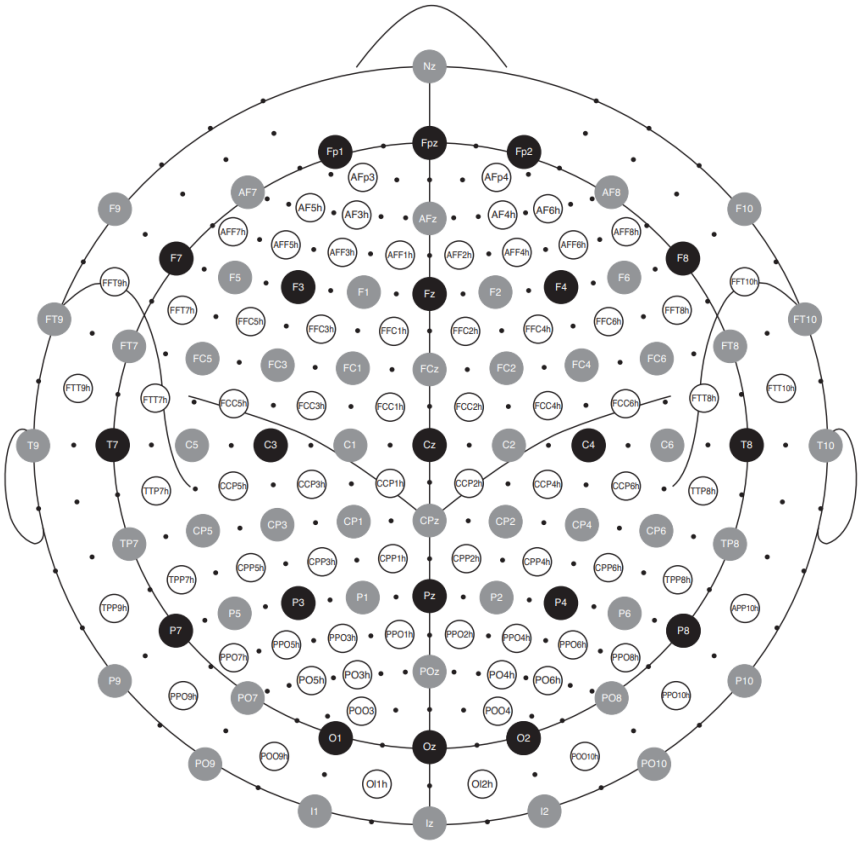

Figure 29: The standard 10–20 montage indicated by the 21 electrodes in black circles. The 10–10 montage consists of the 21 electrodes of the 10–20 montage (black circles) plus 53 additional electrodes indicated in grey. The black dots and the open circles indicate the different electrodes of the 10–5 montage. Note that electrodes on the right side have even numbers, electrodes on the left side have odd numbers, and electrodes along the midline are indicated by z. [17]

The principal waveforms recorded in the EEG are:

I. **Delta** rhythm: < 3.5 Hz originates solely within the cortex, frontal and central location; these typically occur during deep sleep, infancy, and severe organic brain disease (throughout the cortex). Not prominent in wakefulness, generalized in a coma or toxic state.

II. **Theta** rhythm: 4-7 Hz elicited during emotional stress, disappointment, and frustration associated with the parietal and temporal lobe's central location, constant but not prominent when awake and active, and sometimes generalized when drowsy.

III. **Alpha** rhythm: 8-13 Hz, during quiet wakefulness, rested state. Predominant activity in adults in resting state with eyes closed. Rhythmic waves are often recorded from the occipital region and sometimes from the parietal and frontal areas. Occur during consciousness and are attenuated by visual and other sensory stimuli. The waves tend to disappear in sleeping or attentive patients. A sub-band of Alpha, the mu-band (10–13 Hz), is affected by imagery, such as imagined limb movements. It has the same range as an Alpha but is associated mainly with the motor cortex and focused over the premotor and sensorimotor cortex. The mu-band modulation is used in building brain-machine interfaces for prosthesis control. Normal resting alpha rhythms may be substantially reduced in amplitude by eye-opening, drowsiness, and, in many subjects,

moderate to complex mental tasks. Like most EEG phenomena, Alpha rhythms exhibit an inverse relationship between amplitude and frequency. For example, hyperventilation and some drugs like alcohol may cause a reduction of Alpha frequencies together with increased amplitudes [12] [17].

IV. **Beta** rhythm: 14–25 Hz; Mainly recorded from parietal and frontal cortical regions. Activation patterns of CNS typically occur when a person is under tension, prominent in wakefulness, seen in light sleep, and intense mental activity, stress, anxiety or tension.

V. **Gamma** rhythm: >30 Hz; The gamma rhythm is associated with the active information processing state of the cortex. This rhythm can be observed during finger movements with an electrode at the sensorimotor area connected to a high-sensitivity recording device. These qualitative labels are often applied based only on visual inspection or by counting zero crossings. They must be carefully used because actual EEG is composed of a mixture of multiple frequency components, as revealed more clearly by spectral analysis [6] [38].

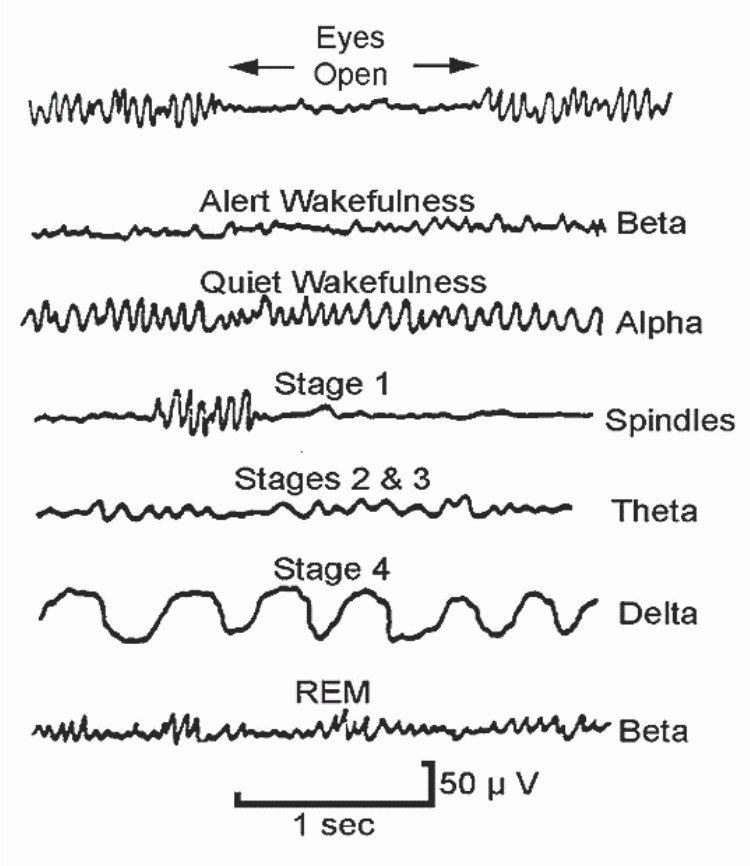

Figure 30: EEG Frequency Bands [37].

4.2 Survey of EEG applications

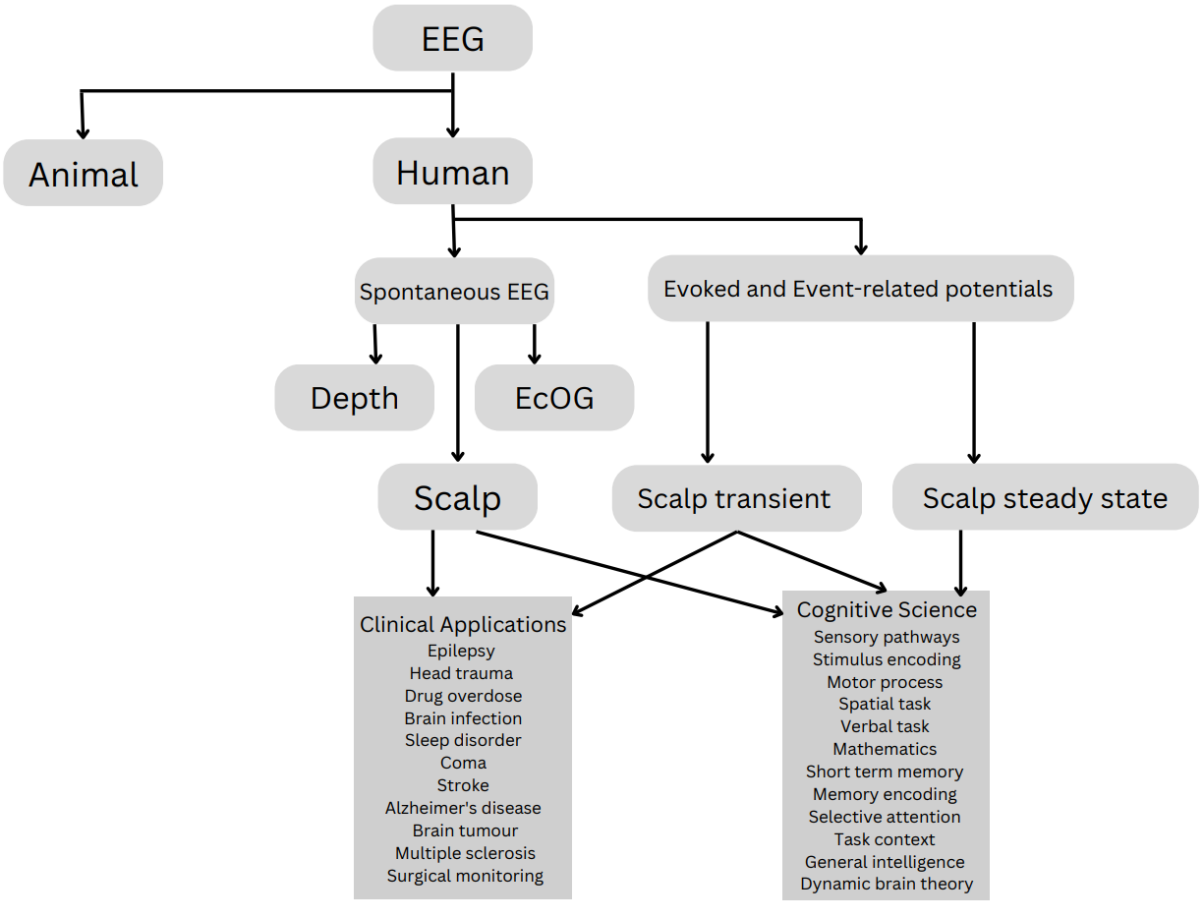

Figure 31: Survey of EEG applications. adapted from Nunez [12]

Survey of EEG Applications in research and clinical diagnosis:

- Epilepsy Monitoring: The EEG can confirm the diagnosis of epilepsy and, depending on the particular pattern of seizure, define the evident seizure type, localize seizure origin and assist in experimental cortical excision of the epileptic focus.
- Sleep Studies: In relaxation or drowsiness, alpha activity rises; if the subject sleeps, the power of lower frequency bands increases. The area of sleep studies is one of the success stories of EEG. Sleep staging is very clearly reflected in a very reactive EEG. Sleep is categorized into two broad types: Non-Rapid Eye Movement (NREM) sleep and Rapid Eye Movement (REM) sleep. NREM and REM occur in alternating cycles; NREM is further divided into stages I, II, III, and IV. The last two stages correspond to deeper sleep, where slow delta waves are shown in higher proportions. With these slower dominant frequencies, responsiveness to stimuli decreases, and so these are indicative of deep sleep. Stage I sleep is typified by slowing disintegration into varying or increasing irregularities. Thus, EEG monitoring finds extensive use in investigating sleep disorders and physiology [2] [6].

- Brain-Computer Interface (BCI): As the EEG procedure is noninvasive and painless, it is widely used to study the brain organization of cognitive processes such as perception, memory, attention, language, and emotion in normal adults and children. The BCI is a communication system that only recognizes a user's commands from their brainwaves and reacts according to them. Simple tasks can consist of desired motion of a cursor, or a pointer displayed on the screen only through the subject's imaging of the movement of his hand. As a consequence of the imaging process, specific characteristics of the brain waves are altered and, thus, recorded so a computer can use them for the user's command recognition, e.g., desynchronizing the motor-associated *mu waves* or altering specific event-related potentials (ERPs) [15] [17] [35] [47] [51].
- EEG Biofeedback: Biofeedback machines create different mind states (e.g., relaxation, top performance) by practically manipulating the brain waves into desired frequency bands through repetitive visual and audio stimuli. Signal analysis methods are needed to interpret the rhythms.
- Monitoring alertness, coma, and cerebral death.
- Locating areas of damage following head injury, stroke, and tumor.
- Testing afferent pathways (by evoked potentials).
- Monitoring cognitive engagement (alpha rhythm).
- Controlling anesthesia depth (servo anesthesia).
- Testing drugs for convulsive effects.
- Investigating mental disorders.
- Providing a hybrid data recording system together with other imaging modalities [2] [35].

4.3 Recordings from Single Neurons In Vitro

Neurons are complex devices. Understanding the biophysical properties of individual neurons would significantly enhance understanding of their collective behaviour in networks. Characterization of individual neurons is especially critical in brain regions built from various neuron types. Most of our knowledge about the biophysical properties of neurons is derived from experiments carried out in brain slice preparations in vitro [6]. Although the brain slice method compromises brain circuits, it provides unprecedented spatial resolution, precision, and pharmacological specificity for the examination of the biophysical and molecular properties of the cell membrane. Brain slices allow recording from local neural circuits [6] [12] [13].

4.4 EEG and Local Field Potential Recording Methods (Depth Electrode (ECoG) and Subdural Grid Recordings)

The local field potential (i.e., local mean field), recorded at any given site in or outside the brain, reflects the linear sum of numerous overlapping fields generated by current sources and sinks distributed along multiple cells. Local field potentials are usually recorded by small-sized

electrodes, e.g., a wire tip placed in the depth of the brain. They reflect the transmembrane activity of neurons in a more confined space than the scalp EEG. By definition, local field potential and EEG are synonymous terms, but for historical reasons, EEG usually refers to scalp-recording field potentials [6] [40].

Depending on the size and placement of the electrode, the volume of neurons that contributes to the measured signal varies substantially. With very fine electrodes, activity recorded by electrodes placed directly on the brain surface is called an electrocorticogram (ECoG). The local field potential reflects the synaptic activity of tens to thousands of nearby neurons. If the electrode is small enough and placed close to the cell bodies of neurons, extracellular spikes can also be recorded. Therefore, in such a small volume of neuronal tissue, one often finds a statistical relationship between local field potentials, reflecting mainly input signals (EPSPs and IPSPs) and the spike outputs of neurons. However, the reliability of such a relationship progressively decreases with increasing the electrode size by lumping together electric fields from increasingly larger numbers of neurons [12]. This is why the scalp EEG, a spatially smoothed version of the local field potential at numerous contiguous sites, has a relatively poor relationship with the spiking activity of individual neurons. However, this is not the case under epileptic conditions when neurons can synchronize within the duration of action potentials. The synchronously discharging neurons create local fields, known as compound or "population" spikes [6] [40] [12].

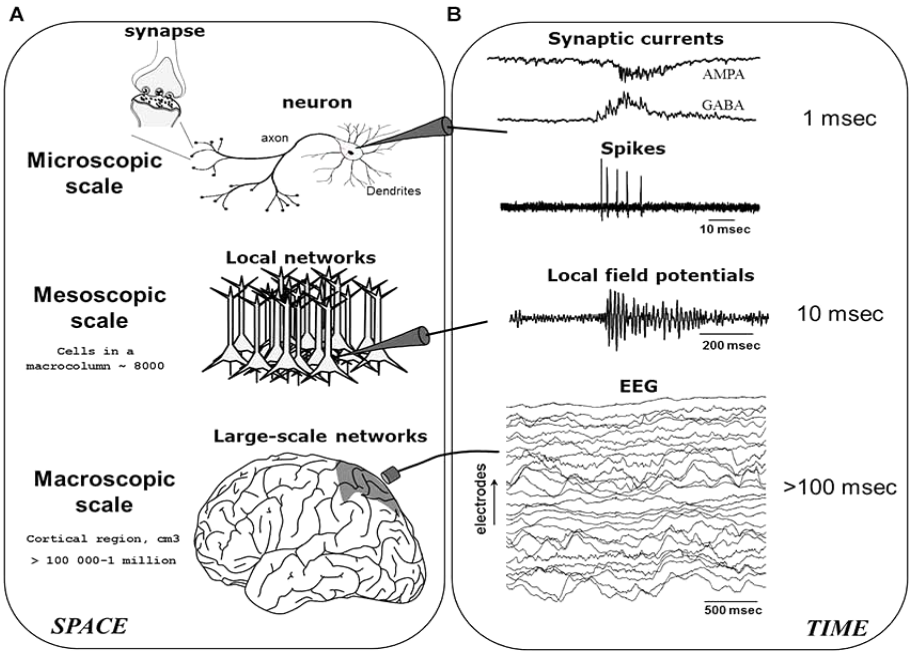

Figure 32: The generation of electroencephalogram (EEG) network oscillations. EEG signals are generated by the integration of neural activity at multiple spatial (A) and temporal (B) scales [41].

The subdural grid electrode is a less invasive approach that yields localization effectiveness somewhere between scalp recording and intracerebral electrodes. The grid, a flexible strip with 20–64 rectangularly arranged electrodes, is introduced subdurally. Although inserting the grid by removing a bone flap in the skull and placing it on the cortical surface requires surgery, its implantation and removal are less invasive and less risky than deep wire electrodes [42] [42].

Electrocorticography (ECoG) is a related modality to EEG, which measures brain biopotentials directly on the surface of the cerebral cortex. Although surgically invasive, the decreased distance from the neural sources allows ECoG to distinguish faster and smaller nuclei of brain activity at higher spatial and temporal resolutions [6] [42]. The amplitude of the ECoG recorded by the grid electrodes is larger than that of the scalp EEG and has a broader frequency bandwidth and higher signal-to-noise ratio. The signals provide better spatial localization because the electrodes integrate activity from a smaller brain area and are essentially free of muscle, eye movement, and other artifacts ubiquitously present in the scalp EEG. Although these are superior features, the invasive grid electrode recording technique cannot be used for research in healthy humans because of ethical considerations. Fortunately, another method can noninvasively increase the spatial resolution while keeping the advantage of the outstanding temporal resolution of the EEG. This technique monitors the brain's magnetic rather than electric fields [43] [44].

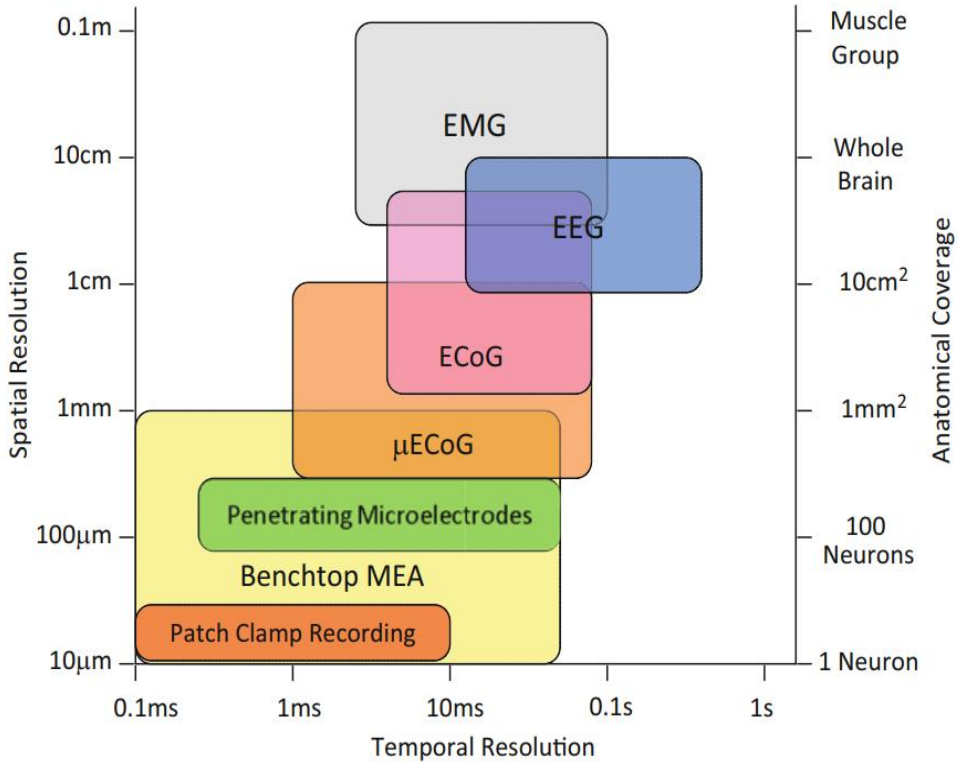

Figure 33: Spatiotemporal characteristics of neural biopotential signals [37]

4.5 Magnetoencephalography (MEG)

Electricity needs a conductor to propagate; as air is a poor conductor, brain currents do not go beyond the scalp. However, the voltage changes created by neuronal cells accompany magnetic field changes. These electromagnetic currents also can be detected and recorded. The magnetic fields that emanate from the brain are only one hundred million to one billionth of the strength of Earth's magnetic field (or < 0.5 Pico tesla). The sensor detecting such weak signals is a SQUID (superconducting quantum interference device). This device operates at–270°C; helium is required in the SQUID to chill the coils to superconducting temperatures. In essence, it consists of a superconductive loop. The SQUID MEG recording requires a laboratory setting.

A modern MEG system is equipped with up to ~300 gradiometers evenly distributed in a helmet shape with an average distance between sensors of 1~2 cm. The detector coils are placed as close to each other as possible, forming a spherical honeycomb-like pattern concentric with the head. This helmet structure is also necessary to provide shielding from external magnetic signals, including the Earth's magnetic field [6] [17] [45].

A practical advantage of MEG is that no electrodes need to be attached to the scalp because the magnetic field emerges from the brain through the skull without distortion. In contrast to the EEG, the MEG signal reflects predominantly intracellular currents. For this reason, MEG and EEG see different types of activity. The spatial resolution of MEG is better than that of the EEG (ideally less than a centimeter), mainly because, in contrast to the EEG, the magnetic fields are not scattered and distorted by inhomogeneities of the skull and scalp. Nevertheless, this technology is still under development as the instrumentation necessary is more sophisticated and expensive. MEG source localization still needs to be more accurate; even under ideal conditions, the improved spatial resolution of MEG is insufficient to obtain information about local circuits and layer-differential effects in the cortex or neuronal spikes [45] [46].

4.6 Functional Magnetic Resonance Imaging (fMRI)

The method is based on detecting and analysing magnetic resonance energy from specific points in a tissue volume. The MRI technique provides far better images than other scanning technologies. Traditional MRI is based on the behaviour of Hydrogen atoms of water, which can align in an orderly way when placed inside a strong magnetic field. In practice, a short pulse of RF energy perturbs these tiny magnets from their preferred alignment. As they return to their original position, they give off small amounts of energy that can be detected and amplified with a "receiver coil" placed directly around the head [17] [47].

Because grey matter and white matter contain different amounts of water, this difference generates a contrast between the surface of the neocortex and the underlying white matter and other areas of the brain that can be used to provide a detailed image of the brain. However, while the MRI method offers exquisite details about the brain's structure, even for deep structures like the amygdala, it does not tell us anything about neuronal activity [15].

As previously mentioned, active neurons consume a lot of energy. In areas with high neuronal activity, this results in a significant difference between the concentration of the oxygenated haemoglobin in the arterial blood and the deoxygenated haemoglobin in the venous outflow. The BOLD (Blood Oxygenation Level Dependent) method can assess these local magnetic field inhomogeneities. When neurons are activated, increases in blood flow are associated with increases in local glucose metabolism and oxygen consumption, so the changes in local deoxyhemoglobin concentration are reflected in the brightness of the MRI image voxels at each time point, hence, (fMRI), which uses the BOLD method, can measure neuronal activity indirectly [6] [12] [49].

Nevertheless, as with any technique, fMRI has its limitations. The first limitation concerns the general statement that "fMRI measures neuronal activity." Neuronal activity has numerous

components, including intrinsic oscillations, EPSPs, IPSPs in principal cells and inhibitory interneurons, action potential generation and propagation along the axon, and release, binding, reuptake, and reprocessing of the released neurotransmitters. Which of these processes, alone or in combination, are responsible for the changes in BOLD has yet to be worked out. Alternatively, different cognitive operations in the same structures can be generated with the same amount of energy, with no expected change in BOLD. This reverse engineering problem is, of course, identical to that of the EEG and MEG. Thus, except for the significantly improved spatial resolution, one cannot expect more from fMRI than from EEG measurements [6] [12].

Another technical drawback of fMRI is its slow temporal resolution. The blood-flow response is delayed about half a second after neuronal activation, and the second-scale temporal resolution of the BOLD imaging method is excessively long for assessing the spatiotemporal evolution of neuronal activity across brain domains. This could affect the usefulness of fMRI in many BCI applications [12] [17] [47].

4.7 Positron Emission Tomography (PET)

Another essential research tool for visualizing brain function is positron emission tomography (PET). A significant advantage of PET is that it provides information about the use and binding of specific chemicals, drugs, and neurotransmitters in the brain. To obtain a PET scan, the subject either inhales or receives an injection of a minimal amount of a radiolabeled compound, which then accumulates in the brain. As the radioactive atoms in the compound decay, they release positively charged positrons. When a positron collides with a negatively charged electron, they are annihilated, and two photons are emitted. The photons move in opposite directions and are detected by the sensor ring of the PET scanner. Reconstruction of the three-dimensional paths of the particles provides information about the maximum accumulation or metabolism of the radiolabeled isotope. PET's spatial and temporal resolutions are inferior to fMRI [6] [12].

Let us pause here to add a few essential details regarding these advanced imaging methods. A single MEG, PET, or fMRI device weighs several tons. They are also impractical for examining behaviour-generated brain changes in the most frequently used small laboratory animals, such as rats and mice. More importantly, even the combined, simultaneous application of these methods must be revised to explain how neurons and neuronal assemblies make sense of the world and create appropriate responses in a changing environment. In the brain, specific behaviours emerge from the interaction of neurons and neuronal pools [6].

4.8 Functional near-infrared spectroscopy (fNIRS)

Functional near-infrared spectroscopy (fNIRS) is another noninvasive technique. It utilizes light in the near-infrared range (700 to 1000 nm) to determine localized cortical regions' oxygenation, blood flow, and metabolic status. It is like BOLD fMRI in terms of imaging contrast; it measures the hemodynamic response. It can produce relatively well-localized signals with a spatial resolution in centimeters and provides information related to neural activity. However, since the images rely on shallow-penetrating photons, NIRS operates effectively only for brain structures on or near the brain surface. NIRS is also inherently limited

in its imaging contrast, which results in a temporal resolution on the order of seconds and a delay of several seconds for feedback [2] [6] [17].

4.9 Brain Computer Interfaces (BCIs)

A BCI system measures CNS activity and converts it into artificial output that replaces, restores, enhances, supplements, or improves natural CNS output [17]. BCIs have emerged as a novel technology that connects and bridges the brain with external devices. They have been developed to decode human intention, leading to direct brain control of a computer or device without going through the natural neuromuscular pathway [47]. The central goal of BCI research and development is for people severely disabled by neuromuscular disorders such as amyotrophic lateral sclerosis (ALS), stroke, spinal cord injury, cerebral palsy, multiple sclerosis, and muscular dystrophies to live enjoyable and productive lives if they can be provided with effective assistive technology [17] [51].

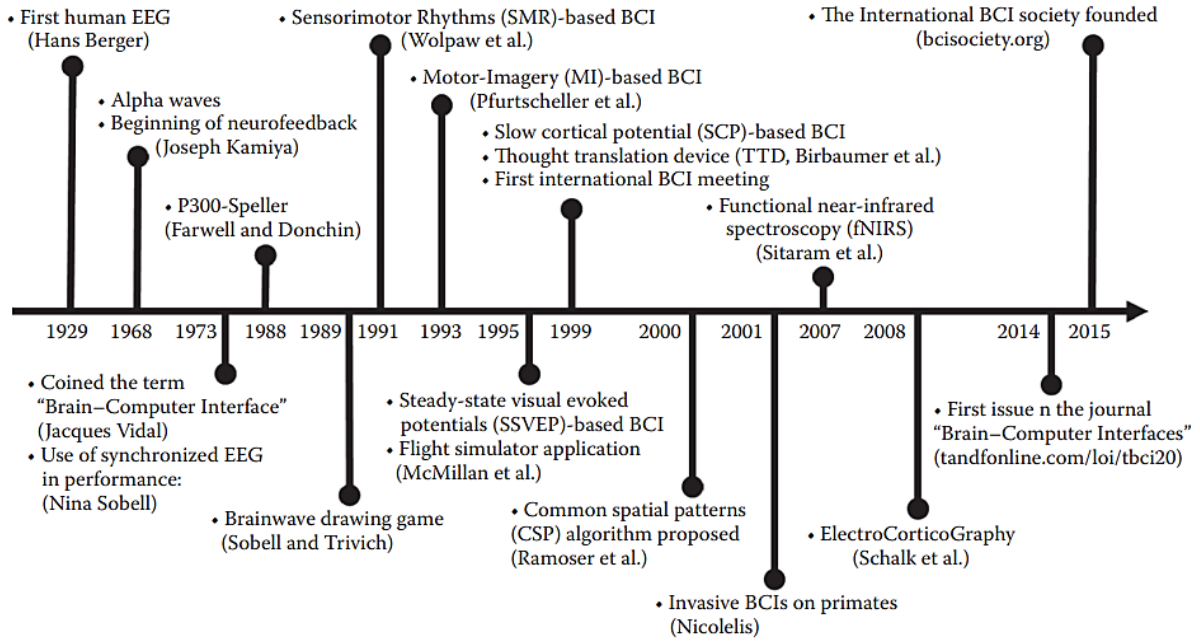

Figure 34: Historical events towards BCI technology [51] [51]

In the 1960s, electroencephalographers' interest in academic institutions shifted from tracing, with all its waves and patterns, to automatic data analysis. Computerization was the direction, with tendencies reaching back to Berger's coworker Dietsch in 1932. However, it only flourished in the 1960s and 1970s. Cooley and Tukey (1965) have been credited with introducing the fast Fourier transforms (FFT) as the basis of power spectral analysis. This work led us into a "brave new world" of EEG computerization, but the automatization of EEG reading was fictional. It was found that EEG is far too complex for such automation; even automatic spike detection had barely reached its earliest stage [2] [6] [12].

The first demonstrations of BCI technology occurred in the 1960s when Grey Walter used the scalp-recorded EEG to control a slide projector in 1964. In the 1970s, Jacques Vidal developed a system that used the scalp-recorded visual evoked potential (VEP) to determine the eye gaze direction (i.e., the visual fixation point) in humans and thus to determine the direction in which

a person wanted to move a computer cursor. At that time, Vidal coined the term brain-computer interface. The pace and breadth of BCI research began to increase rapidly in the mid-1990s, and this growth has continued almost exponentially into the present. In BCIs that measure EEG Sensorimotor Rhythms (SMR), the user typically employs mental imagery to modulate SMR to produce the BCI output [17] [47] [48].

In 1988, Farwell and Donchin proposed the successful BCI paradigm known as the "P300 speller", based on event-related potentials (ERP) in response to a specific event or stimulus [49] [54]. Wolpaw and his colleagues developed a BCI for 1D cursor control based on operant conditioning in 1991 [50] [55]. Gert Pfurtscheller and his team were developing another BCI-based SMR, in which users had to explicitly imagine left or right-hand movements that were translated into a command for the computer by using machine learning; this defined the motor imagery (MI)–based BCIs [56] [57]. Niels Birbaumer and his colleagues worked on a third type of BCI paradigm based on slow cortical potential (SCP) [47] [51]. SCP is caused by shifts in the dendritic depolarization levels of pyramidal neurons in the cortex. Negative SCP generally reflects cortical activation, while positive SCP reflects reduced activation. Yet, Brendan Allison and others have lately rejected this type owing to generally inferior performances [59] [60].

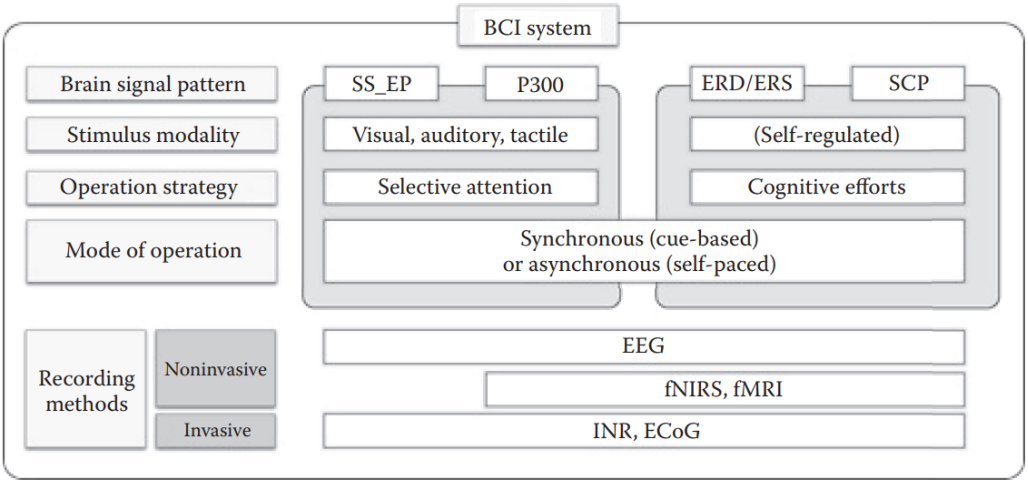

Figure 35: Classification of BCI systems [47].

In general, BCI systems can be categorized as either [(invasive vs non-invasive) (endogenous vs exogenous) (or synchronous vs asynchronous) (active, reactive, or passive) (evoked vs spontaneous) and hybrid] depending on the recording method, brain signal pattern, stimulus modality, mode and strategy of operation. Considering the user's attention, efforts, cognitive/mental state, and engagement [17] [47] [49].

A system-level description can usually be formulated with a block diagram describing the major components required for realization in hardware and software. Neural biopotentials are sensed through a specialized electrode and an analogue front-end (AFE), which contains amplifiers and analogue signal processing circuits conditioning the signal for subsequent digitization by an analogue-to-digital converter (ADC).

Sampling must be performed to digitize the signal without changing the continuous signal's statistical properties. EEG can be sampled at equidistant time intervals. The sampling frequency choice is based on The Nyquist-Shannon sampling theorem to find the minimum acceptable sampling rate. "It states that perfect reconstruction can be achieved only by sampling the analogue signal at a rate at least double the highest frequency of the analogue signal". This threshold is the Nyquist sampling rate (Nyquist criterion or Nyquist limit). Suppose the sampling rate for a particular signal is less than the Nyquist sampling rate; in that case, the information contained in the sequence of samples is distorted and not representative of the actual spectral characteristics of the original signal (aliasing). A sampling rate above double the Nyquist limit is acceptable but unnecessary and will require more data storage space. This way, the entire EEG signal (Ensemble) is represented as Realizations (Samples) at Sequential moments [36].

Quantization approximates a continuous signal using discrete symbols or integer values. The digitized EEG signal values can be considered realizations of one stochastic variable and may be characterized when a histogram assumes stationarity. Calculations of a probability distribution, mean, standard deviation, skewness & Kurtosis may help analyze the signal. A complete description of the properties of the signal generated by a random process can be achieved by specifying the joint probability density function (PDF). A simpler alternative to this description is to compute some averages characteristic of the signal, such as covariance, correlations, and spectra. These averages do not necessarily describe a stochastic signal completely, but they may be beneficial for a general description of signals such as EEG. Digital signal processing (DSP) may further condition the signal or extract relevant physiological information. The digital output data stream can then be logged for local storage or wirelessly transmitted for further external processing [35] [36] [37] [47] [48].

BCI signal processing aims to extract features from the acquired signals and translate them into logical control commands for BCI applications. A feature in a signal can be viewed as a reflection of a specific aspect of the physiology and anatomy of the nervous system. Based on this definition, the goal of feature extraction for BCI applications is to obtain features that accurately and reliably reflect the intent of the BCI user. Artifact/Noise removal and signal enhancement are required to minimize the noise in the signal and are essential to understand its sources; different Feature Extraction methods, in addition to Feature selection and dimensionality reduction, are part of the process of promoting neuroplasticity to restore lost function and to analyze sleep spindles and K complexes, which are challenging to diagnose automatically, probably because of their large variability [6] [12] [17] [35] [37].

However, the translation of intent into action depends on the expression of the intention in the form of measurable signals. Each signal acquisition method is associated with an inherent spatial and temporal resolution. EEG is the most prevalent, popular and promising signal acquisition method for BCIs; even though it has a low spatial resolution, it has excellent temporal resolution and zero clinical risk. Also, increased mobility and portability, in addition to being low cost and feasible to manufacture, make it favoured among researchers. Signals from 2,4 or 8 up to 256 electrodes can be measured at the same time [17] [49] [51].

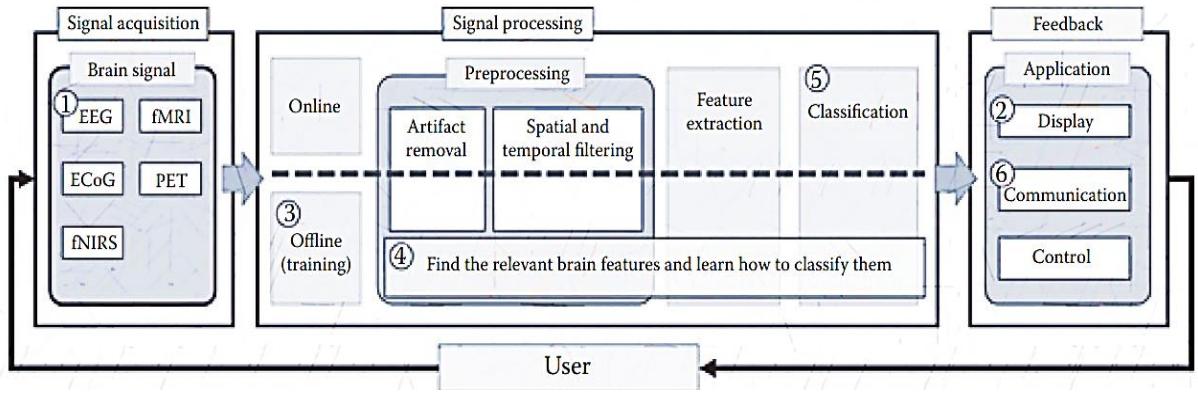

Figure 36: Overview of a general BCI system framework [47].

So, a BCI system has four main components:

I. Signal acquisition,

II. Feature extraction,

III. Feature translation, and

IV. Classification to device output commands or neurofeedback training paradigm [15] [17] [50].

4.9.1 Event related Potentials (ERPs)

Exogenous ERPs are responses that occur in the EEG at a fixed time after a particular visual, auditory, or somatosensory stimulus. The most common way to derive ERP from EEG recording is by aligning the signals according to the stimulus onset and averaging them. Exogenous ERPs generally have shorter latency and are determined almost entirely by the evoking stimulus In comparison, *Endogenous ERPs* have longer latency. They are determined by spontaneous concurrent brain activity (the nature of the task in which the BCI user is engaged in) as in MI studies. ERPs reflect the activity in the ongoing EEG phase locked by the stimuli. The ERP most commonly used in BCIs is the visual evoked potential (VEP), which occurs in response to a visual stimulus. One frequently used VEP is the steady-state visual evoked potential (SSVEP). It depends on the user's gaze direction and thus requires muscle control [15] [17] [51].

The P300 is an endogenous ERP component in the EEG and occurs in the 'oddball paradigm' context [17] [49] [51]. This ERP component is a natural response and is thus especially useful in cases where sufficient training time is unavailable or the user cannot be easily trained. P300-based BCIs are the only BCIs in daily use by severely disabled people in their homes [61].

The P300 speller uses EEG to detect and analyze the P300 wave, a signal in the brain associated with cognitive processing, selective attention, and decision-making in the brain, particularly the recognition of essential stimuli, such as a target among distractors. When using the P300 speller, the user is presented with a matrix of letters or symbols on a computer screen and instructed to focus on the desired letter or symbol as it flashes in a random sequence. As the

brain responds to the target stimulus, the P300 wave is detected by the EEG and translated into a selection on the computer screen [15] [17].

The P300 speller has effectively enabled communication and improved the quality of life for individuals with severe motor impairments. However, it requires significant concentration and training to use effectively and may only be suitable for some as it may accompany uncomfortable fatigue and workload. Advances in BCI technology continue to improve the accuracy and ease of use of the P300 speller and other BCIs, offering hope for improved communication options for individuals with disabilities. The P300 speller technology has demonstrated high accuracy rates, with users able to type at speeds of up to 10 characters per minute. It has been mainly used for communication but has potential in virtual gaming and neuro-rehabilitation applications. The P300 speller was first developed in the 1980s and has undergone significant refinement and optimization, resulting in various versions of the system. The technology is being continuously developed and improved, with ongoing research focused on enhancing its usability, reliability, and accessibility for individuals with diverse needs and abilities [56] [51] [57] [58].

ERD/ERS is a time-locked ERP associated with sensory stimulation or mental imagery tasks. Task-related modulation in SMR usually manifests as an amplitude decrease in the low-frequency components (alpha/beta band), also known as Event-Related Desynchronization (ERD), a decrease in oscillatory activity. In contrast, an amplitude increase in mu and gamma frequency bands is known as Event-Related Synchronization (ERS) that occurs before movement onset. Such characteristic changes in EEG rhythms can be used to classify brain states relating to the planning/imagining of different types of limb movement. This is the basis of neural control in BCIs [53] [56] [51] [57] [58].

Voluntary movements result in a circumscribed desynchronization in the upper alpha and lower beta bands, localized over sensorimotor areas. The desynchronization starts over the contralateral Rolandic region and becomes bilaterally symmetrical with movement execution. The contralateral mu desync's time course is almost identical in swift and slow movements, starting more than 2 seconds before movement onset. ERD and ERS phenomena are found with EEG and MEG recordings [17] [51] [56] [58]. Also, mental imagery can produce replicable EEG patterns in primary sensorimotor areas. This is per the concept that motor imagery is realized via the same brain structures involved in the programming and execution of actual movements [56] [58].

An increased widespread ERD could result from the involvement of a more extensive neural network in information processing. Due, for example, to increased task complexity or the need for more effort and attention. Moreover, with training, people can learn to increase and decrease sensorimotor rhythm amplitude. However, a substantial training period is typically required for users to develop the skill to maintain and manipulate various mental states to enable control. This can be pretty demanding for users, especially disabled users [64] [68].

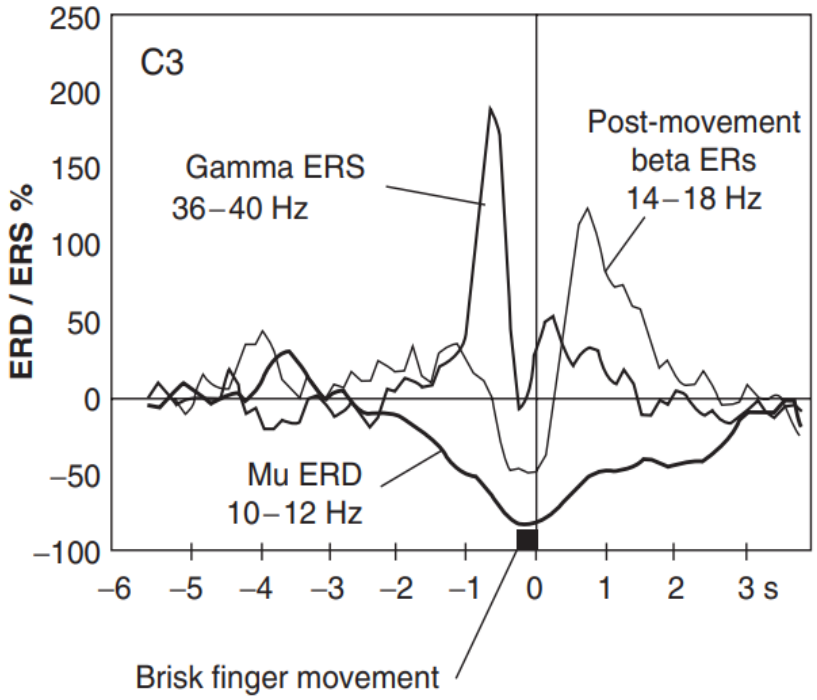

Figure 37 Superposition of different band power versus time courses triggered to brisk finger movement offset. The duration of the index finger extension and flexion was 0.2 seconds. Note the relatively long-lasting mu rhythm (10 to 12 Hz) desynchronization starting about 2 seconds before movement onset, the postmovement beta (14 to 18 Hz) ERS following a beta ERD and the short-lasting power increase around 40 Hz before movement onset. ERD and ERS from one normal subject during self-paced voluntary movement. EEG recorded from C3. The results for three frequency bands are shown: alpha band (mu) 10–12 Hz ERD; beta 14–18 Hz ERD–ERS, and gamma 36–40 Hz ERS. (From Pfurtscheller et al. 1993) [17] [56] [58].

Techniques used to extract ERD and ERS from raw EEG signals [15] [35] [57].

I. First, the raw EEG signal from each trial is bandpass filtered.

II. Second, the amplitude samples are squared to obtain the power samples.

III. Third, the power samples are averaged across all trials.

IV. Finally, variability is reduced, and the graph is smoothed by averaging samples over time.

Noise can be captured from neural sources when the brain signals not related to the target signal are recorded or non-neural sources such as lousy electrode contact or signals from EMG, eye movements electrooculography (EOG), and heart muscle activity (electrocardiography (ECG)), cross talk and power line interference. Mechanical effects from electrode or cable movement typically induce low-frequency (<2 Hz) oscillations, abrupt baseline shifts, or high-frequency transients.

To remove such artifacts and obtain a Clean EEG signal [17] [35] [39]:

- Simple instructions to the user not to use facial muscles can help.
- Trials that contain such artifacts can be disregarded.
- Use a low-pass filter set to ensure the removal of power at frequencies above the Nyquist criterion or notch filters.

- Mathematical operations such as amplitude windows, linear transformations and component analyses are also used for artifact removal.

A bandpass filter preserves signal power within a specified continuous frequency range while attenuating signal power outside of this range. A notch filter is the converse of a bandpass filter; it attenuates signal power within a specified continuous frequency range while preserving signal power outside of this range [17] [35].

High-pass Spatial filters enhance the Signal to Noise ratio (SNR). The bipolar derivation calculates the first spatial derivative and emphasizes the difference in the voltage gradient in a particular direction. Moreover, the surface Laplacian improves spatial resolution by making the electrode more sensitive to activity from superficial, radial, and localized sources underneath the electrode and less sensitive to activity from deep or broadly distributed sources. It can be approximated by subtracting the average of the signal at four surrounding nodes from the signal at the node of interest. It is the second derivative of the spatial voltage distribution and, thus, is an effective spatial high-pass filter [6] [35].

4.9.2 Time-Frequency Analysis

The exact characteristics of EEG signals are, in general terms, unpredictable. One cannot precisely foresee an EEG wave's amplitude or duration. Therefore, an EEG signal is a realization of a random and stochastic process. Obeying Maxwell's and Ohm's laws, brain fields have a direction and magnitude; therefore, they must be represented as vector functions. It is possible to determine some statistical measures of EEG signals that show considerable regularity, such as an average amplitude or frequency. This is a general characteristic of random processes, characterized by probability distributions and their moments (e.g. mean, variance, skewness, and Kurtosis) or by frequency spectra or correlation functions [6] [35] [35].

Such description implies a mathematical, but not a biophysical model, modern mathematical tools are used to analyze EEG signals, assuming that signal generation can be described using sets of complex Nonlinear Differential Equations such as Correlation Dimensions. This field of mathematical research is called "Deterministic Chaos". Thus, it is difficult to distinguish whether EEG signals are generated randomly or by high-dimensional nonlinear deterministic processes [6] [12].

A fundamental signal feature is simply a direct measurement of the signal (e.g., the voltage difference between a pair of electrodes at a particular time after a stimulus). By themselves, fundamental signal features usually provide limited information. Hence, it is more common for BCIs to use features that are linear or nonlinear combinations, ratios, statistical measures, or other transformations of multiple fundamental features detected at multiple electrodes and time points. If selected appropriately, such complex features can reflect the user's desires more accurately than the fundamental features. Most features used in BCI applications are based on spatial, temporal, and spectral analyses of brain signals or their relationships. This set of features is referred to as a feature vector [17] [30].

The most appropriate method for analyzing brain signals would be a “time-frequency analysis” algorithm that would describe changes in all frequencies as a function of time. However, frequency and time cannot be mixed; mathematically, they are orthogonal. This counterintuitive relationship explains why the two major classes of analytical tools used for analyzing brain signals are the “frequency domain analysis” and “time domain analysis” [6]. Fourier transform theory assumes that the signal is analyzed for an infinite duration, which expresses a waveform as a weighted sum of sines and cosines. It decomposes or separates a waveform or function into sinusoids of different frequencies that sum to the original waveform. After the signal is decomposed into sine waves, a compressed representation of the relative dominance of the various frequencies can be constructed. This frequency versus incidence illustration or the autocorrelation function is the power spectrum. It gives the distribution of the squared amplitude of different frequency components [6] [12] [17] [35].

The Fourier method transforms the signal defined in the time domain, into one defined in the frequency domain. Although this representation ignores the temporal variation of the EEG signal, it provides a quantitative answer regarding the power relationship between the frequencies. The inverse relationship between oscillation classes and the magnitude of neuronal recruitment offers some interesting clues about the brain’s long-time and large-scale behaviour, as slow rhythms involve a vast number of cells that can be “heard” over a long distance. In contrast, localized fast oscillations involve only a small fraction of neurons and may be conveyed only to a few partners. Furthermore, faster waves are attenuated more than slow waves. The “loudness” feature of the various network oscillations can be quantified easily by Fourier analysis [6] [12].

A significant advance in computing power spectra has been achieved by introducing a new algorithm for computing the discrete Fourier transform, the fast Fourier transform (FFT). The short-time Fourier transform (STFT) is a practical solution to the time versus frequency orthogonality issue, quantifying frequency content changes over time. This modified analysis divides the brain signal into multiple short epochs, and the Fourier transform is calculated for each epoch. The successive spectra can display the evolution of frequency content with time. The STFT is a compromise of joint time-frequency analysis. A wide temporal window will give good frequency resolution but poor time resolution. In contrast, a narrow window will give good time resolution but poor frequency resolution. Accepting this compromise, this modified method can analyze short sequential epochs, and the frequency structure can be displayed as a function of time [6] [12] [17] [35].

Another popular way of analyzing short-time segments of selected EEG patterns is called “wavelet” analysis. The wave refers to the fact that this function is oscillatory; the diminutive form refers to the fact that this (window) function is of finite length or a fast-decaying, oscillating waveform. The wavelet transform refers to the representation of a signal in terms of a finite length. Rather than analyzing the distribution of all frequencies, the wavelet first selects a “frequency of interest.” Therefore, all wavelet transforms are forms of time-frequency representation. Wavelet transforms broadly classified into the discrete wavelet transform (DWT) and the continuous wavelet transform (CWT) [12] [35].

Coherence is a measure of phase covariance, quantified as the cross-spectrum of two signals divided by the product of the two auto spectra. Because it measures spectral covariance, it cannot reliably separate amplitude and phase contributions. Phase-locking statistics can quantify phase coherence between two signals independent of the amplitudes of the respective signals. Phase-locking or phase-coupling can also occur between oscillatory and non-oscillatory events, such as phase-locked discharge of irregularly spiking neurons and an oscillator. Cross-frequency phase synchrony can occur between two or more oscillators of different integer frequencies when the oscillators are phase-locked at multiple cycles. If two oscillators differ in frequency and cannot fix their phases, they can produce a transient and systematic interaction called phase precession or retardation [6].

Chapter 5: Datasets, Materials, Methods & Results

5.1 Datasets description

Three different data sets were used in our method's evaluation process, the Physionet EEG Motor Movement/ MI Dataset, which the developers of the BCI2000 system recorded. It has a 64-electrode EEG setup, sampled at 160 Hz. The data contains recordings of motor execution, as well as MI tasks. There are recordings from 109 different subjects performing two different MI tasks (left/right fist or both fists/feet) in two-minute runs of each MI of the two tasks. One trial consists of 2 s rest, 4 s of cued MI, and again 2 s of rest before the next trial starts [78].

The BCI Competition IV-2a dataset is also publicly available. It contains recordings from nine subjects who performed four motor imagery tasks (Left Hand, Right Hand, Both Feet and Tongue). The data collection is divided into short runs, each containing 48 trials of each motor imagery activity. The data was collected in two sessions in two days, comprising six runs per session with a short break between them. So, the data contains 288 trials of each motor imagery activity. The EEG data were recorded with 22 Ag/AgCl electrodes arranged in a standard 10-20 system, sampled at 250 Hz and band pass-filtered between 0.5 And 100 Hz. The amplifier sensitivity was set to 100 microvolts. An additional 50 Hz notch filter was enabled to suppress line noise. In addition, three mono-polar Electrooculography (EOG) channels were recorded and sampled at 250 Hz [79].

The third dataset used in this research is the MTA-TTK dataset from the Hungarian Academy of Sciences, which belongs to Peter Pazmany Catholic University. It contains 25 recording subjects, 63 EEG sensor channels, and a 500 Hz sampling frequency. Five classes were considered: rest, imagined movements of the left hand, right hand, left leg, and right leg. No filtering was applied to the original raw signals; however, a 0.5-Hz low-pass filter removes the DC component from the signal and enhances its accuracy.

5.2 Materials

The following Python Packages were used:

- MNE: an open-source Python package for exploring, visualizing, and analyzing human neurophysiological data: MEG and EEG and more.
- Numpy, Scipy, Sklearn & Keras.
- Tensorflow: An end-to-end machine learning platform.
- Matplotlib: A library for creating static, animated, and interactive visualizations.

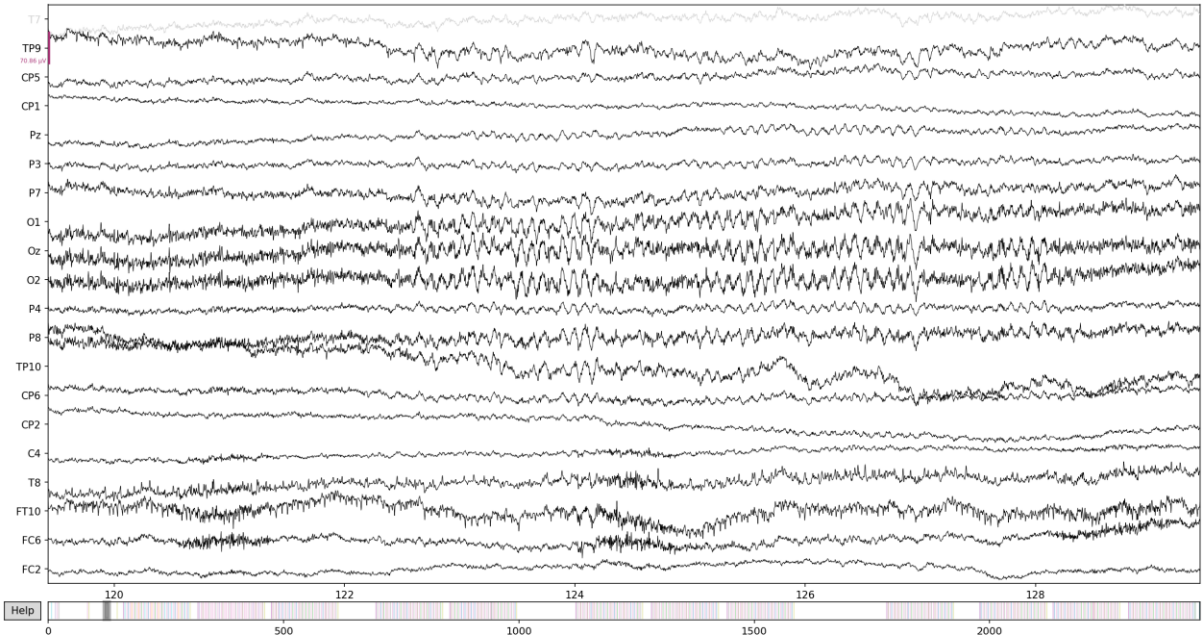

Figure 38: TTK dataset - raw data

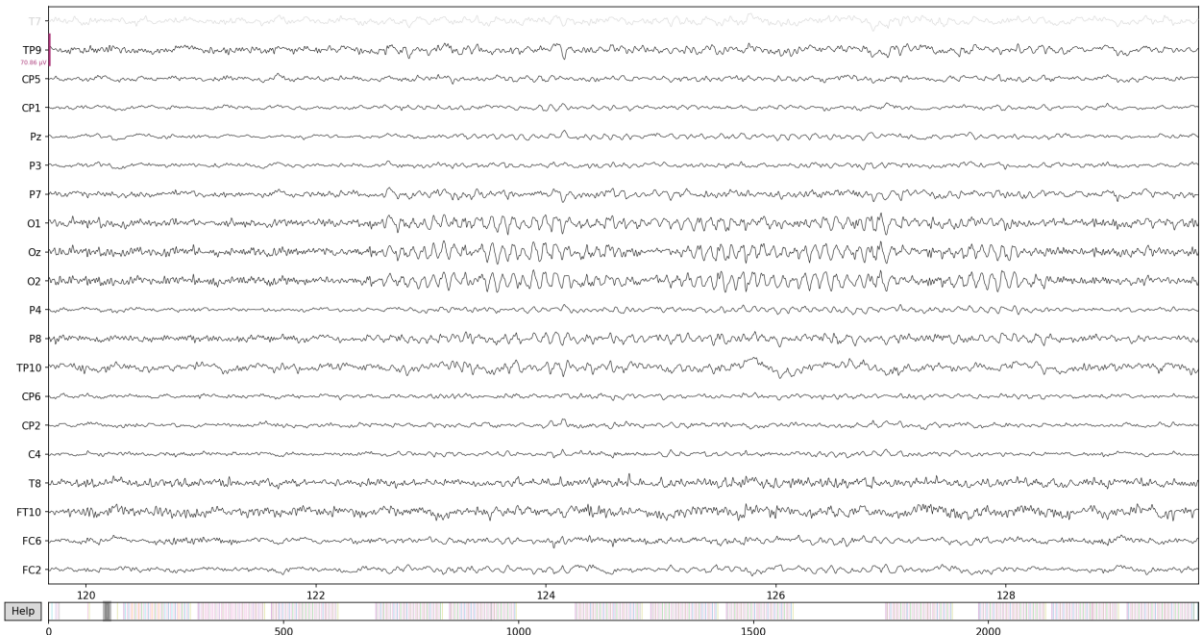

Figure 39: TTK dataset - Filtered data

5.3 Methods

A BCI translation algorithm uses features extracted from brain signals to produce device commands that convey the user's intent. The core component of an effective translation algorithm is an appropriate model. A model is a mathematical abstraction of the relationship between independent variables (i.e., brain signal features) and dependent variables (i.e., the user's intent as expressed by the BCI outputs). The two other components of a translation algorithm are the method for selecting the features used by the model and determining the model's parameters and weights. The primary goal in developing a translation algorithm is to maximize its ability to generalize to new data since BCIs must operate online in real-time.

Although helpful in developing an algorithm, more than success in post hoc data analysis is required to yield the development and use of adaptive translation algorithms [17].

Classification algorithms depend on the label output type, whether learning is supervised or unsupervised, and whether the algorithm is statistical or non-statistical. Statistical algorithms can be further categorized as generative or discriminative. The algorithms in supervised classification procedures predicting categorical labels are Linear discriminant analysis (LDA), Support vector machine (SVM), Decision trees, Naive Bayes classifier, Logistic regression, K-nearest-neighbor (kNN) algorithms, Kernel estimation, Neural networks (NN), Linear regression, Gaussian process regression, Kalman filters and more [35].

Unsupervised classification attempts to find inherent patterns for unlabeled data that can then be used to determine the correct output value for new data instances. Some standard algorithms of unsupervised machine learning classification are K-means clustering, Hierarchical clustering, Principal Component Analysis (PCA), Kernel Principal Component Analysis (Kernel PCA), Hidden Markov Models, Independent Component Analysis (ICA), Categorical mixture model, etc. Semi-supervised learning is a combination of the two classification procedures [37].

Principal Component Analysis (PCA) is a well-established method for feature extraction and dimensionality reduction in which the dimensional data is represented in a lower-dimensional space. Such a representation would reduce the degrees of freedom and the space and time complexities. *Independent Component Analysis (ICA)* helps segregate the brain and non-brain components from the acquired EEG. It converts random signals with multiple variables into one, which measures the frequency strength at a time. They properly visualize the EEG waves to get the frequency wave bands [6] [83].

Common Spatial Pattern (CSP) is a signal processing technique used in neuroscience and machine learning to enhance EEG, MEG, fMRI and ECoG data information. CSP is a supervised machine learning method that exploits the information about differences in brain signals between cognitive tasks/states or motor commands. It involves finding the spatial filters that maximize the contrast of variance in brain signals between two classes of conditions.

CSP has been shown to improve the classification accuracy and speed of BCI systems, which can be applied to assistive technology for people with motor disabilities or to enhance the performance of healthy individuals in tasks requiring neurofeedback training. CSP has been successfully applied in various BCI applications, including motor imagery, speech recognition, and emotion recognition. It has also been used in clinical applications, such as detecting seizures in epilepsy patients and diagnosing Alzheimer's disease. One of the advantages of CSP is that it is a data-driven method, meaning that it can be applied to any EEG data without requiring prior knowledge of the underlying neural mechanisms or signal characteristics. However, it does require a sufficient amount of training data to learn the optimal spatial filters [17] [35].

Overall, CSP is a powerful technique for feature extraction in EEG-based BCIs. Its effectiveness in enhancing the SNR and increasing classification accuracy has been demonstrated in various neuroscience and machine learning applications.

Support vector machine (SVM) is a supervised machine learning algorithm that can be used for classification, regression or outlier detection purposes. The algorithm was developed by Vladimir Vapnik and his team in the 1990s. The basic idea behind SVM is to find the optimal hyperplane that separates the different classes by maximizing the margin between them. The margin is the distance between the hyperplane and the closest data points from each class, and SVM finds the hyperplane that maximizes this distance [84].

SVM works by transforming the input data into a higher-dimensional space using a kernel function, which allows it to identify complex nonlinear relationships between the features. The most commonly used kernels are linear, polynomial and radial basis functions (RBF) or sigmoid functions. SVMs can be used for both linear and nonlinear classification. It effectively handles noise and outliers in data and can be used for binary and multi-class classification problems. Additionally, SVM has a regularization parameter that can be used to control overfitting and improve generalization performance [85].

Nevertheless, SVM can be sensitive to kernel function and hyperparameters, which requires careful tuning. Moreover, the training time of SVM can be slow in high-dimensional datasets, which can be computationally expensive, especially for large datasets. However, various optimization techniques, such as stochastic gradient descent, have been developed to overcome this issue. In summary, SVM is a robust and widely used algorithm in machine learning, and it has been shown to perform well in various applications [86].

While conventional methods like LDA, AR, KNN, CSP along variants of different filter banks and augmentation strategies, SVMs, Riemannian, Laplacian and Bayesian methods, have made significant progress in terms of classification accuracy, deep transfer learning-based systems have shown the potential to outperform them. Deep learning (DL) techniques, especially convolutional neural networks (CNNs), have been extensively used in the field of BCI motor imagery (MI) signal analysis for their high classification accuracy and simple construction procedure. Many trials were conducted using a combination of a long short-term memory (LSTM) network and a spatial CNN, or a multiscale fusion CNN based on an attention mechanism, separable convolution, depth-wise convolution, or temporal convolution network (TCNs). Compared to CNNs, RNNs were originally used to model data that involve sequential characteristics such as time series, language modeling, and speech synthesis, to name a few. Because of their ability to model sequential dependencies, RNNs are a natural choice to use for EEG-based BCI, where brain signals are treated as time series. Trade-offs must be invected in selecting from these general family models. Complex models fit existing data better than simple models, but they may not generalize as well to new data. Limiting the model to only the most relevant signal features often improve its generalization ability [17] [37] [74].

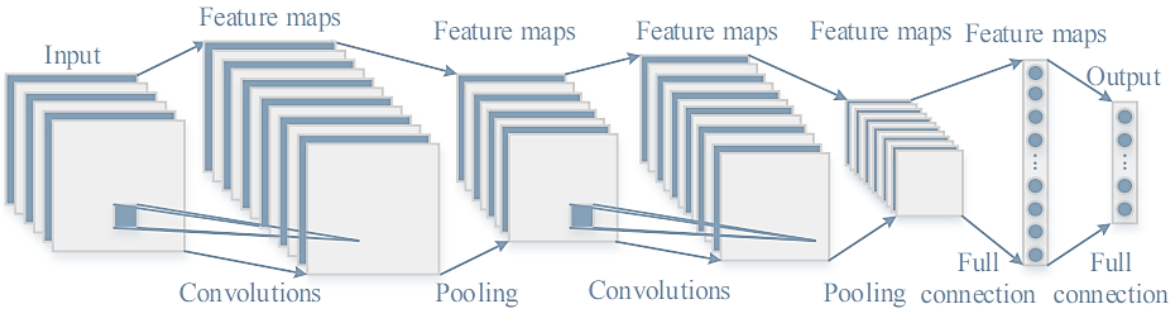

Figure 40: Basic CNN structure

CNN is a deep neural network that is renowned for image processing applications. The convolution operation takes place by applying multiple filters to the data to extract features generating feature maps from the data set. Following up is typically a pooling operation in which the dimensionality of feature maps is reduced. Therefore, CNN proved very useful in classifying motor imagery signals since the raw EEG signal can be used directly as an input without needing a preprocessing stage, like a WT. A CNN model can be integrated within a BCI-based system for real-time applications. Nevertheless, it depends on the software development kit available to perform predictions and commands [37] [35].

Tuning Deep Neural Networks can help improve a deep learning model's classification accuracy or generalization capabilities. Batch normalization is typically applied to normalize intermediate representations between layers, improving generalization and accuracy, especially for CNNs. Dropout layers combat overfitting by randomly disabling a certain percentage of neurons in a layer; this ensures that a network learns generalized features rather than relying on individual neural connections. Dropout is only used during the training phase and turned off for validation and testing. Regularization is also used to reduce overfitting by penalizing weights. Data augmentation aims to produce more training data from available data artificially. In the case of image data, it is possible to rotate, scale or flip the images without changing the meaning. By feeding augmented data to the network, the network learns some degree of invariance to this type of image transformation [75] [76] [92].

Thesis 1

"In this research, I co-created a software code utilizing Python named *Coleeg*, an open-source initiative for facilitating the evaluation of EEG signal classification using neural networks. It is a platform to compare the performance of different CNN architectures [80]."

First, we systematically studied the following models:

- [Basic] represents the simplest neural network model with only one layer and no convolution. This model is not suggested for real-life applications but rather for performance comparison.
- [CNN1D], which performs convolution along the time axis only.

- [CNN2D], where time and sensor channels are considered for two-dimensional convolution.
- [CNN3D and TimeDist] are video classification models that convert the sensor channels into a 2D image that changes with time. 3D convolution and time-distributed 2D convolution are used in CNN3D and TimeDist models, respectively. A simplified diagram for the proposed models is shown below (Fig 39).
- We also added the models [EEGNet] [81], [ShallowConvNet], and [DeepConvNet] [82] proposed in the literature.

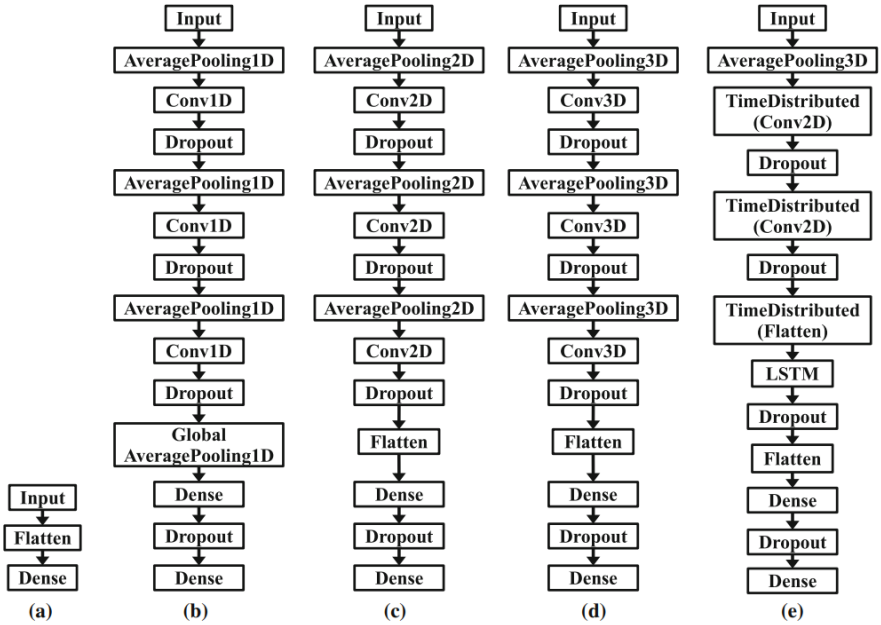

Figure 41: A simplified diagram for the models: a Basic. b CNN1D. c CNN2D. d CNN3D. e TimeDist

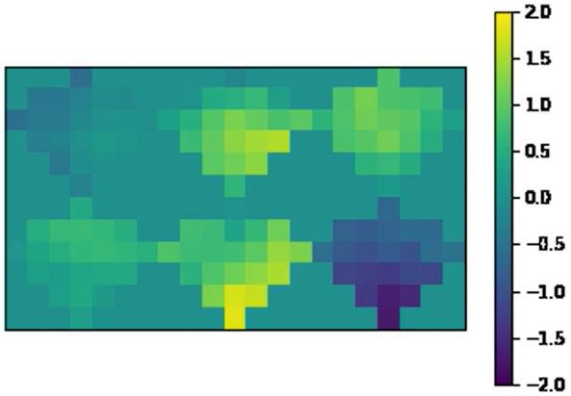

Figure 42: 2D Mapping visualization of Physionet dataset sensors

Three arrays are produced from reading each dataset:

- ***data_x***, which contains time samples obtained from the dataset with the following dimensions: time-epochs x time-samples x sensors x frequency-bands.
- ***data_y*** contains the class label corresponding to each time epoch.

- ***data_index*** has two columns; the first is the index of the first epoch for each subject, and the second is the subject number.

5.4 Results

The models CNN2D, CNN3D, and TimeDist show low accuracy while having high training times, and this might be because of the increased complexity of the models, which makes them tend to have an over-fitting problem and require more training time. The ShallowConvNet architecture was designed specifically to extract log band power features; in situations where the dominant feature is signal amplitude, as in ERP BCIs, ShallowConvNet performance tended to suffer. The opposite situation occurred with DeepConvNet; its architecture was designed to be a general-purpose architecture not restricted to specific feature types, such as extracting frequency features, so its performance was lower when frequency power was the dominant feature.

Table 1: Physionet accuracy values

	Basic	1D	2D	3D	LSTM	EEGNet	Shallow-ConvNet	Deep-ConvNet	CNN1D_MF
Accuracy	40.6 %	52.5%	52.2%	51.6%	47.0 %	53.9%	53.8%	54.3%	58.0
Time	20:28	28:06	1:19:27	6:15:55	2:29:41	1:20:13	1:12:41	48:38	42:20

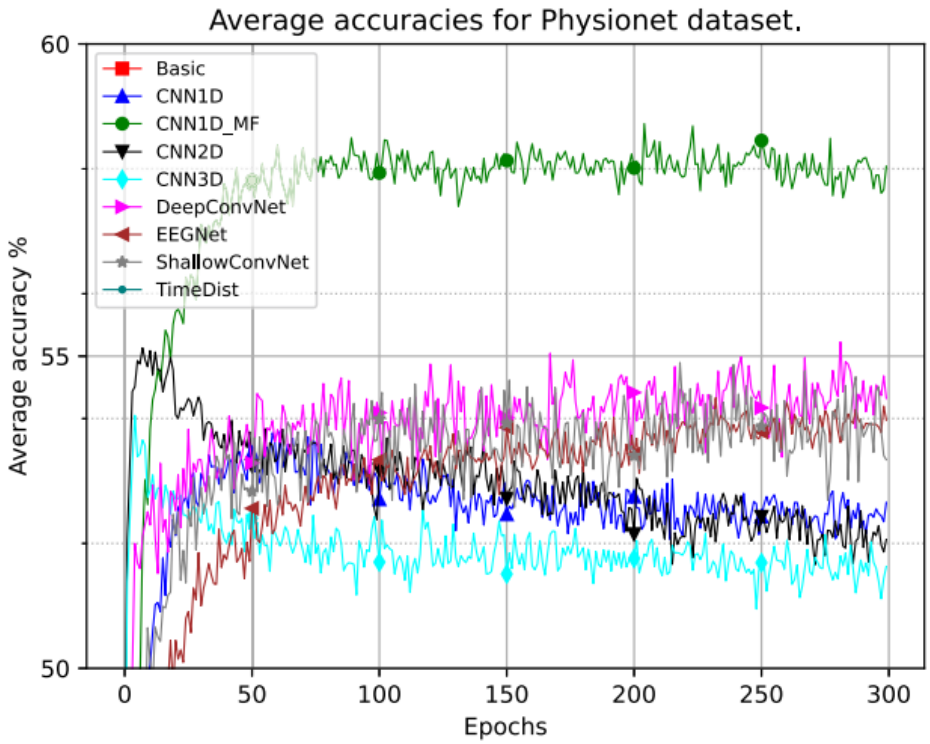

Figure 43: Average Accuracies for Physionet dataset

Table 2: BCI Competition IV-2a accuracy values

	Basic	1D	2D	3D	LSTM	EEGNet	Shallow-ConvNet	Deep-ConvNet	CNN1D_MF
Accuracy	54.1%	65.1 %	59.5 %	60.7%	55.1%	64.7 %	65.1 %	68.3 %	69.2 %
Time	10:12	14:38	31:27	2:24:09	1:06:49	23:46	19:01	2:49	17:01

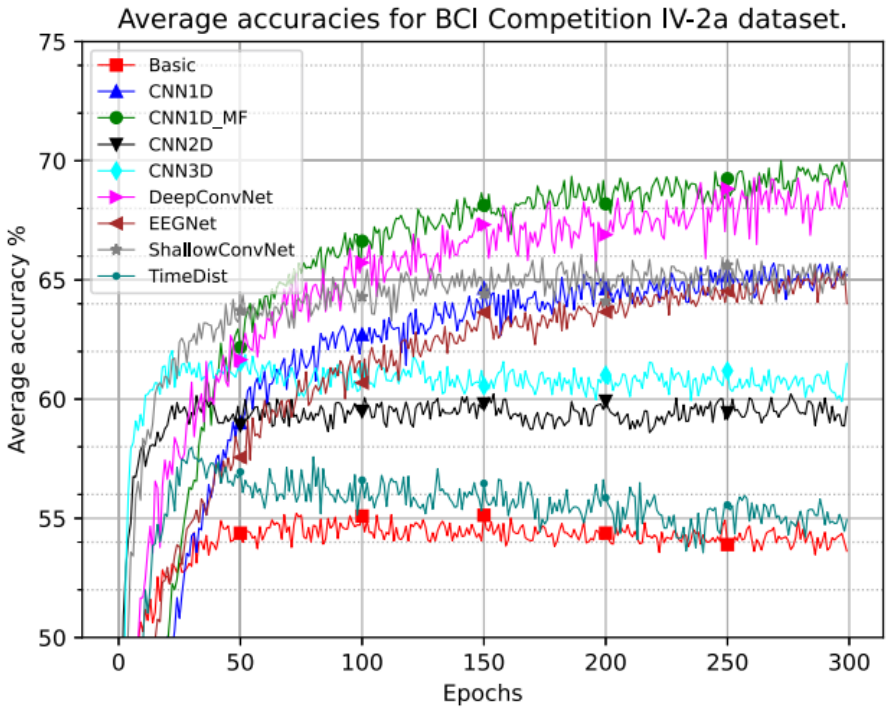

Figure 44: Average accuracies for BCI Competition IV-2a dataset

Then we modified the CNN1D model to have a multiband frequency input CNN1D_MF; doing so has improved the accuracy significantly. Any other model can accept multiple frequency band inputs. However, only the CNN1D model has been considered because it performs best among other proposed models. The subbands are 0.5–8.0 Hz, coinciding with the combined delta (δ) and theta (θ) waves. The band 8.0–13.0 Hz contains the alpha (α) rhythm, while the band 13.0–40.0 Hz coincides with the beta (β) wave and some of the lower parts of the gamma (γ) wave. A finite impulse response (FIR) filter with a linear phase and Hamming window define the bands. Results are presented in Tables 1 and 2 for the Physionet and BCI competition IV-2a datasets, respectively.

Thesis 2

"I present a novel "Multifrequency Band Fusion Method (MFBF)" for EEG MI decoding. Its mechanism divides the signal spectrum into multiple frequency bands and feeds each band into duplicates of the selected CNN model. All the model duplicates are then concatenated to give the required classification."

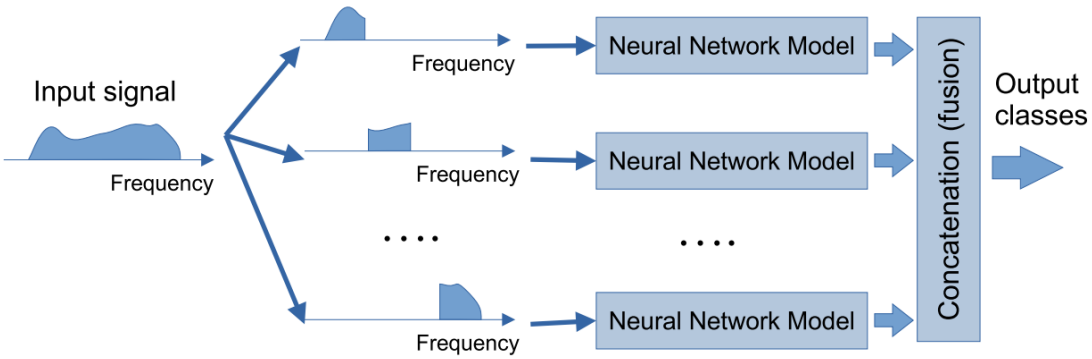

Figure 45: MFBF method illustration

The CNN1D model and the frequency bands mentioned above were used in the experimental evaluation to form the CNN1D-MFBF model. Considering two scenarios, it was evaluated against the EEGNet-fusion model on the three datasets. The first one is where no multiband filtering is used, and it was applied to the CNN1D and the EEGNet-fusion models. The second scenario is applied to the CNN1D and CNN1D-MFBF models. The preprocessing applied to the EEG signals was resampling all datasets to 100 Hz. The data were also normalized to have zero mean and a standard deviation of 1. The results are shown below in Tables 3, 4 and 5 siding their corresponding figures.

Table 3: Physionet accuracy values

	CNN1D No multiband filtering	CNN1D With multiband filtering	CNN1D_MFBF With multiband filtering	EEGNET_fusion No multiband filtering
Accuracy	52.2	57.9	58.7	57.0
Time	0:38:15	0:59:48	1:22:18	8:32:04

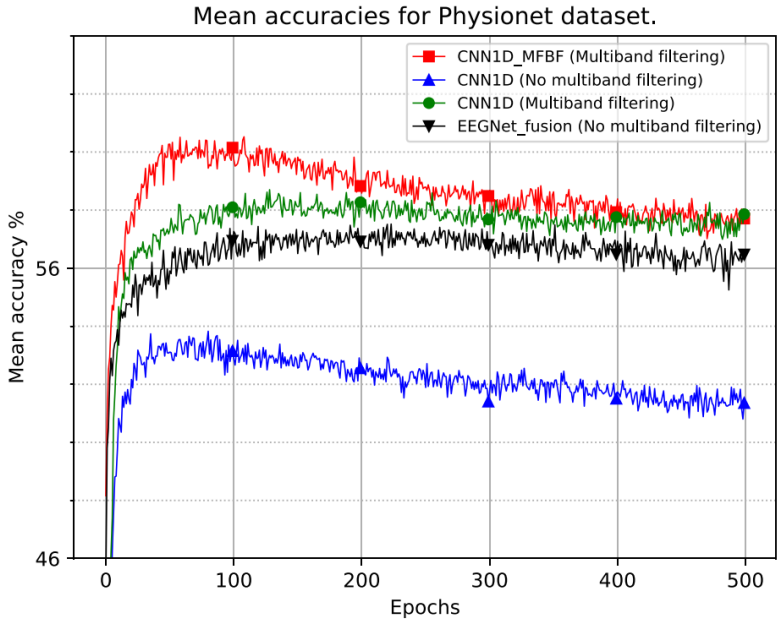

Figure 46: mean Accuracies for Physionet dataset

Table 4: BCI Competition IV-2a accuracy values

	CNN1D No multiband filtering	CNN1D With multiband filtering	CNN1D_MFBF With multiband filtering	EEGNET_fusion No multiband filtering
Accuracy	65.0	68.1	72.8	73.5
Time	0:12:51	0:17:55	0:24:16	2:12:00

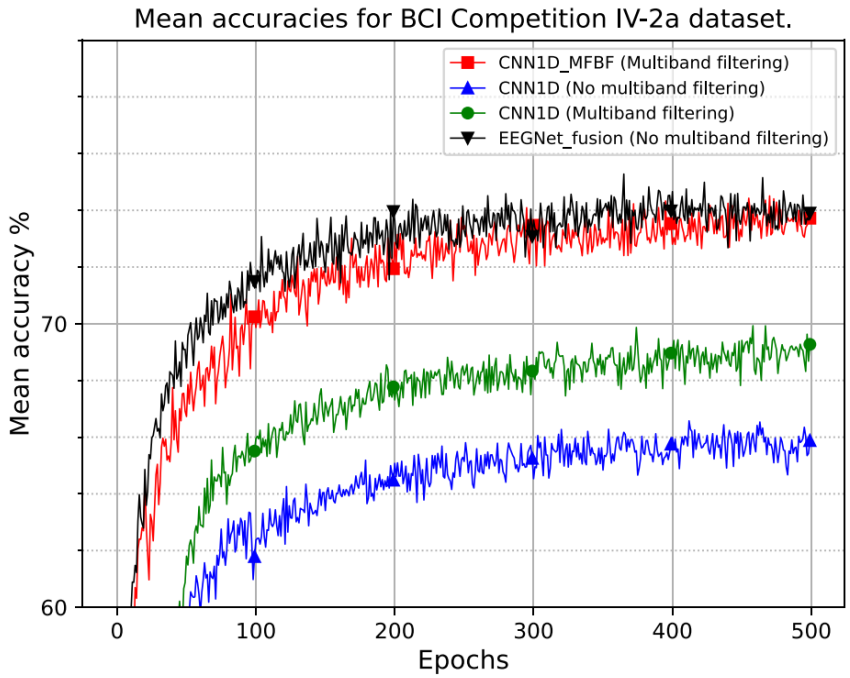

Figure 47: Mean accuracies for BCI Competition IV-2a dataset

Table 5: MTA-TTK

	CNN1D No multiband filtering	CNN1D With multiband filtering	CNN1D_MFBF With multiband filtering	EEGNET_fusion No multiband filtering
Accuracy	37.3	42.5	47.6	45.1
Time	0:25:57	0:36:28	0:56:59	4:53:15

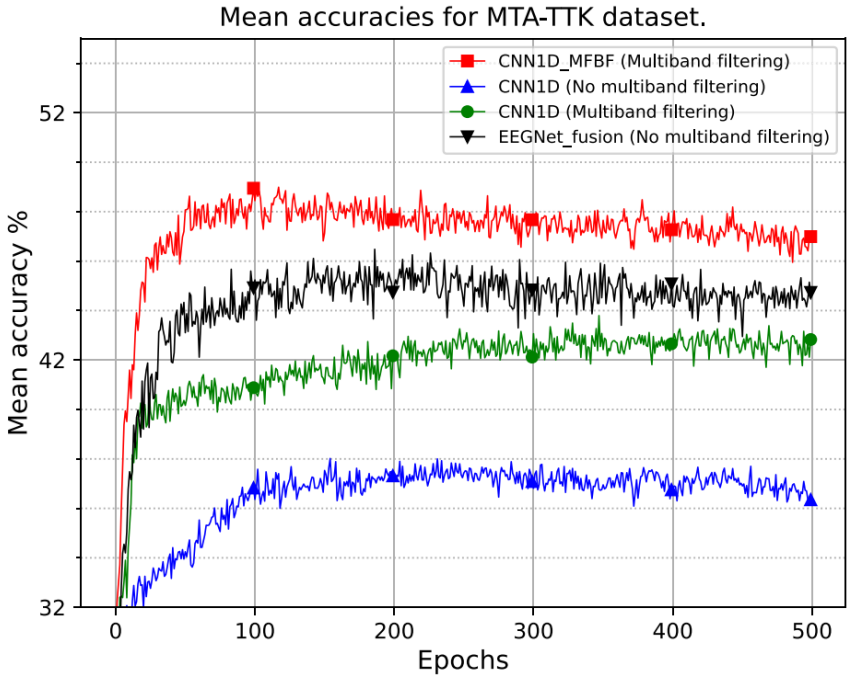

Figure 48: Mean accuracies for MTA-TTK dataset

Our experimental result shows that CNN1D_MFBF has the best accuracy and training time performance, as it takes advantage of the convolution process while keeping the model as simple as possible. They also show that applying multiple filter bands on the input data increases the accuracy results significantly, mainly due to data augmentation. Additional minimal improvement in accuracy was obtained by using 4 s of the trial time instead of 2 s and performing cross-validation for every subject at the expense of increased computational time and cost.

Coleeg has matured to provide many utility functions that facilitate dealing with different datasets and models, such as applying different filter bands, applying notch filters, resampling data, specifying included and excluded subjects, classes and shuffling, visualization and augmentation features were also added along the choice, to use local runtime, which allows researchers to utilize the power of local hardware and overcome the limitations imposed by Colab-hosted runtime, in addition to evaluation metrics, like Cohen Kappa, specificity and sensitivity and plotting the results and saving the plots as pdf files [80].

5.5 Discussion

Most EEG-based BCIs use the P300 evoked potential, sensorimotor rhythms (SMRs), or steady-state visual evoked potential (SSVEP). All three BCI types can help to restore essential communication and control to people with severe neuromuscular disabilities. At present, their capabilities are limited. Improved EEG recording methods are needed to provide stable, high-quality signals in all environments, be comfortable, and be easy to use. New dry-electrode systems have considerable promise. Improved signal analysis algorithms that can consistently maintain accurate performance are also required. While much algorithmic development has relied on offline analyses of archival data, online testing of new algorithms is essential because

it considers the ongoing adaptive interactions between the user and the BCI. BCIs, particularly SMR-based BCIs, also show promise as new methods for enhancing functional recovery for people with strokes or other chronic disorders. Several strategies for using BCIs to induce beneficial plasticity are under study. Evidence that these methods can enhance recovery beyond what can be achieved by conventional methods alone is just beginning to emerge [90] [109].

Recent advances in digital recording and signal processing, together with the leaps in computational power, are expected to spawn a revolution in the processing of measurements of brain activities, primarily EEGs and ERPs. This will enable the implementation of more complicated denoising techniques of ERP than ensemble averaging and more complicated EEG quantification analysis methods than the amplitude and frequencies, including nonlinear dynamics and higher-order statistics [17]. Furthermore, this will help implement various techniques describing the interactions between different regions of the brain, which offer more insights into the functional neural networks in the brain [69].

Current DL-based EEG classification studies aim to improve classification accuracies, proposing a new way to interpret the features and enhancing real-time feasibility. The ability of DL models to properly clean the artifacts and learn from neurological signals still needs to be improved and needs further research. It is crucial in EEG to understand what was learned in the model because the end goal of EEG-based studies is to understand the brain and utilize the signals extracted from the brain. Many studies still need to open-source the data and code, which would be vital in increasing replicability. Open sourcing the data could also help the community train the DL model and transfer the knowledge to a target domain where such a large dataset is unavailable [89] [90].

End-to-end DL classification in EEG data processing and modelling pipeline has the potential to remove the necessity of preprocessing that tends to rely on either specific domain knowledge or visual interpretation by experts. Also, it allows us to focus on one optimization model from the beginning to the end. However, at the current stage, end-to-end is still difficult without a thorough analysis of how and what the DL is learning and relying on to make decisions and proper interpretation and decoding [90].

DL for EEG neural classification is still in the emerging stage. There is growing interest in increasing the reliability and usability of such models with the intent of using them for real-time implementation. However, **no real-time implementations currently employ these deep learning models for EEG decoding tasks**. Several attempts to analyze EEG signals using CNN models were postulated. Many showed promising accuracy results concerning motor imagery and laterality of motion. None proved superior or reliable, but experiments are ongoing, searching for better, well-formed software to extract more information from EEG signals [51] [90] [92].

EEG has several benefits compared to other imaging techniques. The most prominent benefit of EEG is its excellent time resolution; that is, it can take hundreds to thousands of snapshots of electrical activity across multiple sensors within a single second. EEG is an ideal technology for studying the precise time course of cognitive and emotional dynamics, most occurring

within tens of milliseconds. The second reason that EEG is an advantageous technique for studying neurocognitive processes is that it allows the direct measure of neural activity. EEG signals directly reflect biophysical phenomena occurring in neuron populations. This is a clear advantage over other methods, such as fMRI, that do not directly measure neural activity but introduce an extra relationship between what is measured (changes in blood flow in the case of fMRI) and the actual neural activity. Finally, EEG is non-invasive, and the required equipment is relatively cheap, portable and relatively easy to operate [6] [12].

On the other hand, the main disadvantage of EEG is its poor spatial resolution. Neural activity is conducted through the brain volume to the scalp and electrodes by volume conduction. The concept of volume conduction carries important implications for surface EEG measurements as currents are not restricted to the immediate neighborhood of the source, and the electrical activity measured between electrodes has more to do with their orientation to the actual generator than with the proximity of the electrodes to the generator. Because the skull is a poor conductor, current tends to "splash off of it", and each electrode receives signals from millions of neurons, reducing potential spatial localization. This is exacerbated by the fact that the head tissues' conductivities vary across individuals and within the same individual due to variations in age, disease state, and environmental factors. The inference of the location of the current sources from electrode voltage measurements on the scalp is known as the EEG inverse problem. It is comparable to reconstructing an object from its shadow; only generic features are uniquely determined [6] [12] [17] [47].

EEG is also very sensitive to subject movement and external noise. Electrodes used in EEG recording do not discriminate the electrical signals they receive. Intrinsic and extrinsic Artifacts contaminate the recordings in both temporal and spectral domains within a wide frequency band. The internal source of artifacts may be due to the subject's physiological activities (e.g., eye movement, electrocardiographic activity, sweat or muscle artifacts) or their movement. External sources of artifacts are environmental interferences such as power line interference, improper contacts between electrodes and skin, or interferences from recording equipment and cable movement [6] [12] [17] [47].

Four criteria are a must for a system to function as a BCI system:

- The system must rely on activity recorded directly from the brain.
- Intentional control: At least one recordable brain signal, which can be intentionally modulated, must provide input to the BCI (electrical potentials, magnetic fields or hemodynamic changes).
- Real-time processing: Signal processing must occur online and yield a communication or control signal.
- Feedback: The user must obtain feedback about the success or failure of his/her efforts to communicate or control.

The primary goal has been to introduce and articulate a framework capable of synthesizing some results and theories in motor control, imagery, perception, and perhaps even cognition

and language rather than providing compelling data for its adoption. These considerations are not theoretically insignificant but are also quite far from conclusive. BCI development relies heavily on offline analyses of data gathered during BCI operations or various open-loop psychophysiological studies. These analyses can be instrumental and imperative in comparing different models, feature selection, and parameterization methods and testing alternative algorithms.

5.6 Conclusion

The path of the signal:

"Brain – scalp-electrode interface – electrodes (composition material, specifications and configuration) – Amplification and Filtering (Analog circuitry) – ADC – Signal processing (Artifact removing – Feature extraction, dimension reduction, feature selection and classification) – then to application circuit (Digital/analogue commands) leading to intention decoding & neuro-control".

BCI is an emerging field where EEG techniques are used as a direct nonmuscular communication channel between the brain and the external world. BCI research and development is a highly complex, interdisciplinary, and demanding endeavour that depends on carefully evaluating and comparing many different brain signals, signal processing methods, and output devices. Most current BCI systems' inflexibility, unreliability and limited capabilities significantly pose a considerable challenge for designers and users alike. A few people with severe disabilities already use a BCI for essential communication and control in their daily lives. With better signal-acquisition hardware, clear clinical validation, viable dissemination models, and increased reliability, BCIs may become an essential new communication and control technology for people with disabilities and possibly the general population [17].

The present report sheds light on the difficulties encountered in BCI technology. Problems in the field today are accuracy, reliability, and number of commands, Bandwidth as the Information Transfer rate (ITR) (i.e., speed of the system) and new applications and paradigms, and lack of shared codes. Users' comfort needs to be addressed as cognitive workload and mental fatigue may appear as side effects of using the system. Calibration is also challenging in BCI because the SNR is unfavorable, and the subject-to-subject variability is immense.

Visual ERP-based BCIs often have the advantage that the stimulus presentation mode leads to a unique structure of the collected brain signal data, which supervised and unsupervised learning methods may exploit. Without significant improvements, the real-life usefulness of BCIs will, at best, remain limited to only the most basic communication functions for those with the most severe disabilities. In current BCIs, the BCI, rather than the user, typically determines when output is produced. Ideally, BCIs should be self-paced so that the BCI is

always available, and the user's brain signals alone control when the BCI output is produced [66].

EEG phenomena's complexity requires computer simulations to understand the underlying generation processes. New tools for studying nonlinear dynamic systems have been introduced in this domain of theoretical neurophysiology. Furthermore, the availability of powerful computer tools opens new possibilities for modelling complex membrane phenomena and network properties. Academic studies are justified if combined with experimental investigations (hence, offline and online examinations, invasive and noninvasive techniques). In this way, one may obtain new insights about the generation of EEG patterns and formulate hypotheses to be tested under experimental conditions. In the last decades, a shift of attention from models describing the behaviour of neuronal networks in the temporal domain toward models considering complex networks' spatial and spectral properties has occurred. The person interested in interpreting the EEG must draw conclusions based on the brainwaves' frequency, amplitude, morphology, and spatial distribution. However, the diversity of EEG patterns cannot be wholly explained by any single mathematical or biological model available today. Therefore, EEG interpretation remains a phenomenological medical discipline with undoubted prospects in the BCI domain.

'It remains sadly true that most of our present understanding of mind would remain as valid and useful if, for all we knew, the cranium were stuffed with cotton wadding' [96] [97].
[Ralph Gerard (1949), Robert Maxwell Young (1970), Christopher Lawrence (2021)]

Publications

- Wahdow, M., Alnaanah, M., Fadel, W., Adolf, A., Kollod, C. and Ulbert, I., 2023. Multi frequency band fusion method for EEG signal classification. Signal, Image and Video Processing, 17(5), pp.1883-1887.
- Alnaanah, M., Wahdow, M. and Alrashdan, M., 2023. CNN models for EEG motor imagery signal classification. Signal, Image and Video Processing, 17(3), pp.825-830.
- Köllőd, C., Adolf, A., Márton, G., Wahdow, M., Fadel, W. and Ulbert, I., 2022. Closed loop BCI System for Cybathlon 2020. arXiv preprint arXiv:2212.04172.
- Fadel, W., Kollod, C., Wahdow, M., Ibrahim, Y. and Ulbert, I., 2020, February. Multi-class classification of motor imagery EEG signals using image-based deep recurrent convolutional neural network. In 2020 8th International Winter Conference on Brain-Computer Interface (BCI) (pp. 1-4). IEEE.
- Fadel, W., Wahdow, M., Kollod, C., Marton, G. and Ulbert, I., 2020. Chessboard EEG images classification for BCI systems using deep neural network. In Bio-inspired Information and Communication Technologies: 12th EAI International Conference, BICT 2020, Shanghai, China, July 7-8, 2020, Proceedings 12 (pp. 97-104). Springer International Publishing.

References

1. Gloor, P., 1969. Hans Berger on electroencephalography. American Journal of EEG Technology, 9(1), pp.1-8.
2. Schomer, D.L. and Da Silva, F.L., 2012. Niedermeyer's electroencephalography: basic principles, clinical applications, and related fields. Lippincott Williams & Wilkins.
3. Coenen, A. and Zayachkivska, O., 2013. Adolf Beck: A pioneer in electroencephalography in between Richard Caton and Hans Berger. Advances in cognitive psychology, 9(4), p.216.
4. Berger, H., 1929. Über das elektroenkephalogramm des menschen. Archiv für psychiatrie und nervenkrankheiten, 87(1), pp.527-570.
5. Adrian, E.D. and Matthews, B.H., 1934. The Berger rhythm: potential changes from the occipital lobes in man. Brain, 57(4), pp.355-385.
6. Buzsaki, G., 2006. Rhythms of the Brain. Oxford university press.
7. Stone, J.L. and Hughes, J.R., 2013. Early history of electroencephalography and establishment of the American Clinical Neurophysiology Society. Journal of Clinical Neurophysiology, 30(1), pp.28-44.
8. Jasper, H.H., 1991. History of the early development of electroencephalography and clinical neurophysiology at the Montreal Neurological Institute: the first 25 years 1939-1964. Canadian journal of neurological sciences, 18(S4), pp.533-548.
9. Ginzberg, R., 1949. Three years with Hans Berger a contribution to his biography. Journal of the History of Medicine and Allied Sciences, 4(4), pp.361-371.
10. Millett, D., 2001. Hans Berger: From psychic energy to the EEG. Perspectives in biology and medicine, 44(4), pp.522-542.
11. Brazier, M.A., 1961. A history of the electrical activity of the brain: The first half-century.
12. Nunez, P.L. and Srinivasan, R., 2006. Electric fields of the brain: the neurophysics of EEG. Oxford University Press, USA.
13. Standring, S. ed., 2021. Gray's anatomy e-book: the anatomical basis of clinical practice. Elsevier Health Sciences.
14. Netter, F.H., 2014. Atlas of human anatomy, Professional Edition E-Book. Elsevier health sciences.
15. Rao, R.P., 2013. Brain-computer interfacing: an introduction. Cambridge University Press
16. Haines, D.E., 2004. Neuroanatomy: an atlas of structures, sections, and systems (Vol. 153, No. 2004). Lippincott Williams & Wilkins.
17. Wolpaw, J.R., 2013. Brain–computer interfaces. In Handbook of Clinical Neurology. Elsevier.
18. Schiller, F., 1997. The cerebral ventricles: from soul to sink. Archives of neurology, 54(9), pp.1158-1162.
19. Hartman, A.L., 2009. Normal anatomy of the cerebrospinal fluid compartment. Cerebrospinal fluid in clinical practice, pp.5-10.
20. Hendelman, W., 2005. Atlas of functional neuroanatomy. CRC press.
21. Blank, S.C., Scott, S.K., Murphy, K., Warburton, E. and Wise, R.J., 2002. Speech production: Wernicke, Broca and beyond. Brain, 125(8), pp.1829-1838.
22. Ocklenburg, S. and Gunturkun, O., 2017. The lateralized brain: The neuroscience and evolution of hemispheric asymmetries. Academic Press.
23. Hellige, J.B., 2001. Hemispheric asymmetry: What's right and what's left (Vol. 6). Harvard University Press.

24. Davidson, R.J. and Hugdahl, K. eds., 1996. Brain asymmetry. Mit Press.
25. Olton, D.S., Becker, J.T. and Handelmann, G.E., 1979. Hippocampus, space, and memory. Behavioural and Brain sciences, 2(3), pp.313-322.
26. Andersen, P., Morris, R., Amaral, D., O'Keefe, J. and Bliss, T. eds., 2007. The hippocampus book. Oxford university press.
27. LeDoux, J., 2007. The amygdala. Current biology, 17(20), pp.R868-R874.
28. Aggleton, J.P., 2000. The amygdala: a functional analysis. Oxford University Press.
29. Davis, M. and Whalen, P.J., 2001. The amygdala: vigilance and emotion. Molecular psychiatry, 6(1), pp.13-34.
30. He, B. ed., 2005. Neural engineering (pp. 221-262). Norwell, MA: Kluwer Academic/Plenum.
31. Sörnmo, L. and Laguna, P., 2005. Bioelectrical signal processing in cardiac and neurological applications (Vol. 8). Academic press.
32. Teplan, M., 2002. Fundamentals of EEG measurement. Measurement science review, 2(2), pp.1-11.
33. Elmslie, K.S., 2001. Action potential: ionic mechanisms. e LS.
34. Ruben, P.C., 2001. Action potentials: Generation and propagation. eLS.
35. Subasi, A., 2019. Practical guide for biomedical signals analysis using machine learning techniques: A MATLAB based approach. Academic Press.
36. Nunez, M.D., Nunez, P.L., Srinivasan, R., Ombao, H., Linquist, M., Thompson, W. and Aston, J., 2016. Electroencephalography (EEG): neurophysics, experimental methods, and signal processing. Handbook of neuroimaging data analysis, pp.175-197.
37. He, B., Yuan, H., Meng, J. and Gao, S., 2020. Brain–computer interfaces. Neural engineering, pp.131-183.
38. György Buzsáki, M.D., 2019. The brain from inside out. Oxford University Press.
39. Mavros, P., Austwick, M.Z. and Smith, A.H., 2016. Geo-EEG: towards the use of EEG in the study of urban behaviour. Applied Spatial Analysis and Policy, 9, pp.191-212.
40. Herreras, O., 2016. Local field potentials: myths and misunderstandings. Frontiers in neural circuits, 10, p.101.
41. Ros, T., J. Baars, B., Lanius, R.A. and Vuilleumier, P., 2014. Tuning pathological brain oscillations with neurofeedback: a systems neuroscience framework. Frontiers in human neuroscience, 8, p.1008.
42. Buzsáki, G., Anastassiou, C.A. and Koch, C., 2012. The origin of extracellular fields and currents—EEG, ECoG, LFP and spikes. Nature reviews neuroscience, 13(6), pp.407-420.
43. Rubehn, B., Bosman, C., Oostenveld, R., Fries, P. and Stieglitz, T., 2009. A MEMS-based flexible multichannel ECoG-electrode array. Journal of neural engineering, 6(3), p.036003. Xcv
44. Dubey, A. and Ray, S., 2019. Cortical electrocorticogram (ECoG) is a local signal. Journal of Neuroscience, 39(22), pp.4299-4311.
45. Schwartz, E.S., Edgar, J.C., Gaetz, W.C. and Roberts, T.P., 2010. Magnetoencephalography. Pediatric radiology, 40, pp.50-58.
46. Supek, S. and Aine, C.J., 2016. Magnetoencephalography. Springer-Verlag Berlin An.
47. Nam, C.S., Nijholt, A. and Lotte, F. eds., 2018. Brain–computer interfaces handbook: technological and theoretical advances. CRC Press.

48. Lotte, F., 2014. A tutorial on EEG signal-processing techniques for mental-state recognition in brain–computer interfaces. Guide to brain-computer music interfacing, pp.133-161.

49. Clerc, M., Bougrain, L. and Lotte, F. eds., 2016. Brain-computer interfaces 1: Methods and perspectives. John Wiley & Sons.

50. Lotte, F., Bougrain, L., Cichocki, A., Clerc, M., Congedo, M., Rakotomamonjy, A. and Yger, F., 2018. A review of classification algorithms for EEG-based brain–computer interfaces: a 10 year update. Journal of neural engineering, 15(3), p.031005.

51. Lotte, F., Nam, C.S. and Nijholt, A., 2018. Introduction: evolution of brain-computer interfaces.

52. Lotte, F., Bougrain, L. and Clerc, M., 2015. Electroencephalography (EEG)-based brain-computer interfaces.

53. Miranda, E.R. and Castet, J. eds., 2014. Guide to brain-computer music interfacing. Springer.

54. Farwell, L., & Donchin, E. Talking off the top of your head: Toward a mental prosthesis utilizing event-related brain potentials. Electroencephalography and Clinical Neurophysiology, 1988, 70, 510–523.

55. Wolpaw, J.R., McFarland, D.J., Neat, G.W. and Forneris, C.A., 1991. An EEG-based brain-computer interface for cursor control. Electroencephalography and clinical neurophysiology, 78(3), pp.252-259.

56. Pfurtscheller, G. and Neuper, C., 2001. Motor imagery and direct brain-computer communication. Proceedings of the IEEE, 89(7), pp.1123-1134.

57. Pfurtscheller, G. and Da Silva, F.L., 1999. Event-related EEG/MEG synchronization and desynchronization: basic principles. Clinical neurophysiology, 110(11), pp.1842-1857.

58. Pfurtscheller, G., Brunner, C., Schlögl, A. and Da Silva, F.L., 2006. Mu rhythm (de) synchronization and EEG single-trial classification of different motor imagery tasks. NeuroImage, 31(1), pp.153-159.

59. Pfurtscheller, G., Allison, B.Z., Bauernfeind, G., Brunner, C., Solis Escalante, T., Scherer, R., Zander, T.O., Mueller-Putz, G., Neuper, C. and Birbaumer, N., 2010. The hybrid BCI. Frontiers in neuroscience, p.3.

60. Allison, B.Z. and Neuper, C., 2010. Could anyone use a BCI?. Brain-computer interfaces: Applying our minds to human-computer interaction, pp.35-54.

61. Pfurtscheller, G., Flotzinger, D. and Kalcher, J., 1993. Brain-computer interface—a new communication device for handicapped persons. Journal of microcomputer applications, 16(3), pp.293-299.

62. Ramoser, H., Muller-Gerking, J. and Pfurtscheller, G., 2000. Optimal spatial filtering of single trial EEG during imagined hand movement. IEEE transactions on rehabilitation engineering, 8(4), pp.441-446.

63. Vidal, J.J., 1973. Toward direct brain-computer communication. Annual review of Biophysics and Bioengineering, 2(1), pp.157-180.

64. Wolpaw, J.R., Birbaumer, N., Heetderks, W.J., McFarland, D.J., Peckham, P.H., Schalk, G., Donchin, E., Quatrano, L.A., Robinson, C.J. and Vaughan, T.M., 2000. Brain-computer interface technology: a review of the first international meeting. IEEE transactions on rehabilitation engineering, 8(2), pp.164-173.

65. McFarland, D.J. and Wolpaw, J.R., 2011. Brain-computer interfaces for communication and control. Communications of the ACM, 54(5), pp.60-66.

66. McFarland, D.J. and Wolpaw, J.R., 2017. EEG-based brain–computer interfaces. current opinion in Biomedical Engineering, 4, pp.194-200.

67. Ahuja, C.S., Wilson, J.R., Nori, S., Kotter, M., Druschel, C., Curt, A. and Fehlings, M.G., 2017. Traumatic spinal cord injury. Nature reviews Disease primers, 3(1), pp.1-21.

68. Palumbo, A., Gramigna, V., Calabrese, B. and Ielpo, N., 2021. Motor-imagery EEG-based BCIs in wheelchair movement and control: A systematic literature review. Sensors, 21(18), p.6285.

69. Alonso-Valerdi, L.M. and Mercado-García, V.R., 2021, May. Updating BCI paradigms: Why to design in terms of the user? In 2021 10th International IEEE/EMBS Conference on Neural Engineering (NER) (pp. 710-713). IEEE.

70. Zhang, D., Yao, L., Chen, K. and Monaghan, J., 2019. A convolutional recurrent attention model for subject-independent EEG signal analysis. IEEE Signal Processing Letters, 26(5), pp.715-719.

71. Roots, K., Muhammad, Y. and Muhammad, N., 2020. Fusion convolutional neural network for cross-subject EEG motor imagery classification. Computers, 9(3), p.72.

72. Morgane, P.J. and Mokler, D.J., 2006. The limbic brain: continuing resolution. Neuroscience & Biobehavioural Reviews, 30(2), pp.119-125.

73. Anon, 2023. Functions of the Brain Stem. Available at: https://med.libretexts.org/@go/page/7619 [Accessed January 31, 2023].

74. Zhang, X., Yao, L., Wang, X., Monaghan, J., Mcalpine, D. and Zhang, Y., 2019. A survey on deep learning based brain computer interface: Recent advances and new frontiers. arXiv preprint arXiv:1905.04149, 66.

75. Wu, Y.T., Huang, T.H., Lin, C.Y., Tsai, S.J. and Wang, P.S., 2018, November. Classification of EEG motor imagery using support vector machine and convolutional neural network. In 2018 International Automatic Control Conference (CACS) (pp. 1-4). IEEE.

76. Mammone, N., Ieracitano, C. and Morabito, F.C., 2020. A deep CNN approach to decode motor preparation of upper limbs from time–frequency maps of EEG signals at source level. Neural Networks, 124, pp.357-372.

77. Xu, B., Zhang, L., Song, A., Wu, C., Li, W., Zhang, D., Xu, G., Li, H. and Zeng, H., 2018. Wavelet transform time-frequency image and convolutional network-based motor imagery EEG classification. IEEE Access, 7, pp.6084-6093.

78. Goldberger, A.L., Amaral, L.A., Glass, L., Hausdorff, J.M., Ivanov, P.C., Mark, R.G., Mietus, J.E., Moody, G.B., Peng, C.K. and Stanley, H.E., 2000. PhysioBank, PhysioToolkit, and PhysioNet: components of a new research resource for complex physiologic signals. circulation, 101(23), pp.e215-e220.

79. Tangermann, M., Müller, K.R., Aertsen, A., Birbaumer, N., Braun, C., Brunner, C., Leeb, R., Mehring, C., Miller, K.J., Mueller-Putz, G. and Nolte, G., 2012. Review of the BCI competition IV. Frontiers in neuroscience, p.55.

80. Coleeg software on github. https://github.com/malnaanah/coleeg.

81. Lawhern, V.J., Solon, A.J., Waytowich, N.R., Gordon, S.M., Hung, C.P. and Lance, B.J., 2018. EEGNet: a compact convolutional neural network for EEG-based brain–computer interfaces. Journal of neural engineering, 15(5), p.056013.

82. Schirrmeister, R.T., Springenberg, J.T., Fiederer, L.D.J., Glasstetter, M., Eggensperger, K., Tangermann, M., Hutter, F., Burgard, W. and Ball, T., 2017. Deep learning with convolutional neural networks for EEG decoding and visualization. Human brain mapping, 38(11), pp.5391-5420.

83. Viola, F.C., Debener, S., Thorne, J. and Schneider, T.R., 2010. Using ICA for the analysis of multi-channel EEG data. Simultaneous EEG and fMRI: Recording, Analysis, and Application: Recording, Analysis, and Application, pp.121-133.

84. Guler, I. and Ubeyli, E.D., 2007. Multiclass support vector machines for EEG-signals classification. IEEE transactions on information technology in biomedicine, 11(2), pp.117-126.

85. Chapelle, O., Haffner, P. and Vapnik, V.N., 1999. Support vector machines for histogram-based image classification. IEEE transactions on Neural Networks, 10(5), pp.1055-1064.

86. Scholkopf, B., Sung, K.K., Burges, C.J., Girosi, F., Niyogi, P., Poggio, T. and Vapnik, V., 1997. Comparing support vector machines with Gaussian kernels to radial basis function classifiers. IEEE transactions on Signal Processing, 45(11), pp.2758-2765.

87. Guyon, I., Weston, J., Barnhill, S. and Vapnik, V., 2002. Gene selection for cancer classification using support vector machines. Machine learning, 46, pp.389-422.

88. Congedo, M., Barachant, A. and Bhatia, R., 2017. Riemannian geometry for EEG-based brain-computer interfaces; a primer and a review. Brain-Computer Interfaces, 4(3), pp.155-174.

89. Mesnil, G., Dauphin, Y., Glorot, X., Rifai, S., Bengio, Y., Goodfellow, I., Lavoie, E., Muller, X., Desjardins, G., Warde-Farley, D. and Vincent, P., 2012, June. Unsupervised and transfer learning challenge: a deep learning approach. In Proceedings of ICML Workshop on Unsupervised and Transfer Learning (pp. 97-110). JMLR Workshop and Conference Proceedings.

90. Nakagome, S., Craik, A., Sujatha Ravindran, A., He, Y., Cruz-Garza, J.G. and Contreras-Vidal, J.L., 2022. Deep learning methods for EEG neural classification. In Handbook of Neuroengineering (pp. 1-39). Singapore: Springer Singapore.

91. Altuwaijri, G.A., Muhammad, G., Altaheri, H. and Alsulaiman, M., 2022. A multi-branch convolutional neural network with squeeze-and-excitation attention blocks for eeg-based motor imagery signals classification. Diagnostics, 12(4), p.995.

92. Abbas, W. and Khan, N.A., 2018, July. DeepMI: Deep learning for multiclass motor imagery classification. In 2018 40th Annual International Conference of the IEEE Engineering in Medicine and Biology Society (EMBC) (pp. 219-222). IEEE.

93. Zhang, P., Wang, X., Zhang, W. and Chen, J., 2018. Learning spatial–spectral–temporal EEG features with recurrent 3D convolutional neural networks for cross-task mental workload assessment. IEEE Transactions on neural systems and rehabilitation engineering, 27(1), pp.31-42.

94. Li, X., La, R., Wang, Y., Niu, J., Zeng, S., Sun, S. and Zhu, J., 2019. EEG-based mild depression recognition using convolutional neural network. Medical & biological engineering & computing, 57, pp.1341-1352.

95. Kappel, S.L., Rank, M.L., Toft, H.O., Andersen, M. and Kidmose, P., 2018. Dry-contact electrode ear-EEG. IEEE Transactions on Biomedical Engineering, 66(1), pp.150-158.

96. Young, R.M., 1990. Mind, brain, and adaptation in the nineteenth century: cerebral localization and its biological context from Gall to Ferrier (No. 3). Oxford University Press, USA.

97. Lawrence, C., 2021. Robert M. Young's Mind, Brain and Adaptation revisited. The British Journal for the History of Science, 54(1), pp.61-77.

98. Padfield, N., Zabalza, J., Zhao, H., Masero, V. and Ren, J., 2019. EEG-based brain-computer interfaces using motor-imagery: Techniques and challenges. Sensors, 19(6), p.1423.

99. Khan, J., Bhatti, M.H., Khan, U.G. and Iqbal, R., 2019. Multiclass EEG motor-imagery classification with sub-band common spatial patterns. EURASIP Journal on Wireless Communications and Networking, 2019, pp.1-9.

100. Thompson, M.C., 2019. Critiquing the concept of BCI illiteracy. Science and engineering ethics, 25(4), pp.1217-1233.

101. Li, X., Peng, M., Chen, S., Zheng, W., Zhang, Y., Gao, D. and Wang, M., 2022, May. EEG Motor Imagery Classification Based on Multi-spatial Convolutional Neural Network. In 2022 5th International Conference on Artificial Intelligence and Big Data (ICAIBD) (pp. 433-437). IEEE.

102. Rodriguez-Bermudez, G. and Garcia-Laencina, P.J., 2015. Analysis of EEG signals using nonlinear dynamics and chaos: a review. Applied mathematics & information sciences, 9(5), p.2309.

103. Sun, B., Zhao, X., Zhang, H., Bai, R. and Li, T., 2020. EEG motor imagery classification with sparse spectrotemporal decomposition and deep learning. IEEE Transactions on Automation Science and Engineering, 18(2), pp.541-551.

104. Echtioui, A., Zouch, W., Ghorbel, M., Mhiri, C. and Hamam, H., 2021, June. Fusion Convolutional Neural Network for Multi-Class Motor Imagery of EEG Signals Classification. In 2021 International Wireless Communications and Mobile Computing (IWCMC) (pp. 1642-1647). IEEE.

105. Mihelj, E., 2021. Machine Learning Applications to Brain Computer Interfaces (Doctoral dissertation, ETH Zurich).

106. Ramoser, H., Muller-Gerking, J. and Pfurtscheller, G., 2000. Optimal spatial filtering of single trial EEG during imagined hand movement. IEEE transactions on rehabilitation engineering, 8(4), pp.441-446.

107. Hossain, K.M., Islam, M.A., Hossain, S., Nijholt, A. and Ahad, M.A.R., 2022. Status of deep learning for EEG-based brain–computer interface applications. Frontiers in computational neuroscience, 16.

108. George, O., Dabas, S., Sikder, A., Smith, R.O., Madiraju, P., Yahyasoltani, N. and Ahamed, S.I., 2022. State-of-the-Art Versus Deep Learning: A Comparative Study of Motor Imagery Decoding Techniques. IEEE Access, 10, pp.45605-45619.

109. Scherer, R., Faller, J., Balderas, D., Friedrich, E.V., Pröll, M., Allison, B. and Müller-Putz, G., 2013. Brain–computer interfacing: more than the sum of its parts. Soft computing, 17, pp.317-331.

110. Halgren, M., Ulbert, I., Bastuji, H., Fabó, D., Erőss, L., Rey, M., Devinsky, O., Doyle, W.K., Mak-McCully, R., Halgren, E. and Wittner, L., 2019. The generation and propagation of the human alpha rhythm. Proceedings of the National Academy of Sciences, 116(47), pp.23772-23782.

111. AlSukker, A.S.M., 2012. An improved EEG pattern classification system based on dimensionality reduction and classifier fusion (Doctoral dissertation).